Cooperative Simultaneous Localization and Mapping Framework

von der Naturwissenschaftlich-Technischen Fakultät (Fakultät IV),

Department Elektrotechnik und Informatik

der Universität Siegen

zur Erlangung des akademischen Grades

Doktor der Ingenieurwissenschaften

(Dr. –Ing.)

genehmigte Dissertation

von

M. Sc. Eng. Ahmad Kamal Nasir

1. **Gutachter: Prof. Dr. –Ing. Hubert Roth**
2. **Gutachter: Prof. Dr. rer. nat. Klaus Schilling**

Tag der mündlichen Prüfung: 19 Februar 2014

Abstract

This research work is a contribution to develop a framework for cooperative simultaneous localization and mapping with multiple heterogeneous mobile robots. The presented research work contributes in two aspects of a team of heterogeneous mobile robots for cooperative map building. First it provides a mathematical framework for cooperative localization and geometric features based map building. Secondly it proposes a software framework for controlling, configuring and managing a team of heterogeneous mobile robots. Since mapping and pose estimation are very closely related to each other, therefore, two novel sensor data fusion techniques are also presented, furthermore, various state of the art localization and mapping techniques and mobile robot software frameworks are discussed for an overview of the current development in this research area.

The mathematical cooperative SLAM formulation probabilistically solves the problem of estimating the robots state and the environment features using Kalman filter. The software framework is an effort toward the ongoing standardization process of the cooperative mobile robotics systems. To enhance the efficiency of a cooperative mobile robot system the proposed software framework addresses various issues such as different communication protocol structure for mobile robots, different sets of sensors for mobile robots, sensor data organization from different robots, monitoring and controlling robots from a single interface.

The present work can be applied to number of applications in various domains where a priori map of the environment is not available and it is not possible to use global positioning devices to find the accurate position of the mobile robot. Therefore the mobile robot(s) has to rely on building the map of its environment and using the same map to find its position and orientation relative to the environment. The exemplary areas for applying the proposed SLAM technique are Indoor environments such as warehouse management, factory floors for parts assembly line, mapping abandoned tunnels, disaster struck environment which are missing maps, under see pipeline inspection, ocean surveying, military applications, planet exploration and many others. These applications are some of many and are only limited by the imagination.

Zusammenfassung

Diese Forschungsarbeit ist ein Beitrag zur Entwicklung eines Framework für kooperatives SLAM mit heterogenen, mobilen Robotern. Die präsentierte Forschungsarbeit trägt in zwei Aspekten in einem Team von heterogenen, mobilen Robotern bei. Erstens stellt es einen mathematischen Framework für kooperative Lokalisierung und geometrisch basierende Kartengenerierung bereit. Zweitens schlägt es einen Softwareframework zur Steuerung, Konfiguration und Management einer Gruppe von heterogenen mobilen Robotern vor. Da Kartenerstellung und Poseschätzung miteinander stark verbunden sind, werden zwei neuartige Techniken zur Sensordatenfusion präsentiert. Weiterhin werden zum Stand der Technik verschiedene Techniken zur Lokalisierung und Kartengenerierung sowie Softwareframeworks für die mobile Robotik diskutiert um einen Überblick über die aktuelle Entwicklung in diesem Forschungsbereich zu geben.

Die mathematische Formulierung des SLAM Problems löst das Problem der Roboterzustandsschätzung und der Umgebungmerkmale durch Benutzung eines Kalman filters. Der Softwareframework ist ein Beitrag zum anhaltenden Standardisierungsprozess von kooperativen, mobilen Robotern. Um die Effektivität eines kooperativen mobilen Robotersystems zu verbessern enthält der vorgeschlagene Softwareframework die Möglichkeit die Kommunikationsprotokolle flexibel zu ändern, mit verschiedenen Sensoren zu arbeiten sowie die Möglichkeit die Sensordaten verschieden zu organisieren und verschiedene Roboter von einem Interface aus zu steuern.

Die präsentierte Arbeit kann in einer Vielzahl von Applikationen in verschiedenen Domänen benutzt werden, wo eine Karte der Umgebung nicht vorhanden ist und es nicht möglich ist GPS Daten zur präzisen Lokalisierung eines mobilen Roboters zu nutzen. Daher müssen die mobilen Roboter sich auf die selbsterstellte Karte verlassen und die selbe Karte zur Bestimmung von Position und Orientierung relativ zur Umgebung verwenden. Die exemplarischen Anwendungen der vorgeschlagenen SLAM Technik sind Innenraumumgebungen wie Lagermanagement, Fabrikgebäude mit Produktionsstätten, verlassene Tunnel, Katastrophengebiete ohne aktuelle Karte, Inspektion von Unterseepipelines, Ozeanvermessung, Militäranwendungen, Planetenerforschung und viele andere. Diese Anwendungen sind einige von vielen und sind nur durch die Vorstellungskraft limitiert.

Acknowledgement

This research work is a result of my endeavor as a PhD student at department of Elektrotechnik und Informatik, University of Siegen, Germany. During my effort I have been supported by many people to whom I wish to express my gratitude.

First of all, I would like to acknowledge the support of my wife Ayesha during my PhD time period. I can't describe in words all the ways in which she encouraged me. I would also like to acknowledge the contribution of my parents, brothers and sisters to support me at every stage of my life and for their moral supports and fond memories.

Especially, I am indebted to Prof. Dr. –Ing. Hubert Roth for providing me a possibility at the institute of control techniques at university of Siegen. I would like to thank him for providing me assistance and freedom to conduct my research work throughout the past three and half years of my doctoral research work. The institute of control engineering department provided me a conducive environment to learn and the resources to perform experiment that resulted in this research work. I would also like to specially thank my colleague Christof Hille for fruitful discussions regarding many issues. Furthermore, I thank Prof. Dr. rer. nat. Klaus Schilling for being my second supervisor. I would also like to thank Prof. Dr.-Ing. habil. R. Obermaisser, Prof. Dr. Roland Wismüller for being my co-examiner in the PhD committee.

At the end I would like to thank HEC Pakistan and DAAD to provide me a scholarship to finish my PhD studies at university of Siegen.

To my lovely family

Table of Contents

List of Figures

List of Tables

Notations

Following acronyms and notations are used throughout this text. Vectors are represented by lower subscripted letters (x_t, z_t) where the matrices are represented by capital letters (A, B, C, K). The notation of x_t is used for the mobile robot pose instead of the x coordinate of the position. Sometime the term single robot is used instead of multiple robots just for bringing clarity and simplicity to the discussion.

CDF	Cumulative Distribution Function
CUDA	Compute Unified Device Architecture
EKF	Extended Kalman Filter
FBM	Feature Based Map
FOV	Field of View
GPS	Global Positioning System
GPU	Graphical Processing Unit
GT	Ground Truth
HSM	Hessian Scan Matching algorithm
ICP	Iterative Closest Point matching algorithm
IMU	Inertial Measurement Unit
KF	Kalman Filter
LASER	Light Amplification by Stimulated Emission of Radiation
LIDAR/LADAR	LIght Detection and Ranging
MSRS	MicroSoft Robotics Studio
OGM	Occupancy Grid Mapping
PDF	Probability Distribution Function

PF	Particle Filter
PSM	Polar coordinate Scan Matching algorithm
RBPF	Rao-Blackwellised Particle Filter
RFID	Radio Frequency IDentification
RGB-D	Red Green Blue – Depth device such as Microsoft Kinect
ROS	Robot Operating System
SIFT	Scale Invariant Feature Transform
SONAR	SOund Navigation and Ranging
SURF	Speeded Up Robust Features
TCP	Transmission Control Protocol
UDP	User Datagram Protocol

Chapter 1.

Introduction

1.1. Motivation

Mobile robots are finding a way more and more in our daily life from vacuum cleaners [1] to autonomous driving vehicles [2]. Furthermore navigate able industrial robots [3] are not very far away. Mobile robots can be used at warehouse, autonomous cargo handling at sea ports. Not to mention to operate in a hazardous environment for humans such as the site of Fukushima daiichi nuclear power plant for debris removal. There was not so much to actually help to overcome nuclear leakage problem due to the aftermath of the earthquake which resulted in the destruction of the plant. The DARPA urban challenge also promoted to develop vehicles capable of driving through traffics [4]. Many institutes have developed the mobile robots for infotainment of visitors [5] at museums and management at libraries [6]. The success of these applications depends highly on the accuracy and robustness of their SLAM implementation.

Multiple robots with heterogeneous capability can mutually assist each other for working toward a common goal. To cooperate among multiple robots there is a need of an interface which addresses the various issues such as (a) Different communication protocol structure for mobile robots. (b) Different sets of capability (sensors) for mobile robots. (c) Sensor data organization from different robots. (d) Monitoring and controlling robots from a single interface. (e) Expansion of existing robot network. (f) Combined map building. In order to enhance the efficiency of a cooperative mobile robot system high modularity and scalability should be maintained. Apart from the above mentioned aspects other issues have also to be addressed in the ongoing standardization process of the cooperative mobile robotics systems. Controlling and managing cooperative multi-robot system is challenging because the system requires handling multiple robots with heterogeneous capabilities and set of sensors and flexible control architecture. One of many challenges in the field of cooperative robotics as stated by Smart [7] is standard software architecture. Robot system developers have to re-implement basic control and communication mechanisms due to the non-interoperability of current implementations. Therefore, in order to enhance multi-robot system control and communication, a new type of multi-robot middleware or interface environment is necessary. The interface should be general enough to allow the addition of another robot within the

network with a different set of sensors and communication protocols. Furthermore, sensor data from different robots should be organized and managed in a structured way. The overall system should be flexible enough to be adopted for the need of robot control.

It is exciting to know how the multiple robots can help each other to solve the SLAM problem, therefore the research work has two ambitions, first is to develop a framework where multiple robots can cooperative with each other. The second is to develop a mathematical SLAM framework for building a centralized geometric map cooperatively. Although many algorithms exist today to solve SLAM problems for single mobile robot in static indoor environment, there is still a challenge to perform cooperative SLAM especially the map merging part. The large, dynamic, sparse and outdoor environment makes the problem further interesting. This research work proposes a cooperative SLAM framework which addresses the issues of cooperative SLAM and building a software framework for cooperation among heterogeneous mobile robots.

1.2. Problem Statement

The cooperative SLAM problem can be formalized as $p(x_t, m|z_t, u_t, c_t)$ where x_t is the state of the robots at time step t, m is the map, z_t is the robots measurements, u_t are the control inputs and c_t is the data association function. One of the goals in this research work is to formalize $p(x_t, m|z_t, u_t, c_t)$ for cooperative SLAM problem among a team of mobile robots, and the second is to develop a software framework where we can control, configure and manage different mobile robots for cooperative map building tasks.

1.3. Research Work Scope

This dissertation gives a brief introduction to the background and developments of SLAM problem. Various SLAM methodologies are discussed in the next section. An EKF based multi-robot SLAM algorithm for heterogeneous features is formulated in this research work. EKF is used as the main estimation engine. The overall solution to SLAM consists of following parts; state estimation, observations, segmentation, feature extraction, measurement prediction, data association and then state and features update. From the implementation point of view the core modules which are mentioned above are also discussed and formulated.

It would also be exciting to know which sensor technologies can be combined to enhance the map accuracy, but the evaluation of various sensor technologies for SLAM problem is not discussed here. Furthermore due to the limitation of available hardware, sensors and resources for validation, some simulations are performed to validate the algorithms. The

research work scope is also limited for indoor environment. The cooperative SLAM algorithm discussed in Chapter 4 assumes that the initial relative robot poses are known.

1.4. Related Works

SLAM in literature is often referred as chicken or the egg causality dilemma. Much research has been done on this topic over the past decades as Hugh Durrant-Whyte [8] states that a solution of SLAM problem is the Holy Grail for the mobile robotics community. SLAM is a hard problem because of big and dynamic robot environment, robot's noisy sensors measurements and robot's motion and control errors. A solution of the SLAM problem requires a big state vector consisting of robot pose and position of all landmarks, which represent the world around the mobile robot. This state vector is updated each time new measurement from the robot sensors are available, therefore, it requires a lot of computational power. SLAM can be performed either using environment features or using scan matching technique in which raw sensor measurements are used. The feature based SLAM is the earlier version of the SLAM which was realized using an EKF. In a scan matching technique one need's to estimate a transformation which consists of a rotation and translation to find relative pose of the robot between two consecutive raw sensor measurements. Many scan matching techniques exists in the literature such as ICP [9], HSM [10] and PSM [11]. For a comparison among different scan matching techniques please refer [12].

The inception of the probabilistic SLAM problem occurred during mid-80's [8]. The research work by Smith et al [13] and Durrant-Whyte [14] described probabilistic estimation technique for correlation among map features and robot pose. The key insight of the high correlation among map features (landmarks) and robot pose described that, these correlations grows with successive continuous observations. Crowley [15] and Leonard [16] performed SLAM using sonar sensors. They used the line segments extracted from ultrasonic sensor data as features. Vandorpe [17] and Gonzalez [18] used laser data to perform SLAM. During that time Faugeras [19] and Ayache performed earliest work in visual navigation and mapping. Lenord [20] worked on to reduce the computational requirements by dividing the state vector into local sub parts. This idea was skipped when later on it was found that for the convergence of the SLAM problem, the huge state-vector is essential and more the correlation among features grows the better solution becomes. So far, the robots pose and landmarks were represented by univariate Gaussian noise model. Murphy [21] introduced a particle filter which is a discretized representation of a complex multi-model probability density function. Using particle filters the robot pose is represented by a set of discrete states, particles. He

furthermore proposed the discretization of the space around the robot in blocks which he termed as occupancy grid mapping. Later on, Montemerlo [22] extended the work to feature based maps, which is known as FastSLAM in which he used Extended Kalman filter to estimate the map where particle filter was used to represent robot pose. GMapping [23] is a grid based SLAM algorithm in 2D. The first working solution of the SLAM problem was based on extended Kalman filter (EKF-SLAM) and then later came the Rao-Blackwellised particle filter (FastSLAM).

The main advantage of a particle filter is to represent a multi model belief about robot states. Many authors like [24] [23] [25] uses grid based maps with PF to address the SLAM problem in large dynamic outdoor environment. Grisetti [23] developed GMapping which is at the moment a very robust tool to build the grid map using a laser scanner and odometry. Haehnel [25] proposed GridSLAM algorithm and Eliazer [24] proposed DP-SLAM. GMapping and GridSLAM reduce the number of particles where DP-SLAM uses a tree based structure. Many of state of the art SLAM algorithm are available on OpenSLAM [26] website as open source packages, furthermore many of the algorithms are also available as ROS [27] packages.

There are many challenges in cooperative SLAM such as a standard framework for data acquisition, robot and their sensor data management, global map representation and the mathematical framework for fusing multi-robot and multi-sensor data. In general cooperative slam can be performed in a centralized [28] [29] or decentralized [30] [31] [32] [33] manner. Jayasekara [34] proposed a method for cooperation based on external tracking of robots which is limited to visual range of the camera and laser scanner. Williams [35] proposed a decentralized cooperative SLAM methodology to manage computational complexity and improved data association. Andrew [31] proposed the method of decentralized cooperative SLAM based on FASTSLAM. The map merging part is performed only when one robot detects other and measures its pose relative to its own. This situation happens less frequent in practical scenarios. Lee [36] proposed the distributed cooperative SLAM using the ceiling vision. Using ceiling vision based data association technique the proposed algorithm detects the overlapping regions, an estimate of the transformation for map alignment. This technique is limited to indoor planer environment. Zhou [37] proposed an algorithm for multi-robot map alignment to build a joint map. Relative pose measurement between robots is used to find the transformation between maps. When there is an overlap between maps i.e. landmarks appear twice in two maps this information helps to increase the map alignment accuracy. Ming [38] proposed a cooperative SLAM technique using vertical lines and colored name plates as landmarks in an indoor office environment.

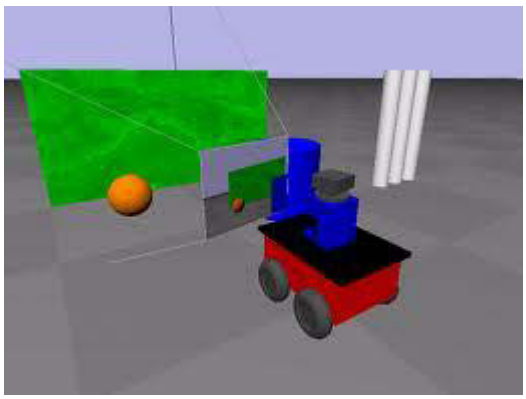

Figure 1.1 Simulation of Pioneer Robot in PSG Environment

Regarding a standard framework for mobile robotics, many set of libraries and tools exist for handling mobile robots. Many of them focus on the single mobile robot while other targets a group of robots but usually such frameworks are application and platform dependent. The player project [39] is a popular open source robot software framework which handles the communication between robot hardware/simulation and the control software clients. PSG (Player Stage Gazebo) consists of a 2D simulator "Stage", a 3D simulator "Gazebo" [40] as shown in Figure 1.1 and robot control interface software "Player". Its client server architecture is based on TCP sockets. The mobile robot's hardware is accessed through drivers and many of the drivers are already implemented in Player, furthermore, PSG can be used for simulating robots. For implementation of player drivers for a custom robot please refer to [41]. Few weakness of PSG systems are as follows. In order to function properly, Gazebo has many non-documented dependencies that include specific versions of the third party libraries. Another important deficiency of Gazebo is that there is no online mesh generation and rendering capability which is important for creating online maps from mobile robots range sensors data. Unfortunately overall PSG system is difficult to install and run due to its complexity [42] and non-documented dependencies, furthermore, it does not provide online map making facility and no structured built-in scheme for storage of robots data.

During STAIR project [43] at Stanford it was also required and realized such a software framework for hardware software integration of various mobile robot modules which later evolved into ROS [44]. ROS [27] is an open source project which provides a framework for communicating data within various running processes and uses existing source code and libraries for managing robot related tasks. It uses IPC (Inter Process Communication) methodology for peer to peer communication among various nodes (executable); therefore, modules do not require to be linked together in one executable. Messages among nodes are communicated through master node; therefore publisher (sender) and listener (receiver) both

are unaware of their existence. Nodes for ROS can be written either using C++ or Python. The ROS specifications are at messaging layer for cross-language development. ROS has various tools for managing, building and running various ROS components. It uses other open source projects code such as PSG for simulation, OpenCV for vision sensors, OpenNI for RGB-D camers, Eigen for matrix algebra libraries and many more. It also provides a data logging and playback mechanism which is missing in PSG system which is a very important aspect for a multi robot system during development. For a conceptual working about ROS system please refer [44]. A 2D planer map image of the second floor of Hölderlinstr F-block building is shown in the Figure 1.2 during the simulation of a robot in Stage-ROS. Figure 1.3 shows the graphical visualization component of the ROS, RVIZ, for displaying robot's laser scanner measurements published as topic.

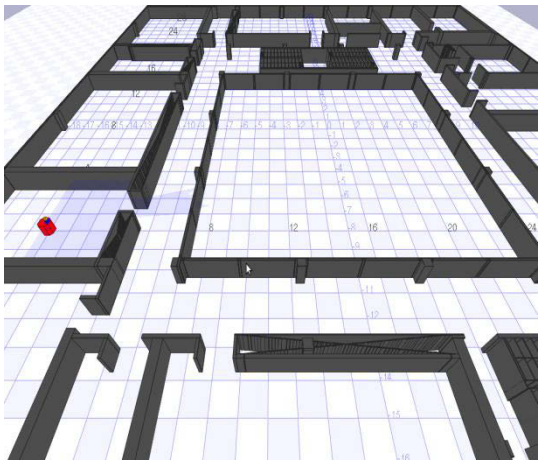

Figure 1.2 Simulation of virtual robot in Stage-ROS

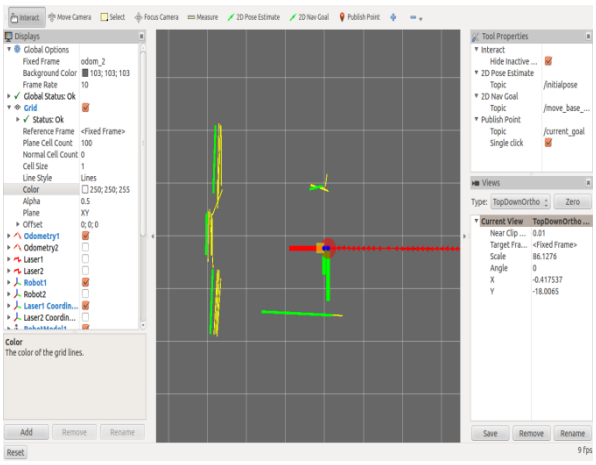

Figure 1.3 Sensor measurement visualization in RVIZ-ROS

CARMEN [45] is another open source robot control software toolkit developed at Carnegie Mellon University. It provides a consistent interface and basic modules for different commercial robots for research purpose. Its design consist of three layers, first layer is for hardware interfacing and control e.g. for low level linear and angular velocity control, integrate motion information from odometry. The second and upper layer provides high level tasks such as localization, tracking and motion planning. The third and the top most layer provides user level tasks which uses modules from second layer. USARSim [46] is an open source robot simulator which incorporates a simulation engine based on a first person shooter game unreal tournament which is used to host a robots competition within the robocup initiative. USARSim is based on the Unreal Tournament game engine. A simulation environment as shown in Figure 1.4 provides virtual ground and aerial robots in a map. The

robot's sensors data are acquired through Gamebots [47] protocol over TCP connection with the game server.

Figure 1.4 Simulation of aerial and ground robot in a virtual environment based on Unreal Tournament game engine

MSRS [48] was a Microsoft initiative in 2006 to provide industry software standards for robot control. Figure 1.5 shows multiple Poineer robots and an NXT robot being simulated in a virtual environment. It provides visual programming tools, 3D simulation and methods to access the robot's sensors and actuator data using C# as programming language.

Figure 1.5: Microsoft Robotics Studio simulation of multiple robots

Marilou [49] is a commercial robot simulation tool which can be used for cooperative robotics. It provides a modeling environment to construct a virtual environment and the mobile robot with sensors, actuators and joints. The simulation runs within physics based engine and allows the user interaction during the simulation run. A test simulation environment is shown in the Figure 1.6. various programming languages such as C/C++/C#/VB/Matlab can be used to interface with the robot's sensor and actuator's data.

Figure 1.6 Marilou based mobile robot simulation

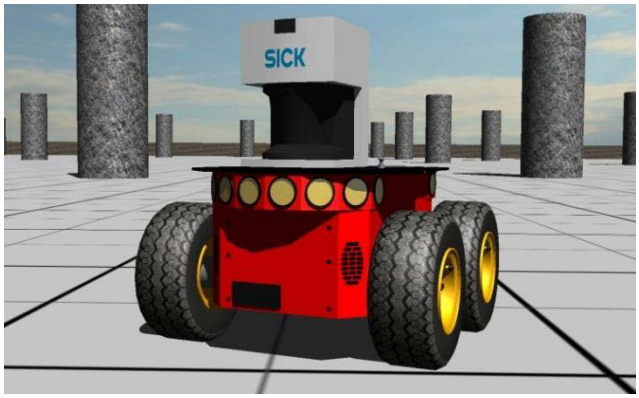

Figure 1.7 Webbot based simulation of Poineer mobile robot

Webbots is a commercial robot modeling, programming and simulation software. Figure 1.7 shows a pioneer robot within a Webbots virtual simulation environment. It also provides the multiple programming languages to interface through API with the running simulation. For a comparison among different robotics frameworks the reader may refer [50]. There exist other cooperative heterogeneous robot applications. For instance, Wei Li [51] uses a down looking monocular camera fixed on an aerial quad-rotor to track a mobile robot while Gaurav [52] achieved aerial robot localization using a single camera by observing the relative positions of it and two ground mobile robots with known location on the ground below it. Those works are more application oriented and self-contained. Therefore, they don't explicitly define a framework of how multiple robots in a cooperative environment should be controlled, managed and configured.

1.5. Methodology

The mathematical formulation for cooperative SLAM is probabilistic in nature and its methodology is as follows. The robots pose and the geometric features in the environment are together represented as state vector. The state vector can be considered as the map. Because of the probabilistic nature of the robot motion and sensor errors the uncertainty of the map is also estimated and maintained at each time step. Kalman filter is used as core estimation

engine for maintaining the robots pose and environment features uncertainty. Two novel sensor data fusion algorithms are also proposed which better helps to localize the robot. From the implementation point of view the SLAM algorithm, range sensor data segmentation, geometric features estimation and data association are also discussed.

The methodology for the cooperative framework in this work is as follows. First of all a universal control board is developed which can be used by different mobile robots. Then a modular firmware is developed which can be configured according to the specific robot's sensor and features. Then a software framework is developed which proposes a general communication protocol interface, general format for configuration of robot's modules features, organized storage of robots sensors data in database and other. The proposed software framework is a decentralized system which runs on multiple computers.

1.6. Applications

SLAM has been applied to number of applications in various domains where a priori map of the environment is not available and it is not possible to use global positioning devices to find the accurate position of the mobile robot. Therefore the mobile robot has to rely on building the map of its environment and using the same map to find its position and orientation relative to the environment. The environment which are perfect candidates for applying SLAM techniques are Indoor environments such as warehouse, mapping abandoned tunnels, disaster struck environment which are missing maps, under see pipeline inspection, ocean surveying, military applications, planet exploration and many others. These applications are some of many and are only limited by the imagination. Various research groups at Freiburg [53], Stanford [54], Zaragoza [55], Sydney [56] and many others [57] [58] [59] are working on the land, air and sea applications of the SLAM problem.

Multi-robot systems can be used in cooperative planetary exploration (map building), firefighting, search and rescue in areas affected by natural disasters and in myriad of other fields which involves environmental dangers to human life. Other advantages are faster objectives completion time, in case of individual robot failure, task can be assigned to other robot; tasks can be done which are beyond the capability of single robot and many others. Furthermore, overall system robustness is increased because of the redundant sensor information.

1.7. Thesis Overview

This thesis is structured as follows; Chapter 1 describes the background and motivation of the research work. It describes also the problem statement, research scope and the related work in this field in chronological order.

Chapter 2 describes the required tools and techniques to solve the SLAM problem. It also discusses the individual components of the SLAM solution algorithm such as localization, mapping and navigation. Since the mapping is closely dependent on robot's pose therefore, two novel pose estimation techniques are also discussed.

Chapter 3 discusses the extended Kalman filter based SLAM approach and its core components in detail. These components are clustering or segmentation, geometric feature extraction, data association or map update and the augmentation of new features into the map.

Chapter 4 discusses the EKF based SLAM process for multiple robots and heterogeneous features.

In Chapter 5 a cooperative SLAM software framework for multiple robots is discussed. It describes the architecture and components of the system, firmware and hardware components for mobile robots. It also describes a simulation environment which can be used for the rapid development of the mobile robots related cooperative SLAM algorithms.

Chapter 6 discusses the implementation of the proposed cooperative architecture on the robot. It discusses the implemented framework and the applied cooperative SLAM algorithm.

Chapter 7 ends the thesis with a discussion about the research work and concludes with the future work direction.

Chapter 2.

Theory and Background

This chapter provides the theoretical bases, mathematical tools and techniques required for this research work. These theoretical backgrounds are not complete in it-self, therefore, for an in-depth understanding the reader is suggested to refer the corresponding references mentioned in the text.

Here we will discuss the structure of the SLAM which is often implemented in Bayesian form. The Bayes rule can be represented in the following form:

$$p(x_t|z_{1:t},u_{1:t}) = \frac{p(x_t|z_{1:t-t},u_{1:t}) \cdot p(z_t|x_t,z_{1:t-1},u_{1:t})}{p(z_t|z_{1:t-1},u_{1:t})} \quad \text{Eq. 2.1}$$

Here, $p(x_t|z_{1:t},u_{1:t})$ represent the posterior probability, $p(x_t|z_{1:t-t},u_{1:t})$ represents the prior probability, $p(z_t|x_t,z_{1:t-1},u_{1:t})$ represents the conditional probability of $z_{1:t-1}$ given x_t and $u_{1:t}$. $p(z_t|z_{1:t-1},u_{1:t})$ is the normalization constant which is often written as η in the literature. In the above equation x_t denotes the robot pose at time step t, $z_{1:t}$ represents all the observations and $u_{1:t}$ represents all the control commands, linear and angular velocity. The two important assumptions which play an important role in probabilistic robotics are Markov process model and the Independence assumption. According to Markov process model the current state x_t depends only on x_{t-1}, we silently assume the state vector is complete, which mathematically can be described as $p(x_t|z_{1:t},u_{1:t}) = p(x_t|x_{t-1},z_t,u_t)$. According to second assumption we will treat that each observation z_t is independent from the other and previous observations z_{t-1}. After introducing the above mentioned assumption and simplification yields the following recursive Bayes law:

$$\begin{aligned} p(x_t|z_{1:t},u_{1:t}) &= \frac{p(x_t|z_{1:t-t},u_{1:t}) \cdot p(z_t|x_t)}{p(z_t|z_{1:t-1},u_{1:t})} \\ &= \eta \cdot p(x_t|z_{1:t-t},u_{1:t}) \cdot p(z_t|x_t) \end{aligned} \quad \text{Eq. 2.2}$$

The term $p(x_t|z_{1:t-t},u_{1:t})$ is called the motion model where the term $p(z_t|x_t)$is called the observation or measurement model. For further information the reader can refer [8][49].

2.1. Probabilistic Motion Model

The robot motion model used in this research work assumes that the robots have holonomic constraints such as differential drive robots and each robot wheels are separated by a distance B. If a differential drive robot is given a motion command comprises of linear and angular velocity $u_t = [v \quad \omega]^T$ then the velocity for right and left motor velocity controller is calculated as follows

$$v_r = v + \frac{B \cdot \omega}{2} \qquad \text{Eq. 2.3}$$

$$v_l = v - \frac{B \cdot \omega}{2} \qquad \text{Eq. 2.4}$$

Such that the positive angular velocity ω induces an anti-clockwise rotation and positive linear velocity v induces a forward motion. Usually a simple kinematic motion model is used for a differential drive robot instead of a dynamic model because of the simplicity of kinematic model and the unavailability of various parameters required for a dynamic model.

Motion model or probabilistic kinematic model for a mobile robot consists of states transition probability distribution $p(x_t|u_t, x_{t-1})$. It predicts the posterior distribution of mobile robot states x_t, which robot assumes, after applying the motion commands u_t at prior distribution of robot states x_{t-1}. The states of a mobile robot consist of its pose or its configuration. Mobile robot kinematics describes the effect of control actions on its configuration. The configuration of a mobile robot in environment is known as its pose. The pose of a mobile robot in 3D is described by six Degree of Freedoms (DOF), Location described by 3D Cartesian coordinate and three Euler angles, i.e.

$$x_t = [x \quad y \quad z \quad \varphi \quad \theta \quad \psi]^T \qquad \text{Eq. 2.5}$$

For a mobile robot in a planar environment its pose is described by three DOF, location described by 2D Cartesian coordinate and an orientation, i.e.

$$x_t = [x \quad y \quad \theta]^T \qquad \text{Eq. 2.6}$$

The robot motion model is called probabilistic because the uncertainties in the input and/or states are explicitly modeled into the system equations. Therefore, it is important to understand the nature of motion noise or uncertainties which affects the robot motion. The motion noise might be deterministic (systematic) or nondeterministic (random or non-systematic) errors. Basically this noise is introduced because of un-modeled effects in to the

robot kinematics. As we know the wheel odometry is subject to two kinds of errors, systematic and non-systematic errors [60]. The kinematic model should be able to handle various error sources such as different wheel diameters, inaccuracy of the wheel attachment, ground unevenness and slip. Two systematic error sources are considered here, the difference in both robot wheel diameters and the wheel base distance. These errors can be modeled as scale factors and can be calculated by a calibration technique such as UMBmark [60] in an offline manner or in an online manner [61]. In the online calibration technique these calibration scale factors are included in the state vector and are also estimated at each time step, which is then used to correct the odometric information. During the experimentation the ground based mobile robot's wheel odometry is calibrated in an offline manner by UMBmark method. The calibration process calculates the scale factors constants, due to non-deterministic errors, that are used to compensate the non-systematic errors in odometry information at each time step. The non-systematic errors are random in nature and mostly happen because of slip or because of surface morphology. These errors can be modeled as Gaussian distribution $\mathcal{N}(0, \sigma^2)$ noise with zero centered mean and standard deviation σ and then added to each state variable.

2.1.1. Robot Motion Model Using Wheel Odometry

Wheel odometry is obtained by integrating the wheel encoder information from ground mobile robot. Similarly flying robot uses inertial odometry to estimate its pose which is obtained by integrating the information obtained from inertial measurement unit but this discussion is limited to wheel odometry. The robot's wheel odometry information is given as an input u_t to the probabilistic motion model. This input can be described either by velocity or by displacement information obtained by the right and left wheel encoders. Usually odometry information in the form of velocity is preferred in motion planning algorithms such as collision avoidance to predict the effect of motion in advance but here the odometry information in the form of linear and angular displacement is used.

Figure 2.1 shows the kinematics of a differential drive mobile robot during a time step ΔT from the robot pose x_{t-1} to robot pose x_t. Due to the linear and angular velocity command $u_t = (v, \omega)^T$ given to the robot, it will traverse a linear distance ΔS and an angle of $\Delta\theta$ during a sampling interval of ΔT. The actual linear and angular displacements traversed by the mobile robot due to the commanded velocity can be calculated by using the left and right wheels encoder's displacement measurements

$$\Delta S = \frac{\Delta S_r + \Delta S_l}{2} \quad \text{Eq. 2.7}$$

$$\Delta\theta = \frac{\Delta S_r - \Delta S_l}{c_b \cdot B_n} \quad \text{Eq. 2.8}$$

Where the displacement measured by left and right wheel encoder is ΔS_l and ΔS_r respectively. These displacements are calculated by the Eq. 2.10 and Eq.2.11. B_n is the nominal separation distance between the left and right wheel which is often known as wheel base. c_b is the correction factor found by the UMBmark calibration method.

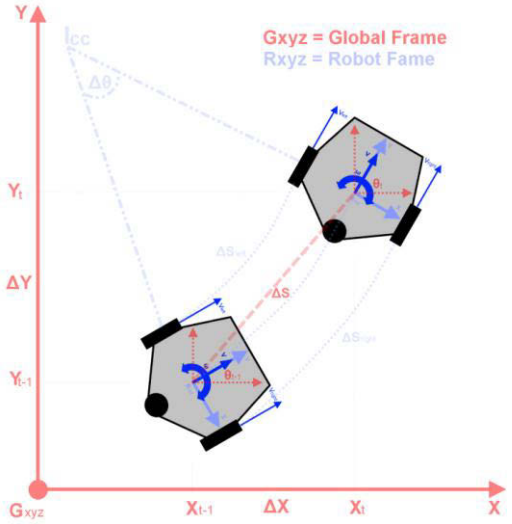

Figure 2.1 Mobile robot odometry process

$$C_m = \frac{\pi \cdot D_n}{n \cdot C} \quad \text{Eq. 2.9}$$

$$\Delta S_l = c_l \cdot C_m \cdot N_l \quad \text{Eq. 2.10}$$

$$\Delta S_r = c_r \cdot C_m \cdot N_r \quad \text{Eq. 2.11}$$

N_l and N_r are the pulses measured by the left and right wheel encoders and D_n is the nominal diameter for the left and right wheels. C is the pulses per revolution constant for wheel encoders and n is the gear ratio between the motor shaft and the wheel. c_l and c_r are also the correction factors found by the UMBmark calibration method. The mobile robot's motion model is calculated by numerical integrating of the odometric information $(\Delta S, \Delta\theta)$ is as follows

$$x_{t+1} = x_t + \Delta S \cdot \cos\left(\theta_t + \frac{\Delta\theta}{2}\right) \quad \text{Eq. 2.12}$$

$$y_{t+1} = y_t + \Delta S \cdot \sin\left(\theta_t + \frac{\Delta\theta}{2}\right) \quad \text{Eq. 2.13}$$

$$\Delta\theta_{t+1} = \theta_t + \Delta\theta \quad \text{Eq. 2.14}$$

Mathematically the complete probabilistic robot motion model using robot kinematics including the non-deterministic effects is defined as follows

$$\begin{bmatrix} x_{t+1} \\ y_{t+1} \\ \theta_{t+1} \end{bmatrix} = \begin{bmatrix} x_t \\ y_t \\ \theta_t \end{bmatrix} + \begin{bmatrix} \Delta S \cdot \cos\left(\theta_t + \frac{\Delta\theta}{2}\right) \\ \Delta S \cdot \sin\left(\theta_t + \frac{\Delta\theta}{2}\right) \\ \Delta\theta \end{bmatrix} + \begin{bmatrix} \mathcal{N}(0, \sigma_x^2) \\ \mathcal{N}(0, \sigma_y^2) \\ \mathcal{N}(0, \sigma_\theta^2) \end{bmatrix} \quad \text{Eq. 2.15}$$

Usually one can move the robot in a predefined trajectory for calibration process. And then by measuring the difference between robot's absolute pose by some means and the estimated pose using odometry process at end position during several runs, one could measure the standard deviation of pose due to non-deterministic errors. Here σ_x, σ_y is the standard deviation of the position error, difference between absolute and estimated position, and σ_θ is the standard deviation of robot orientation error.

2.2. Probabilistic Observation Model

A probabilistic observation model $p(z_t|x_t, m)$ describes a process by which a sensor measurements, landmark or feature are generated given the current robot pose and existing map. The terms features and landmarks are synonymous in the context of SLAM and will be used interchangeably in this text. The observation model is called probabilistic because it accommodate the different type of deterministic and non-deterministic errors such as measurement errors due to sensor accuracy and resolution, unexplained measurements, failure to detect objects and unexpected objects which are not present in the existing map. As statistically each noise source is modeled as a random variable corresponding to a particular distribution; therefore, the probabilistic observation model is a mixture of all such distributions. The probabilistic observation model is in fact a conditional probability which describes the set of observations z_t given the current robot pose x_t and the map m. Because of independence assumption we can describe the probabilistic observation model as follows

$$p(z_t|x_t, m) = \prod_{k=1}^{n} p\left(z_t^k | x_t, m\right) \quad \text{Eq. 2.16}$$

The observation model depends on the type of sensor modality. SLAM algorithms rely on the observation of the environment which is performed by various types of sensors such as range

sensors, camera images and RFID signals. The accuracy and robustness of SLAM algorithms depend on the sensor technology, further information regarding mobile robot sensors can be found in [20]. Recent sensor technologies such as laser range scanners, RGB-D cameras and time of flight cameras are being used now a day to map the environment of a mobile robot. Laser beam based range sensors yield the most exact results both in indoor and outdoor environment and therefore are commonly used. RGB-D cameras such as Microsoft Kinect [62] and ASUS Xtion Pro [63] are limited to indoor use while the time of flight cameras have limited field of view and range but has high frame rate therefore it is considered good candidate for obstacle avoidance but not for SLAM. Modern laser ranger scanners are able to distinguish among the readings which are affected while passing through the glass. We mainly used two types of sensors, a 2D laser scanner and 3D RGB-D camera for our mobile robots. Both sensors fall into the category of range sensors, therefore only beam based observation models will be discussed.

The observation model also depends on the type of map; feature map or grid map. In the feature based map the environment map can compose of certain environmental features or location of objects in the environment. For grid based map there are three types of observation models, beam based range models, likelihood field range model and scan matching. Beam based range models depend mostly on the geometry and physics of the sensor which has two drawbacks, smoothness in cluttered environment and the computational complexity compared to the likelihood field range model. The difference between likelihood based sensor model and scan matching is that scan matching creates a local map of the robot to be compared with the global map which includes the free space and open space where the likelihood based observation model only includes the end point of range scans. All the above three sensor models are based on the raw sensor measurements. For feature based maps the raw sensor measurements are preprocessed to extract features along with its signatures if it is available. Mathematically we can describe the feature extraction process as a function which is operating on the measurements, $f(z_t)$, therefore, the observation model becomes $p(f(z_t)|x_t, m)$. There are a number of features which can be extracted from the environment. Usually the choice of feature is dependent on the choice of sensor and environment. Considering range scan sensors such as laser scanner and RGB-D cameras in partially structured indoor environment, lines, corners and planes are a good choice of features to be extracted from raw range sensor measurements. This research work is based on the feature based maps; therefore a simple observation model will be discussed in the next section.

2.2.1. Observation Model Using Range Sensors

The most common and basic observation model for point feature is range and bearing model. In this model each point feature's range and orientation relative to robot local frame are measured by the feature extractor function along with a feature's unique identifier or signature. The unique identifier helps to solve the correspondence or data association problem. The probabilistic observation model for the point feature uses the geometric laws for range and bearing calculations, which is described by the equation 2.17 as follows

$$\begin{bmatrix} r_t^i \\ \alpha_t^i \\ s_t^i \end{bmatrix} = \begin{bmatrix} \sqrt{(m_{j,x} - x)^2 + (m_{j,y} - y)^2} \\ atan2(m_{j,y} - y, m_{j,x} - x) - \theta \\ s_j \end{bmatrix} + \begin{bmatrix} \mathcal{N}(0, \sigma_r^2) \\ \mathcal{N}(0, \sigma_\alpha^2) \\ \mathcal{N}(0, \sigma_s^2) \end{bmatrix} \quad \text{Eq. 2.17}$$

Where $(r_t^i, \alpha_t^i, s_t^i)^T$ is the expected range, bearing and signature of measurement respectively and (x, y, θ) is the robot pose. Each feature parameters are subjected to an uncertainty specified as Gaussian distribution $\mathcal{N}(0, \sigma^2)$. The errors in each feature's extracted parameters are because of the noise in the sensor measurements. Each feature i is corresponds to a feature j in the map, this is called correspondence. Failure in correspondence leads to failure of the EKF base SLAM algorithm. In case of particle filter multiple hypotheses can be tracked simultaneously, therefore, it is more resilient to data association errors. If a measured feature doesn't correspond to a feature in the map then it is considered a new feature and added to the existing map.

In case of line features first the raw measurements, one complete range scan, from the 2D laser scanner is passed to a function for segmentation. Then the parameters of a line which is defined in hessian normal form is estimated from each segmented cluster of range readings. The line estimation process not only estimates the parameters of the line model but also the uncertainty in the parameters. For detailed discussion refer section 3. Similarly the 3D plane extraction process is described in section 3.3.2.2. The existing features are stored in a KD-tree data structure. Therefore each observed line is searched in the KD-tree to find its corresponding line. For the details of KD-tree data structure please refer section 3.3.3.2.

2.3. Estimation

Estimation techniques such as Extended Kalman Filter and Particle Filters are the main engine of SLAM process. They provide us a framework to keep track of the robot and map states and to update them as new information arrives from sensors. The estimation engines which is used for implementing SLAM process is discussed in the following sections.

2.3.1. Extended Kalman Filter

EKF localization keeps a uni-modal belief $p(x_t|u_t, z_t, m)$ about the localization of a mobile robot and map features. This belief has a Gaussian distribution which can be described by its first and second moment i.e. robot could only be at one place defined by its mean with some uncertainty in its position defined by its variance. The uncertainty in robot position grows as the robot moves in the environment because of noise in robot motion model. In this research work feature based map consist of plane landmarks. The observation model for EKF which is used depends on the type of sensor and is discussed in the next chapter. The robot motion model used for EKF is defined in section 2.1.1.

R. E. Kalman [32] proposed a novel recursive filter technique. His proposed solution can estimate the present, past or future states of a static/dynamic process. The Kalman filter algorithm is a two-step algorithm which requires an appropriate model of the system under investigation and the model of the measurements. The first step estimate the system states according to system model where in the second step the estimated states are refined using the observations. For in-depth knowledge about the Kalman filter and its various derivatives the reader can refer Simon [64]. Extended Kalman filter is very popular, efficient and computational inexpensive for a moderately small non-linear system with not so many states and assumes that the noise present in the system is a uni-model Gaussian. A system can have non-linarites in motion and/or observation model. Because of a non-linear robot motion model an EKF is used. The computational expensive part of the Kalman filter is the calculation of Kalman gains which requires an inverse of the innovation covariance matrix. This operation has a computational cost of $O(n^{2.4})$ where n is the number of states in the system. The challenging part often in the implementation of Kalman filter is the choice of the process noise covariance matrix parameters. Initially the non-diagonal elements, cross covariance's, of the covariance matrix are initialized to zero, that mean there is no correlation between robot pose and features but as the robot start moving and start making observations the covariance matrix becomes dense and both pose and features start becoming correlated. Correlation is very important for convergence.

EKF follows the same cycle of prediction and correction steps. The EKF algorithm steps will be described here in details, for detailed derivation of EKF refer [64]. The prediction or state estimation step is described as follows

$$x_k^- = f(x_{k-1}^+, u_k, 0) \qquad \text{Eq. 2.18}$$

$$P_k^- = F_x \cdot P_{k-1}^- \cdot F_x^T + F_n \cdot Q_k \cdot F_n^T \quad \text{Eq. 2.19}$$

Where the Jacobian matrices F_x and F_n are the partial derivatives of motion model function $f(x_k, u_k, w_k)$ w.r.t. states and state noise respectively as follows:

$$F_x = \frac{\partial}{\partial x} f(x_k, u_k, w_k) \quad \text{Eq. 2.20}$$

$$F_n = \frac{\partial}{\partial w} f(x_k, u_k, w_k) \quad \text{Eq. 2.21}$$

The functions is a parameter of state vector x_k, control vector u_k and noise vector w_k. The important thing to be note is that no noise is added into the state estimation. The uncertainty due to noise is added while propagating the state covariance from the previous step. The uncertainties in the states are modeled by the covariance matrix Q_k and it is propagated by the motion model jacobian F_n with respect to state noise.

The correction step of the EKF is as follows

$$e_k = h(x_k^-) \quad \text{Eq. 2.22}$$

$$E_k = H_x \cdot P_k^- \cdot H_x^T \quad \text{Eq. 2.23}$$

$$z_k = y_k - e_k \quad \text{Eq. 2.24}$$

$$Z_k = E_k + R_k \quad \text{Eq. 2.25}$$

$$K_k = P_k^- \cdot H_x^T \cdot Z_k^{-1} \quad \text{Eq. 2.26}$$

$$x_k^+ = x_k^- + K_k \cdot z_k \quad \text{Eq. 2.27}$$

$$P_k^+ = P_k^- - K_k \cdot H_x \cdot P_k^- \quad \text{Eq. 2.28}$$

H_x is composed of the partial derivatives of measurement model w.r.t. states which is defined as follows

$$H_x = \frac{\partial}{\partial x} h(x_k) \quad \text{Eq. 2.29}$$

Where e_k is the expected states and E_k is covariance of expected states. z_k is the innovation or the amount of new information which is brought into the system and Z_k is the innovation covariance which is the sum of expected states covariance plus the covariance on the new measurements. Eq. 2.26 represents the Kalman gain which is the ratio of expected states gain

and the innovation gain. Eq. 2.27 and Eq. 2.28 represent the correction of the states and their corresponding covariances. During states correction an amount of new information proportional to Kalman gain is added to the existing states. The uncertainties of the states are decreased proportional to the amount of Kalman gain.

2.3.2. Particle Filter

Particle filter is a very powerful tool and used for many applications such as filtering, tracking and navigation where the system is very non-linear and state space is very large. A particle filter is an approximation of Bayes filter which represents the robot pose by an arbitrary multimodal probability distribution using a set of M particles $X_t = \{x_t^1, x_t^2, x_t^3, \cdots, x_t^M\}$. Each robot pose/state/particle x_t^i is associated with an importance weight/factor w_t^i which reflects the probability or likelihood of that particle and is updated after each new observation of the robot. The robot belief X_t which consists of set of particles and their corresponding importance weight is recursively updated from X_{t-1}. First the hypothetical state estimate $x_t^{[i]}$ of a sampled particle is made based on the motion model, previous particle $x_{t-1}^{[i]}$ and the control input u_t. The likelihood of the sampled particle is proportional to the observation probability i.e. $w_t^{[i]} = P\left(z_t \mid x_t^{[i]}\right)$. The observation probability is based on the difference between the current measurement and the predicted measurement according to the stored map of the sampled particle $x_t^{[i]}$. Secondly a resampling step is performed which is very crucial and computationally time consuming. In this step a new particle set is created which reduces the variance of the underlying distribution. Particles with a higher weight will appear more often in the new list than ones with lower likelihoods which means a good hypotheses of robot poses will remain in the non-parametric representation of the state while others disappear. Various resampling techniques which are being employed are Multinomial Resampling, Residual Resampling, Stratified Resampling and Systematic Resampling. For a comparison of resampling strategies the reader is referred to [65]. For the implementation of particle filter one can refer [66]. Resampling could also be dangerous which could lead to deprivation/depletion problem, in which no particle exists in the vicinity of correct state. This problem occurs when numbers of particles are small and it may happen that during resampling good samples are replaced and the final particle distribution loses track of the correct state. The computational effort is proportional to the number of samples. Since the resampling step is crucial, therefore, if the robot stops or if no observations are made then it should be avoided. GMapping [23] and DP-SLAM [67] resample only, if the particle weight

variance is above a certain threshold. The particle weight variance can be calculated as follows:

$$N_{eff} = 1 \Big/ \sum_{i=1}^{M} \left(w_t^{[i]}\right)^2 \qquad \text{Eq. 2.30}$$

The N_{eff} coefficient is maximum for equal weights of the particles and resampling would not reduce the variance of the probability distribution.

Rao-Blackwellised particle filter is a combination of EKF and PF in which the created map of the environment consists of features (edges, corner or planes). In literature this technique is also known as FastSLAM [66] in which the robot pose is estimated by particle filter, which accommodate multiple hypotheses about robot position, and the features are estimated and maintained by EKF. Since each particle represent one hypothesis of a robot pose and contains its own set of map features describing the map. Since the map is estimated by Gaussian therefore, each feature has a mean and variance which are represented by μ and Σ respectively. Therefore, the joint state vector for a particle is defined as follows:

$$x_t^{[i]} = \begin{bmatrix} \begin{bmatrix} x \\ y \\ \theta \end{bmatrix}^{[i]} & \mu_{1,t}^{[i]}, \Sigma_{1,t}^{[i]} & \mu_{2,t}^{[i]}, \Sigma_{2,t}^{[i]} & \dots & \mu_{N,t}^{[i]}, \Sigma_{N,t}^{[i]} \end{bmatrix} \qquad \text{Eq. 2.31}$$

The RB-PF can also be divided into two phases for ease of understanding, in the first phase the particles are sampled using the motion model which is similar to simple PF approach. Then the correspondence among observation and map features is calculated and represented by correspondence variable c_t. The simplest data association strategy is nearest neighbor approach [68] with a defined distance measure. If a new feature is found its mean and variance is calculated and added to the feature map, mean is the transformation of feature measurement from robot local coordinate frame to global coordinate frame. Otherwise, using the standard EKF approach its mean and covariance is propagated and the importance weight is calculated from the innovation covariance of the feature. The resampling process is similar to the PF. The optimized version which is known as FastSLAM 2.0 [22] basically includes the different distribution which takes in account the current measurement into account.

The particle motion model does not implement a drift and all particle position would remain the same while only heading angle is affected by the Gaussian noise. While in Gaussian probabilistic motion model the position is also affected. This behavior is requested to model the real robot kinematics. The real challenge in both cases is to find the appropriate noise

control parameters. For choosing noise control parameters factors such as robot architecture, sensor's characteristics and environment factors should be kept in mind. In case of the particle filter the noise has a direct influence on the variance of particle weights. Other issue in particle filter is too often resampling which can be avoided by sampling based on the variance of the particle filters.

2.4. Localization

The use of absolute positioning system devices/sensors obviates the localization problem. Since the mobile robot pose cannot be determined directly because of the unavailability of sophisticated global positioning sensors or the noise in the observations and uncertainty in robot motion, therefore, robots pose has to be inferred from the noisy measurement measurements. The other problem which makes the localization problem hard is the incompleteness of a single measurement, e.g. consider a SONAR sensor can't decide the object shape even from a single noise free measurement which might be necessary to determine its location with respect to that object. When there is error in the robot executed command and actual motion performed by the robot this uncertainty will affect the future observations of the robot because they are referenced according to robot's local coordinate frame. Mobile robot localization deals with determining the pose of mobile robot given the robot controls (odometry), sensor measurement and map of the environment. Mathematically it is described as $p(x_t|u_t, z_t, m)$. The environment map could be a feature based map or location based (occupancy grid) map. A single observation is usually not enough to localize the robot within the map, due to feature correspondence; therefore, the robot has to integrate the observations over time to determine its pose. The severity of localization problem depends on various factors such as the knowledge of the mobile robot's initial position, state of the environment, robots interaction with the environment and cooperative localization among multiple robots. The localization algorithms here are probabilistic in nature and we will assume the unknown correspondence, i.e. we don't know the true identity of the detected landmark from the robot measurement.

2.4.1. Pose Estimation

Accurate pose estimation is fundamental to mobile robots' navigation, guidance, localization and mapping. To compensate the characteristic deficiencies of individual sensor measurements and to merge measurements from redundant sensors, data fusion can be performed to get the optimal estimate of the mobile robot pose. The research work [69] describes a method for combining data from multiple on-board sensors to determine a mobile

robot pose. An error model for a gyroscope, a dual-axial accelerometer and wheel encoders are derived for estimating the mobile robot's pose. A tri-axial magnetometer measures the magnetic field strength which is used as a criterion for acceptance of electronic compass readings to correct the azimuth of the mobile robot's orientation. The errors in each sensor are estimated mutually rather than independently considering each sensor error model.

Multi-sensor data fusion method reduces deterministic and stochastic errors during mobile robot operation hence provides a best estimates of a robot pose without the use of external positioning system for longer period of time. A robust data fusion algorithm must address the problems such as different sensors sampling rates, asynchronous sensors sampling and reliable availability of estimated data in the presence of sensor failures. Kalman Filter can be applied for the multi-sensor data fusion directly over the state vector or indirectly over the error in state vector. Therefore following Kalman filter data fusion schemes are possible: (1) Direct Pre-Filter, (2) Direct Filter, (3) Indirect Feed Backward Filter, (4) Indirect Feed Forward Filter.

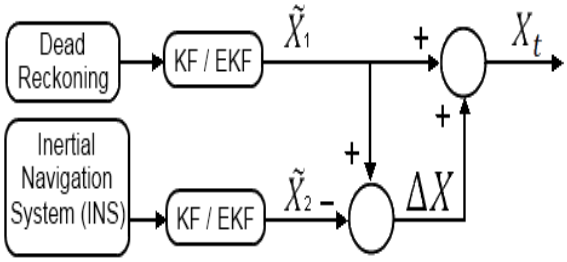

Figure 2.2 Direct Pre-Filtering

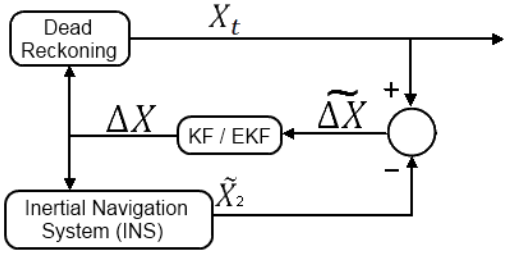

Figure 2.3 Indirect Feed Backward Filtering

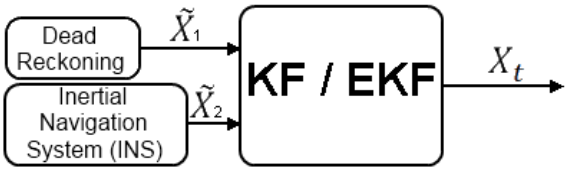

Figure 2.4 Direct Filtering

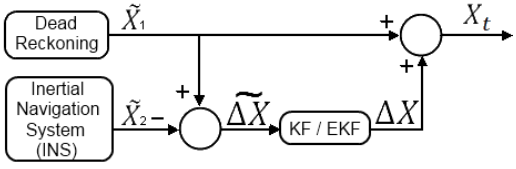

Figure 2.5 Indirect Feed Forward Filtering

In direct pre-filter scheme dead reckoning measurement and inertial navigation system measurements are filtered separately and the errors between these filtered measurements are used to correct measurement from any one method as shown in Figure 2.2. The direct filter formulation uses the states such as position/velocity and orientation calculated from wheel encoders as state variables and the measurements are the inertial and other sensors outputs, Figure 2.4. In direct formulation Kalman filter is inside the navigation loop therefore filter has to suppress the noisy measurements from the INS as well as to estimate of mobile robots position/velocity and orientation. Due to accurate kinematics estimation and being

inside the navigation loop the filter has to be updated faster than the dynamics of the navigation system. This is off-course a computational burden because Kalman filter gain calculations require inverse and square operations on matrix which are very costly in term of computation. Another disadvantage is since encoder and gyroscope/accelerometer models are independent from each other therefore it suppress the errors exclusively according to respective sensor model.

The indirect feedback Kalman filter feeds back the error estimates to one of the mobile robot's dead reckoning or inertial navigation algorithm to mutually compensate the errors as shown in Figure 2.3. The error models for the sensors are described in Appendix A. The filter estimates the systematic errors of encoder (wheel scale factor, wheel distances) and stochastic errors of gyroscope (scale factor, bias) mutually and explicitly. These scale factor errors are fed back to compensate the respective sensor output. Furthermore, the pose errors are feedback into navigation system. In indirect feed-forward formulation the signals measured from sensors are compared before fed into the Kalman Filter and the estimated error is added into one of the dead reckoning system or inertial navigation system as shown in Figure 2.5.

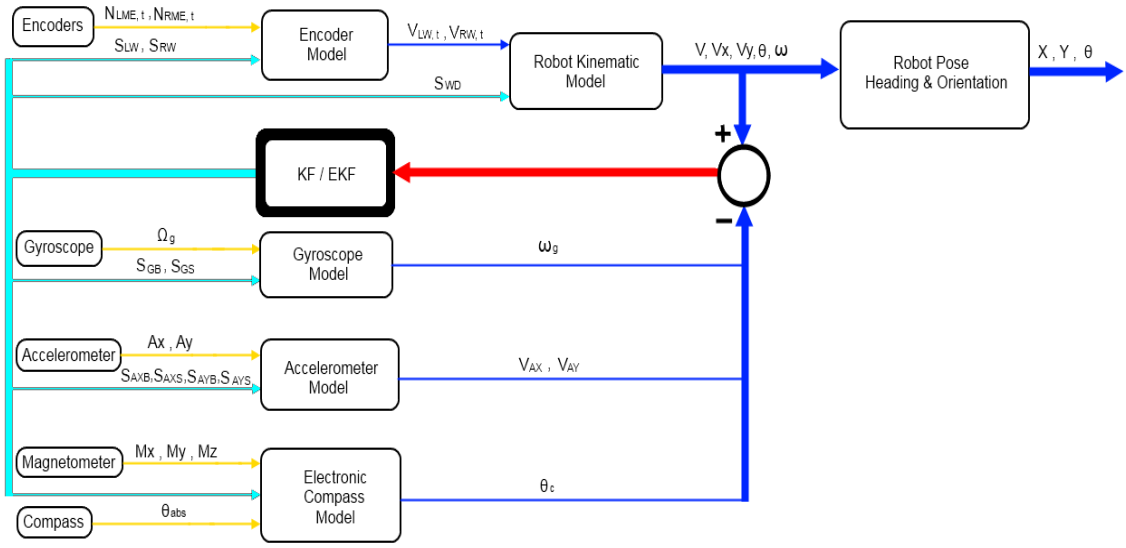

Figure 2.6 Block diagram for multi-sensor data fusion for mobile robot's pose estimation

The proposed multi-sensor data fusion algorithm is elaborated by a block diagram as shown in the Figure 2.6. It is based on the indirect feedback Kalman filter data fusion methodology.

For the evaluation of the proposed methods an experiment is conducted in which TOM3D is commanded to move along a straight line at a speed of 28 cm/sec for 25 sec, for a linear trajectory of 700cm. Figure 2.7 shows the experiment environment in which the robot has

moved along a wall. The straight wall provided a reference for PMD camera distance measurement.

The nearby ferromagnetic materials and electronic sources effect the electronic compass. The implemented algorithm monitors the earth magnetic field strength measured by the magnetometer as a criterion to accept the compass measurements, which are used to correct the robot's orientation. A set of waypoints trajectory is sent to the robot by wireless transceiver. During the execution of the linear trajectory along the wall, the robot acquires the earth magnetic field strength at the start point of the linear trajectory and then uses it as a criterion for acceptance of compass measurements if the field strength varies less than the threshold value calculated from the start point value. Figure 2.8 shows the trajectory of the TOM3D by wheel encoders, fusion algorithm and PMD camera. At the end of experiment a manual measurements of final robot position were taken which reported the final robot position is 4cm (Y-axis, toward wall) and 15cm (X-axis, along corridor) away from the desired end position.

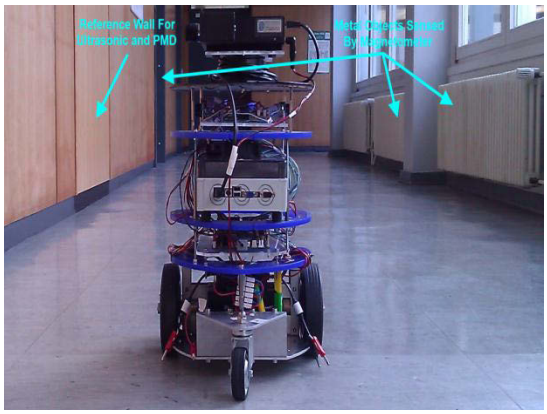

Figure 2.7 Experiment Environment with ferromagnetic interferences and reference wall for measurements

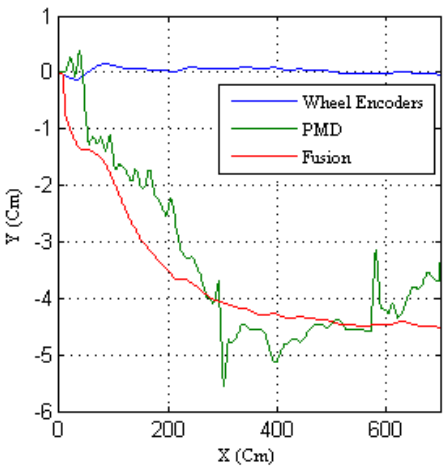

Figure 2.8 Trajectory estimation by wheels encoders , PMD Camera and fusion algorithm

Another research work [70] is performed to estimate the mobile robot's orientation by using a novel combination of stereo vision and gyroscope. The temporal gyroscope drift and bias are the main source of errors. The proposed solution helps to eliminate the gyroscope unbounded drift errors. Since the gyroscope offers a higher bandwidth and availability of angular velocity it is corrected with the stereo vision system which has lower bandwidth and availability but bounded errors. The data fusion between gyroscope and stereo vision system is implemented by using Kalman filtering scheme as shown in Figure 2.10. Gyroscope and vision system samples are asynchronous and their sampling rates are different because of the processing

requirements of stereo vision system. Therefore, to accommodate the delayed measurements from the vision system the approach mentioned in [71] is used.

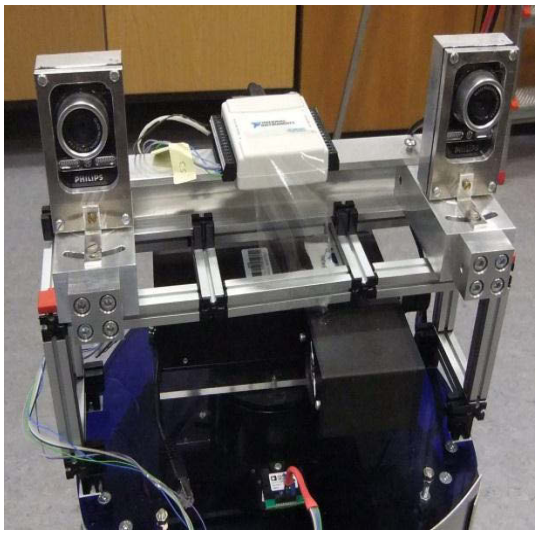

Figure 2.9 Stereo Camera and Gyroscope Setup on TOM3D

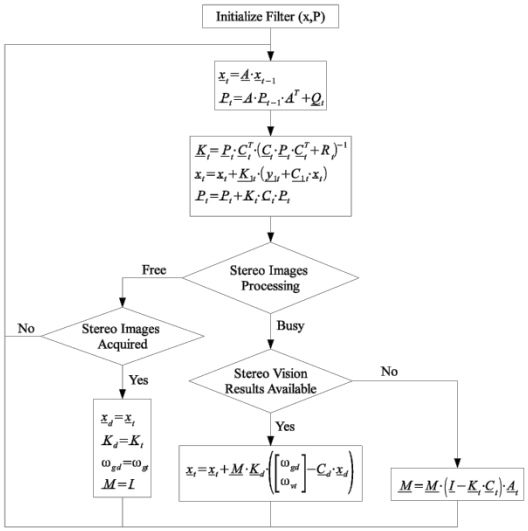

Figure 2.10 Stereo-Gyro Data Fusion Flowchart

An experiment to evaluate the above mentioned fusion approach is conducted on the TOM3D mobile robot which was equipped with stereo camera and gyroscope as shown in Figure 2.9.

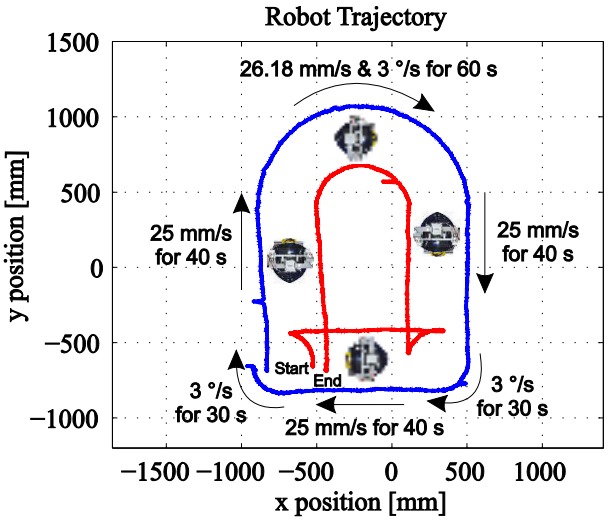

Figure 2.11 Experiment trajectory for Stereo-Gyro data fusion experiment

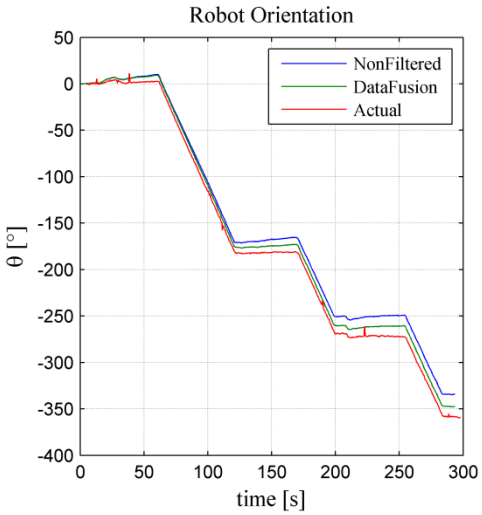

Figure 2.12 Stereo-Gyro data fusion experiment result

Tom3D moved in a trajectory as shown in the Figure 2.11 during the experiment. To measure the absolute position of the robot the 3D measurement system V-Scope [72] is used. A more important result is the integrated angle, which is depicted in Figure 2.12, where all parts of the motion commands can be easily identified. It can be clearly seen that the estimated angle is very accurate compared to the non-filtered integrated angle and very close to the V-Scope

measurements. After the experiment the raw gyroscope value is reporting -334.1°, whereas the fusion process reports -355.6° and the angle calculated from the V-Scope measurement is -358.3°.

2.5. Mapping

For localization of a mobile robot into an environment we need to have a map of the environment. One can create a map by composing set of features present in the environment or by decomposing the spatial environment of the mobile robot in to discrete units. The resulting map is usually called feature based map and grid based map respectively. Feature based maps consists of features such as corners, edges, planes and others. There are other types of maps but for SLAM implementation point of view they will not be discussed here, the interested reader may refer [66].

2.5.1. Grid Based Mapping

An occupancy grid map discretized the whole spatial environment into small cells and uses raw data observations directly to estimate the robot trajectory. Each cell value can represent a Boolean value or a likelihood of cell being occupied. The accuracy of objects shape and position in the environment is a function of the sensor modality which is being used to sense the environment and the resolution of the cell which discretize the environment. There is a compromise between the accuracy of representing the objects shape and the grid cell size which affects the memory requirements.

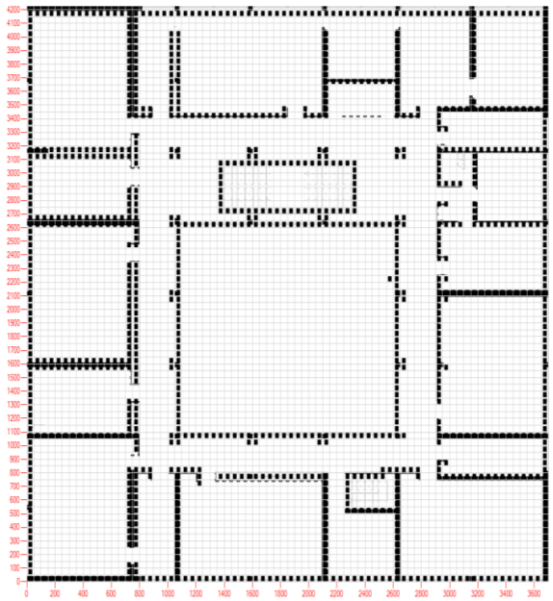

Figure 2.13 Manual occupancy grid map creation

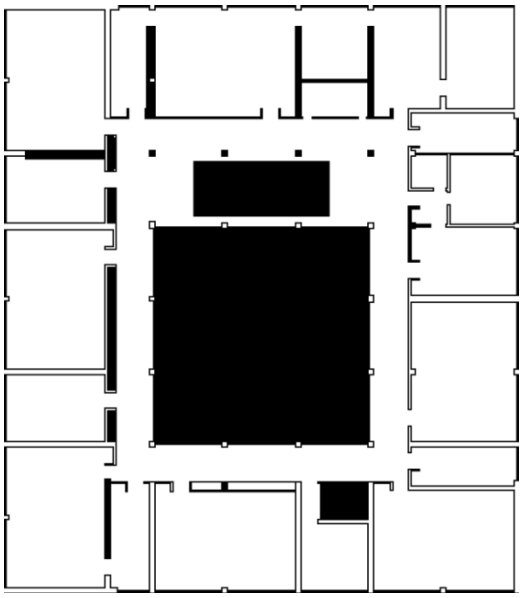

Figure 2.14 Automatic occupancy grid map creation

OGM is robust against outliers and very desirable for navigation and path planning. OGM for large environment, especially 3D, require a huge amount of memory. These maps are also limited to geometry information obtained from range sensors. Some efficient details of implementing OGM can be found in [23]. Grid maps are classical way of representing environment based on Cartesian location. Grid based map representation are costly in term of memory requirement but good for path planning and autonomous map building.

Figure 2.13 and Figure 2.14 shows the creation of occupancy grid map manually and automatically respectively when a plan image of the environment is provided. In case of manual occupancy grid map generation process, a grid of desired size is overlaid over the plan image and then using the mouse left, right and middle button occupancy grid value are assigned either as occupied, free or unknown respectively to each grid cell. The final hand drawn occupancy grid map information along with some relevant information as header is stored in a XML file format which is described as follows

<MAPINFO>
<MAPORIGIN>0,0</MAPORIGIN>
<MAPSIZE>3700,4223</MAPSIZE>
<GRIDSIZE>50,50</GRIDSIZE>
<GRIDDATA>1,1,1…0</GRIDDATA>
</MAPINFO>

Table 2.1 Occupancy Grid Map XML Output file's format

In the above example the picture pixels are calibrated to cm and the grid cell size is chosen as 50cm x 50cm. The resultant XML file contains the grid cell data, 6250 values each of which is corresponding to the grid state. 0 means empty, 1 means occupied and -1 means unknown. One can also edit the already created grid map generated by automatic OGM generator application for fine adjustment of the artifacts. The application to generate the OGM automatically works as follows. It requires four arguments as input in addition to map file name. The first two arguments specify the grid cell width and height and the other two specify the thresholds to determine a cell as occupied, unoccupied and unknown. These two thresholds represents the percentage of block to be considered as unoccupied and unknowns. In the first step of automatic OGM generation the plan image is converted into a black and

white image. Then in the second step the plan image is processed block by block where each block size is specified as grid cell size. If the percentage of the non-zero elements are greater than or equal to unoccupied threshold then the cell is considered as unoccupied else if the percentage of non-zero elements are between unoccupied and unknown then they are considered as unknown otherwise if it is less than unknown threshold then the block is assumed as free. At the end the block information is stored as occupancy grid map in the same XML grid map file format as described above in Table 2.1.

2.5.2. Feature Based Mapping

Feature based map is an alternative approach to represent the environment in which only certain characteristics of the environment are used to model the map. FBM can handle arbitrary features such as planes, corners, edges, SIFT, SURF, barcodes etc. FBMs are very efficient regarding the data association, map update and memory requirements especially for large environments. FBM are not as robust to senor noise and outliers as the OGM because the model estimation uncertainty in the feature extraction process. This could lead to wrong data association which is very crucial to Kalman filter based SLAM implementation. The choice between FBM and OGM depends also on the sensors e.g. SONAR and 2D Laser scanner favors the OGM where vision based sensor favors FBM. Figure 2.15 shows the example map of environment as a plane image where the Figure 2.16 shows the FBM composed by extracted lines from the map image.

If one has the map of the environment in the form of a planner image then he can create a line feature based map from the image. Similarly if one has the 3D point cloud he can create the plane feature based map from the image. The following application is used to extract the 2D lines defined in polar coordinate. The coordinate frame is assumed at the center of image. The application is used to create a feature based map for mobile robot localization. For the localization the robot uses its laser range scanner to estimate the lines from the raw measurements and then find a correspondence of the line with the existing line features.

To extract the lines from an input intensity image, first a Canny [73] edged detection operation is applied over the input image. As a preprocessing step before implementing canny edge detection algorithm the input image is converted to a gray-scale image to reduce the computational requirements and simplification. The gray-scale image is in fact a matrix with rows and columns equal to image width and height in pixels respectively. The result of canny edge detection algorithm is a binary image which contains only the non-zero pixels value

corresponding to edges i.e. sudden changes in the image contrast. The canny algorithm consists of the following four steps:

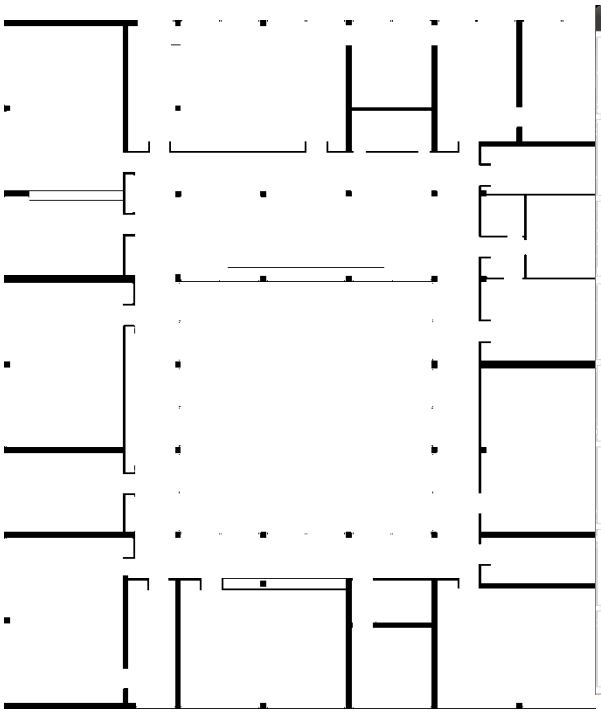

Figure 2.15 Original map image of the environment

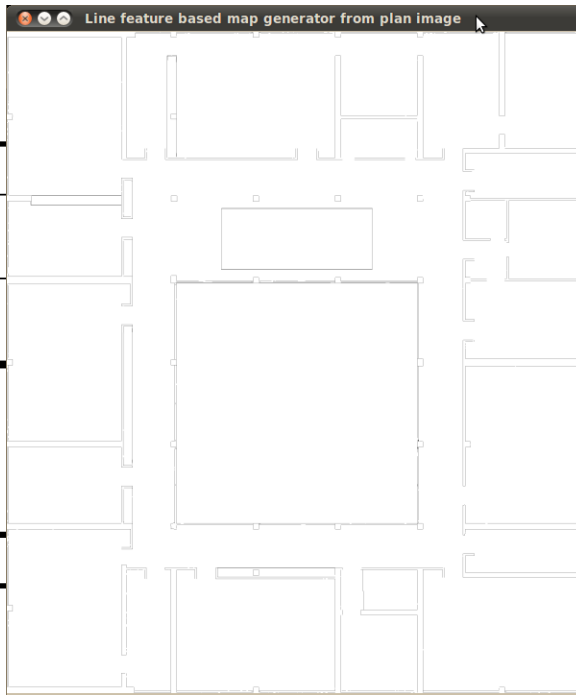

Figure 2.16 Extracted line features from the map image

Step 1: Gaussian filter is applied to remove the noise. The filter consists of a kernel or mask, a matrix, with a certain standard deviation. The resulting image is a blurred image which is a result of convolving or sliding the kernel across the gray-scale image from left to right starting from top to bottom.

Step 2: Since the edges are the gradient in the intensity of the image. The magnitude and direction of the gradient for each pixel in the smoothed image is determined using Sobel [74] technique. To get the edge intensity and direction, Sobel technique determines components of the gradient along the x and y axis by convolving a 3x3 X-kernel and Y-kernel respectively with the intensity image. The gradient magnitude is determined by using Euclidean distance measure. Manhattan distance measure can be used to reduce computational complexity. The gradient direction is calculated by using arctangent function.

Step 3: The edges which are found in the previous step are thick; therefore, they must be narrowed. To thin down the thickness of edges the following algorithm is applied. Since there

are eight neighboring pixels of any pixels except the border pixels, therefore the gradient orientation is divided into eight regions of 45 each. The decision to keep the pixel gradient value is based on the following condition. If the gradient value of the current pixel is greater than the gradient values of the pixel in gradient direction and opposite of gradient direction then its value is kept otherwise set to zero.

Step 4: The edges found in the image may be the true edges or it may be formed because of the noise or rough surface. Usually fake edges are short, disconnected and irregular. Distinction between true and fake edges can be made using thresholding. Using a single threshold short discontinuous edges are formed because of the noise in the discontinuous region. The canny edge detection algorithm discerns between true and fake edges using two thresholds T1 and T2. If the gradient intensity is above T1 it is considered as strong edge. Strong edges can be treated as true edge because it is unlikely to be caused by noise. If the magnitude of the gradient is between T1 and T2 it is considered as weak edge otherwise discarded. The weak edges may be true edges or because of color variation or noise. The weak edge is considered as the true edge only if it is connected with a strong edge otherwise discarded. Because if a weak an edge is connected with a true edge, it is likely to be a true edge but because of the noise it is suppressed and considered as weak edge. Where the disconnected weak edges are likely due to color variation or noise and therefore they are independent of the strong edges thus discarded. The Tracking of weak edges adjency with strong edges can be checked using Grass-fire, flood-fill, algorithm.

After the edge detection probabilistic Hough transformation is applied over the binary image. Each non zero pixel in the image space is used for voting phase in Hough space. The voting phase is also known as Hough transformation. The Hough space or accumulator is the discretization of line's parameters space, i.e. a 2D space where each axis correspond to a parameters of the line equation. Since one point can corresponds to many lines, therefore, one point in image space corresponds to many points in the Hough space. Similarly, one line can have correspondence with many points; therefore, each point in Hough space corresponds to many points into the image space. To reduce the computation requirements in standard Hough transformation, probabilistic Hough transformation uses two random non zero points to form a line which vote for a point in Hough space. After a certain number of iterations the Hough space points above a certain thresholds are treated as lines. The corresponding endpoints of the line are then extracted from the image space. The extracted line segments parameters ρ and θ along with the line segment's end points are stored in a XML file format

which later can be retrieved by the localization module during the loading of the map at startup.

2.5.2.1 Plane Extraction and Map Building Using a Kinect Equipped Mobile Robot

3D Map building is fundamental to the autonomous navigation of the mobile robots in real world environment. Furthermore it could help mobile robots to reason about environment. State of the art mobile robots use 3D range scanning devices such as laser scanner, time of flight cameras, stereo cameras and RGB-D cameras to sense the spatial environment and construct the map from acquired point clouds. Traditional computer vision solutions to construct 3D maps from multi-view videos or related images are computational resource demanding and time consuming. Geometric features such as lines and planes are prevalent into the manmade environments such as offices and factory floors. Mobile robots can use such geometric features to construct a map for collision free autonomous navigation and localization in such environments.

This research work uses the plane detection algorithms to detect the planes from the raw Kinect data and registers them using octree data structure. During this experiment a geometric feature (3D plane) based map is created using a differential drive mobile robot equipped with a Microsoft Kinect camera in an indoor office environment as shown in Figure 2.17. To create the model of the environment several scans have to be fused. The fusing process is easy if the position of the scanner is known otherwise scan registrations have to be performed to estimate the pose of the scanner. This experiment does not concentrate on the scan registration process. It is also assumed that the mobile robot has been already localized thus an accurate mobile robot pose is available for mapping.

Kinect is an inexpensive RGB-D camera which provides a color image stream and a depth image stream in an indoor environment in real time which can be very useful for dense 3D color mapping in cluttered indoor environments. Despite of the impressive acquisition rate the raw data is unsuitable for navigation and real-time 3D mapping because of the enormous amount of the data to be processed. Therefore, geometric features such as planes are extracted from the raw 3D point clouds.

Since Kinect sensor acquires enormous amounts of data, 9.2 million 3D points in one sec, it is challenging to process the data in real time because of the limited amount of computation resources available on mobile robots, furthermore, raw 3D point clouds from Kinect sensor are

not directly useable. Some processing is required to reduce this amount of data to extract features information present in the raw 3D point cloud. The features could be point features, line features, color segmentations and shape detections. Extracting multiple geometric features from the range data is computationally demanding and directly related to the number of parameters required to represent the geometric model to be found in the raw point clouds. In this geometric mapping approach 3D planes as geometric features are used because a plethora of 3D planes are available in structured environments. Two algorithms namely RANSAC and Hough transformation are tested to extract the 3D planes from the raw point cloud so that we can compare the performance of real-time geometric map building from the Kinect equipped ground mobile robot.

From the resulted 3D generated map by the RANSAC, Figure 2.19, and the Hough Transform, Figure 2.18, both produce a visually comparable result. The difference between the two resulted maps is in the top left corner, where the RANSAC fails to find the correct planes, because the corresponding point clouds contain a high number of invalid points. In term of the execution time RANSAC took on average 50 mSec to extract the first plane, whereas the Hough Transform took an average of 170 mSec to extract a plane. Since no loop closure was used the difference between start and end point in both maps was expected.

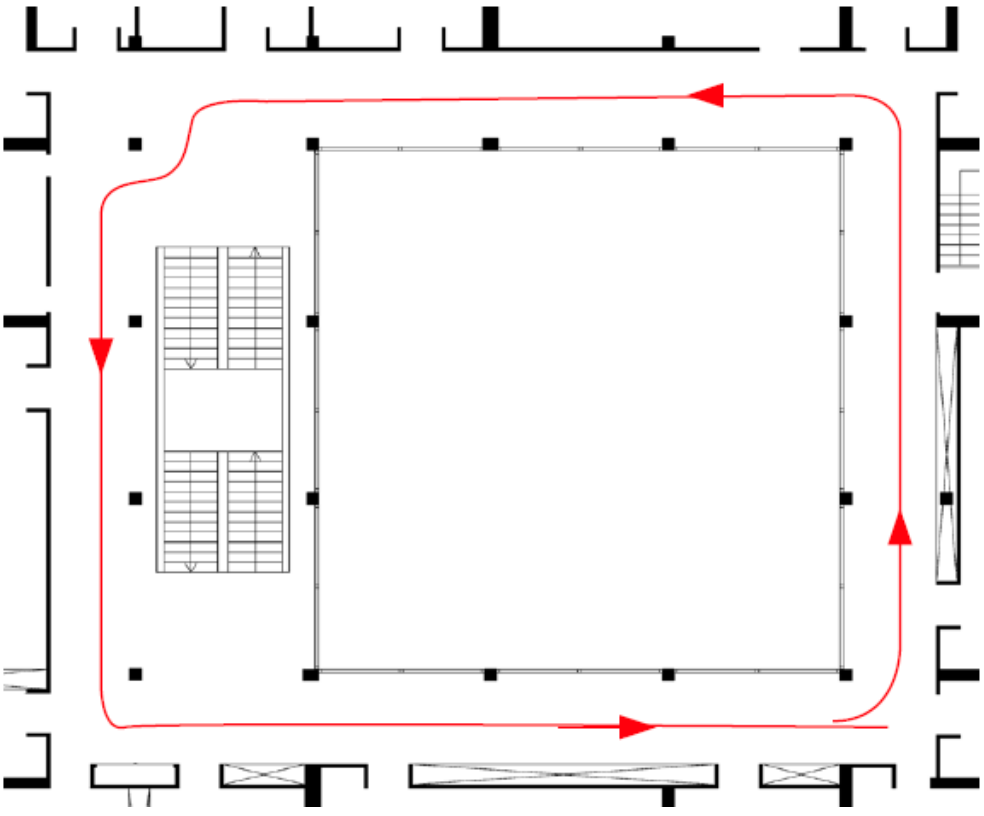

Figure 2.17 Robot trajectory in the mapped environment

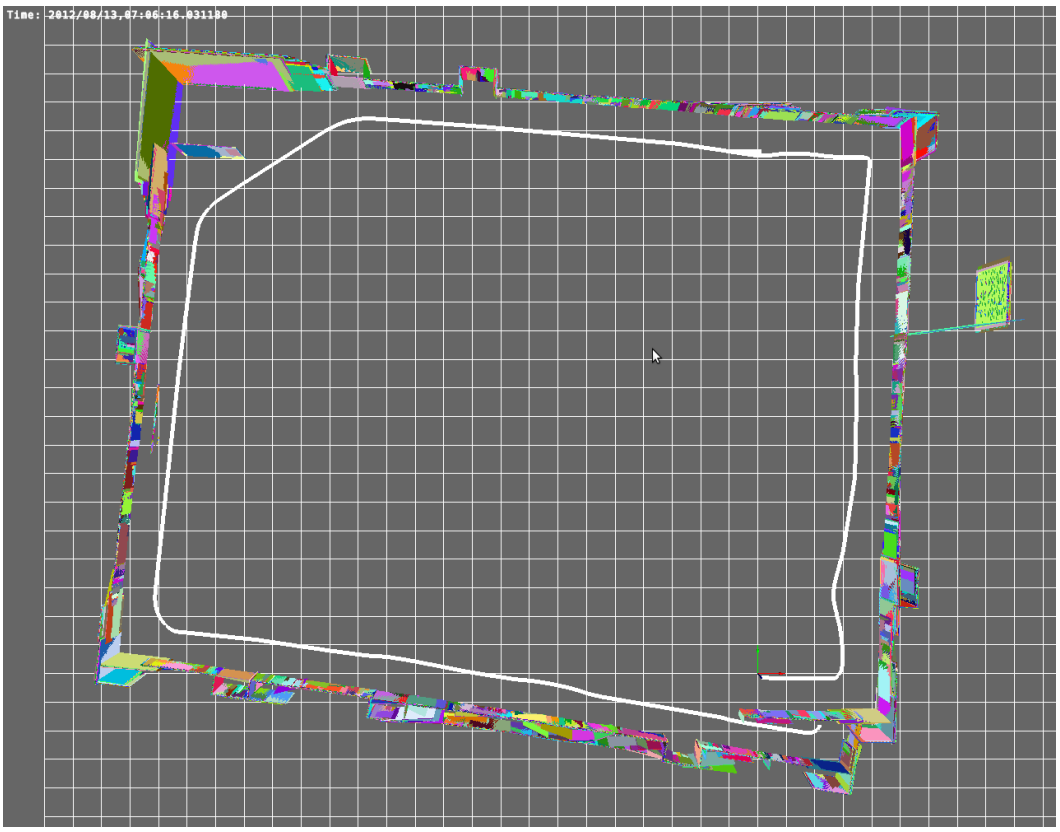

Figure 2.18 Geometric map created using Hough transformation

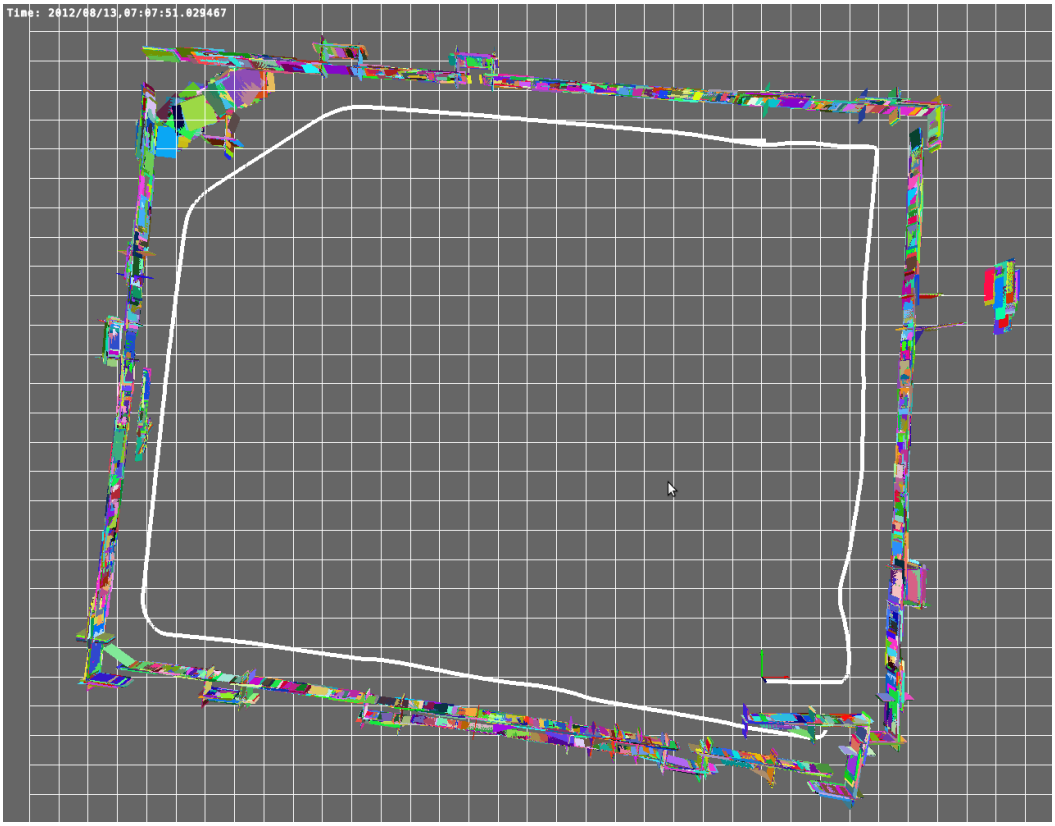

Figure 2.19 Geometric map created using RANSAC algorithm

2.6. Navigation

Navigation is not a part of SLAM process but it is an essential task to navigate a mobile robot in the environment and avoiding obstacles. A* is a path finding algorithm between two points on an OGM. It can work on rectangular, triangular, hexagonal or any other type of grid map. It is a deterministic algorithm which will find a path if one exists. Peter Hart, Nils Nilsson and Bertram Raphael of Stanford Research Institute first described the algorithm [75] in 1968 which is an extension of Edsger Dijkstra's algorithm [76] in 1959. For the further discussion it will be assumed that a rectangular grid map is available to the robot, given as input in case of localization scenario or build up by the robot in SLAM scenario, and each unoccupied grid has the same cost value. Furthermore, the starting grid cell position, current grid cell position and end grid cell position on the grid map are denoted by s, p and e respectively. A* combines the best of greedy best-first search algorithm and Dijkstra's algorithm; furthermore one can tune algorithm speed versus shortest path. Greedy best-first algorithm takes into account the distance from current position to the target without considering the already travelled path distance, therefore, it reaches to the target as quickly as possible by using a heuristic function to guide its way toward the goal. But there is a caveat, the quickest path might be longer if there comes obstacles in the way and the algorithm has to re-plan the path. Therefore, the problem lies in looking only for shortest distance toward the goal and neglecting the already traversed distance from the start. Dijkstra's algorithm takes into account only the distance travelled from start position to the current position, therefore, it try to reach to the target in a shortest path without considering the target direction which results it into longer time to find the shortest path.

A* algorithm evaluates at current grid cell location (node) a heuristic function which consists of two parts as follows:

$$f(p) = g(p) + h(p) \qquad \text{Eq. 2.32}$$

The first part $g(p)$ is a function which returns the length of the already traversed path from starting position to the current position p. The second part $h(p)$returns the estimate of an acceptable distance of the remaining path from current position to the target position. By acceptable distance means a distance which is close to optimal distance from current position to the destination. And this is the estimated one because we don't know the path we will take to reach the end point. After evaluation of the above heuristic function for the current point p's neighbors the algorithm follows a path from point $p's$ neighbor with least heuristic function value. A* algorithm speed VS shortest path performance is depended on the chosen

heuristic functions. If $h(p)$ is zero then A* algorithm act like Dijkstra's algorithm which results into the shortest path. On the other extreme if $h(p)$ is very high compared to $g(p)$ than it will try to find the path as quickly as possible without considering if it's the shortest, therefore act like Greedy Best First algorithm.

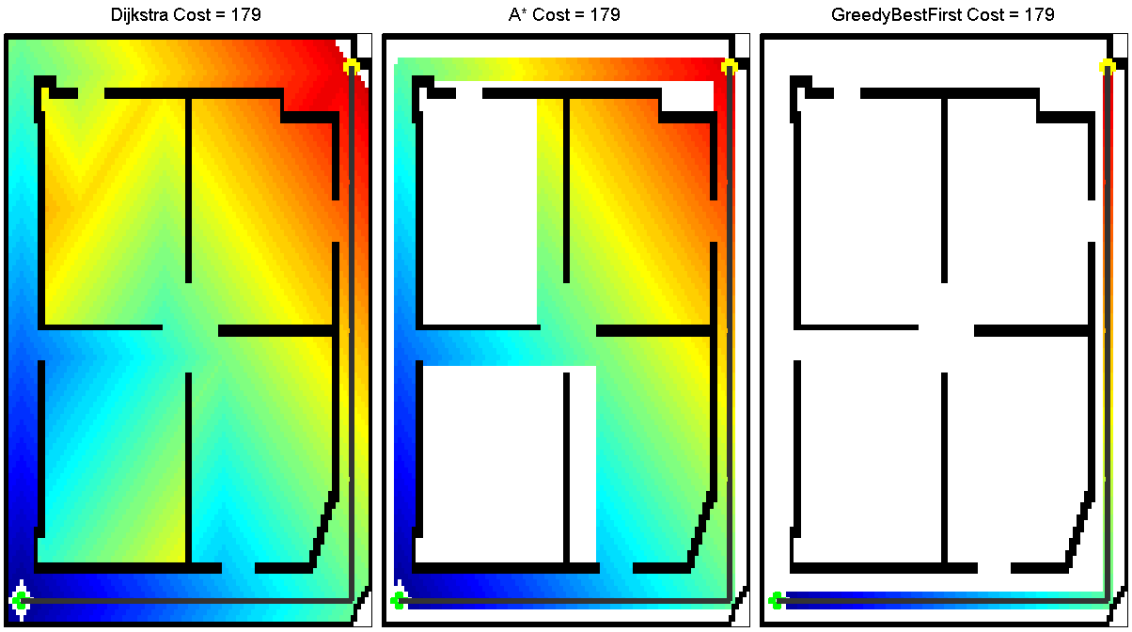

Figure 2.20 Visual comparison of three path finding algorithms in scenerio-1

If $h(p)$ result's less than the optimal path length from point p to the destination then the resultant path will be the shortest but other frontiers are also explored and thus make the algorithm runs slower. If $h(p)$ result is equal to the optimal path length from point p to the destination then the result will be the shortest path without exploring other frontiers. Basically what happens is that $g(p)$ matches with $h(p)$ so that $f(p)$ doesn't change and the point on left and right of p are of higher distance value, therefore don't explore other frontiers. If $h(p)$ result is greater than the optimal path length from point p to the destination than the resultant path may not be the shortest path but the one found quickly without exploring more frontiers.

Use a distance heuristic function that matches the robot movement. On a square grid where robot movements are limited to front, back, left and right use Manhattan distance (L_1-Norm).

$$h(p) = |p.x - e.x| + |p.y - e.y| \qquad \text{Eq. 2.33}$$

If the robot can also move diagonal in addition to basic four movements then use the Diagonal or Chebyshev distance (L_∞-Norm).

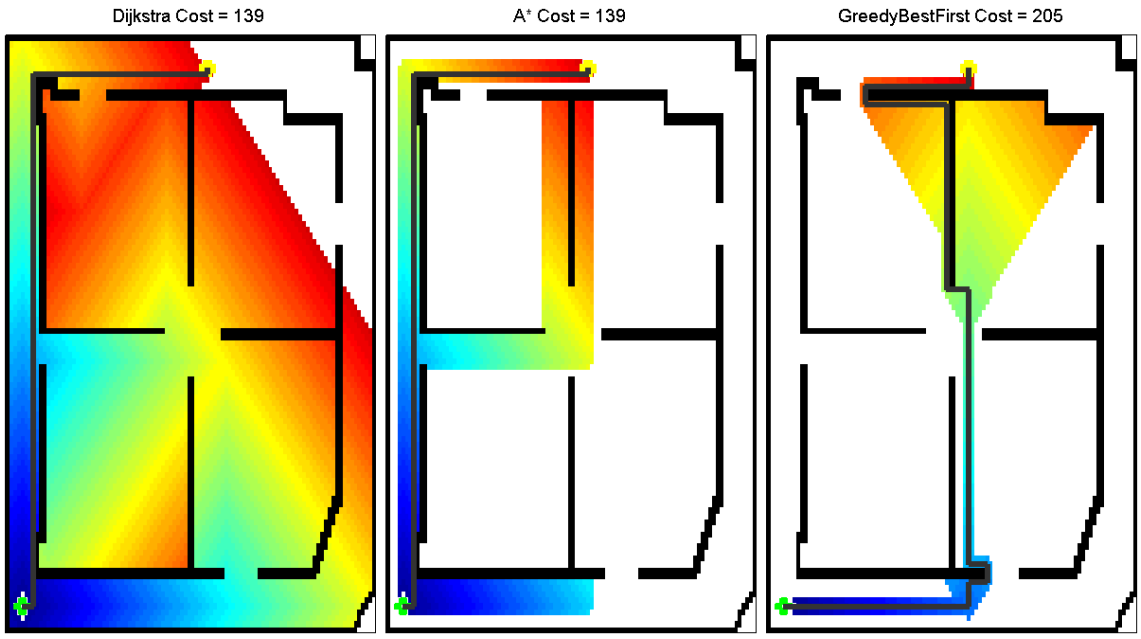

Figure 2.21 Visual comparison of three path finding algorithms in scenerio-2

$$h(p) = \max(|p.x - e.x|, |p.y - e.y|) \quad \text{Eq. 2.34}$$

If the robot can maneuvers in any direction then use the Euclidean distance (L_2-Norm). One caveat to the Euclidean distance heuristic is that it takes longer to run the A* algorithm to find the shortest path because $h(p)$ will be smaller than $g(p)$. The Euclidean distance calculated by $h(p)$ is always smaller than the Manhattan or Chebyshev distance calculated by $g(p)$.

$$h(p) = \sqrt{(p.x - e.x)^2 - (p.y - e.y)^2} \quad \text{Eq. 2.35}$$

If there are multiple end locations of same priority then A* algorithm can reach any one of the location by the following modification. Instead of evaluating the $h(e_1)$, evaluate $min(h(e_1), \dots, h(e_n))$ while rest of the algorithm remains the same.

The performance of the A* algorithm also depends on one of the important detail i.e. in case of the different frontiers of the same f value which one to choose, there are different strategies which produces different results. One approach is to choose the point with lowest h value. Another approach is to calculate the magnitude of the cross product between vectors formed from start point to end point and from the frontier point to the end point and selecting the frontier with smaller resultant area.

Figure 2.20 and Figure 2.21 show the visual comparison of the three above mentioned navigation algorithm with same starting position while different end position. The colored gradient visually depicts the cost of reaching at that point. From Figure 2.20 it seems that

Greedy Best First algorithm is the best but one can see from Figure 2.21 that it traps within the obstacles and even the found path which is shown by thick bold line is not the shortest. Where the Dijkstra's algorithm always find the shortest path if one exists but it will take longer to execute because it searches the path in all direction from the starting point.

2.6.1. Implementation

The A* algorithm uses priority list for its implementation. A priority list is an data structure where each element stored has a priority value attached to it and when a data value is asked from the priority list then the data value with the highest priority is returned. Each grid cell is called a node in A* implementation. A node consists of following variables; grid cell location, grid cell state (Occupied, Unoccupied), a pointer to parent node and variables for storing f, g and h value. There are two lists maintained by the algorithm, let's call them FRONTIERS and VISITED. A FRONTIER is a priority list which contains the nodes that are the valid candidates for examining. The f value is used as the priority value of the FRONTIERS priority list. When the FRONTIERS list is queried then the node with minimum f value shall be returned. A VISITED list contains nodes which have been already examined; they are the interior of the frontiers cells.

In the beginning both lists are empty; to start the algorithm the starting node is added to the FRONTIERS list. Then we start our search loop. A node from the FRONTIERS list is queried which is called current node. If the current node matches to the destination node then we add the current node to our resultant path list and backtrack all the nodes using the parent field of the nodes in the VISITED list until we reach to the starting node. Otherwise the current node is added to the VISITED list. The neighboring nodes, 8 in 2D or 26 in 3D, to the current node are examined; the nodes which are un-occupied and already not in the FRONTIERS or VISITED list, there h, g and f value are calculated and their parents field is set as current node and then added to the FRONTIERS list. The h value is calculated using the chosen heuristic value the g value is the sum of current nodes g value plus moving cost from current node to the neighboring node. Then re-query the updated FRONTIERS list for the next current node. This process is repeated until there are no more nodes in the frontiers, in that case no path exists, or the destination node matches the current node which means the path is found.

2.7. Summary

In this chapter the background concepts related to mobile robot SLAM and navigation are discussed. First of all the probabilistic motion model for differential drive robots and range sensor models are discussed.

Then a Kalman filter and particle filter based probabilistic estimation techniques are introduced which are the core part of SLAM solution.

Afterwards the data fusion strategies are discussed which are used for the accurate mobile robot pose estimation.

Both the grid based map and feature based map construction process are discussed which directly affect the SLAM algorithm implementation.

And finally A* navigation algorithm is discussed which is very important for the autonomous mobile robot navigation.

Chapter 3.

Simultaneous Localization and Mapping

3.1. SLAM

The knowledge of the environment and mobile robot's pose is essential for autonomous navigation, obstacle avoidance, cooperation and path planning. The end product of SLAM can be seen as an accurate map of an unknown environment built by the robot(s). Accurate means while building the map the robot localizes itself using the same map, therefore, it results into an accurate map. Maps could be an occupancy grid map or feature based maps as described in section 2.5. Various state of the art SLAM methods were mentioned in the related work section 1.4. Despite past two decades efforts to find robust and general purpose solution to SLAM, the problem is not fully solved especially in case of large outdoor environment and multi map fusion.

In general the probabilistic SLAM solution consists of two parts, prediction step and the update step. In the prediction step the robot states are updated using robot motion model and in the update step the estimated states are corrected using the observation or measurement made by the robot using its sensors. Observations can be the observations of new features or re-observations of the old features. In the case of re-observation of the existing features, this information is used to update the previous belief of the robot about its pose and existing features.

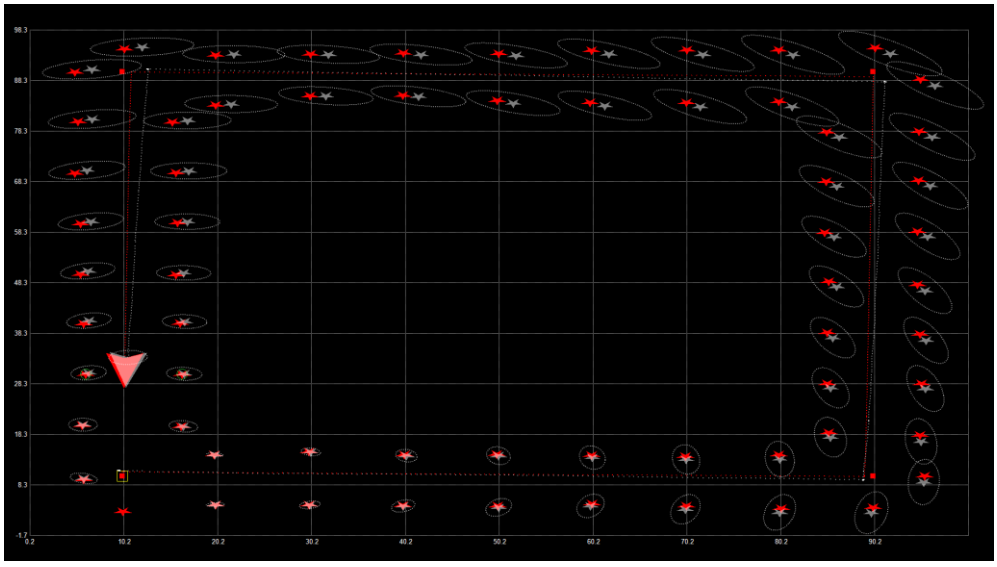

Figure 3.1 Simulation of range-bearing based EKF SLAM

Figure 3.1 displays the result of an EKF based Range-Bearing SLAM algorithm for known data association. The robot's pose uncertainty, shown by ellipse, increases as it moves as shown in the above figure. In the simulation shown above, fig. 3.1, the robot moves inside a cloister. The red stars represent the columns of the cloister which can be detected by a factitious Range-Bearing sensor system mounted on the robot. The factitious sensor can provide the range and bearing of the column with respect to the robot pose with some uncertainty in the measured range and bearing. These columns can be considered as landmarks or point features. The factitious robot sensor can also determine the unique ID printed on the column for resolving the problem of data association or ambiguity among the same columns. The small red squares represent the waypoints which the robot has to traverse. The red dotted line represents the nominal trajectory of the robot while the gray dotted line represents the estimated trajectory of the robot. The grey dotted ellipse represents the uncertainty in the position. Two important results can be seen. First the gray stars represent the map generated by the robot and the second is the robot pose uncertainty which never grows unbounded because it uses the map to localize itself.

SLAM algorithms can be roughly classified by their estimation techniques and their map representation. This chapter discusses the implementation of an EKF based SLAM algorithm. The strength and weaknesses of the map representation have been discussed in section 2.5. EKF is used as estimation engine for robot pose and features position estimation. The EKF maintains and updates the mean and covariance of the states at each time step. The state vector consist of robot pose x_r and set of features parameters m which are considered as map

$$x = \begin{bmatrix} x_r \\ m \end{bmatrix} \quad \text{Eq. 3.1}$$

Where the covariance matrix is as follows

$$P = \begin{bmatrix} P_{rr} & P_{rm} \\ P_{mr} & P_{mm} \end{bmatrix} \quad \text{Eq. 3.2}$$

The EKF-SLAM consists of two phases' prediction and correction.

3.2. Prediction

The prediction phase estimates the robot pose and the map after the robot has executed a motion command or when motion data is available from odometry. The map or set of landmarks are assumed to be constant or time invariant, therefore

$$x_{t+1} = \begin{bmatrix} f(x_r, u_t, w_t) \\ m \end{bmatrix} \quad \text{Eq. 3.3}$$

The kinematic motion model $f(x_r, u_t, w_t)$ of the differential drive robot to estimate the pose states is as follows:

$$f(x_r, u_t, w_t) = \begin{bmatrix} x_t + \Delta s \cdot \cos\left(\theta_t + \frac{\Delta\theta}{2}\right) + \mathcal{N}(0, \sigma_x^2) \\ y_t + \Delta s \cdot \sin\left(\theta_t + \frac{\Delta\theta}{2}\right) + \mathcal{N}(0, \sigma_y^2) \\ \theta_t + \Delta\theta + \mathcal{N}(0, \sigma_\theta^2) \end{bmatrix} \quad \text{Eq. 3.4}$$

Where $x_r = (x_t,\ y_t,\ \theta_t)^T$ is the current robot pose, $u_t = (\Delta s,\ \Delta\theta)^T$ is the odometry inputs which consist of linear and angular distance measured by the robot wheel encoders. Here it is assumed that the robot pose error is due to the non-systematic errors because of robot wheel slip and interaction of the wheel with the ground. These errors $w_t = \left(\mathcal{N}(0, \sigma_x^2),\ \mathcal{N}(0, \sigma_y^2),\ \mathcal{N}(0, \sigma_\theta^2)\right)^T$ are assumed to have a normal or Gaussian distribution and they are un-correlated. The systematic errors such as due to difference of left and right wheel diameters and difference of wheel base length from the nominal value are also assumed to be corrected by the odometry calibration procedure such as UMBmark [60].

After estimating the state vector as a result of robot motion, the uncertainty of the robot and map features states are calculated as follows:

$$\begin{bmatrix} P_{rr,k} & P_{rm,k} \\ P_{mr,k} & P_{mm,k} \end{bmatrix} = \begin{bmatrix} F_r \cdot P_{rr,k-1} \cdot F_r^T + F_n \cdot Q \cdot F_n^T & F_r \cdot P_{rm,k-1} \\ P_{mr,k-1} \cdot F_r & P_{mm,k-1} \end{bmatrix} \quad \text{Eq. 3.5}$$

Where $P_{rr,k}, P_{mm,k}$ are the new robot and map uncertainties and $P_{rm,k}$ is the cross covariance between robot and map features. $P_{rr,k-1}, P_{mm,k-1}, P_{mr,k-1}$ are the old robot uncertainties. It can be seen from above equation that the uncertainty of the robot pose $P_{rr,k}$ is propogated from the previous robot state uncertainty in addition to the uncertainty due to the noise. The uncertainty of the map features $P_{mm,k}$ remain the same but the covariance between the robot and map feature changes. Where F_r and F_n are the Jacobians of the robot motion model with respect the pose vector and noise vector. These Jacobians have the following values

$$F_r = \frac{\partial}{\partial x_r} f(x_r, u_t, w_t) = \begin{bmatrix} 1 & 0 & -\Delta s \cdot \sin\left(\theta_t + \frac{\Delta\theta}{2}\right) \\ 0 & 1 & \Delta s \cdot \cos\left(\theta_t + \frac{\Delta\theta}{2}\right) \\ 0 & 0 & 1 \end{bmatrix} \quad \text{Eq. 3.6}$$

$$F_n = \frac{\partial}{\partial w_t} f(x_r, u_t, w_t) = \begin{bmatrix} 1 & 0 & 0 \\ 0 & 1 & 0 \\ 0 & 0 & 1 \end{bmatrix} \quad \text{Eq. 3.7}$$

In Eq. 3.5 Q is the covariance matrix of the non-systematic errors which is defined as follows:

$$Q = \begin{bmatrix} \sigma_x^2 & 0 & 0 \\ 0 & \sigma_y^2 & 0 \\ 0 & 0 & \sigma_\theta^2 \end{bmatrix} \quad \text{Eq. 3.8}$$

3.3. Correction

The correction phase of the EKF based SLAM algorithm is very complex. It consists of clustering, feature extraction, expected feature prediction, map update and mapping new features. Each of these steps is described in details as follows.

3.3.1. Clustering or Segmentation

Segmentation is usually the first step after range sensor data acquisition, sometime it is followed by filtering. The real depth data from range measurement sensors contains more than one geometric model or features present in the real environment, therefore, as a preprocessing step to feature extraction clustering or segmentation is performed. Segmentation groups the related set of data so that the geometric model of the feature is estimated from the range data segment.

The SICK PLS-101 laser-scanner is mounted on one of the robot, TOM3D. Because of the 2D range scan measurements provided by the SICK laser scanner line features are selected for performing SLAM. The laser-scanner has a CCW rotating mirror at 25 rpm (40msec/scan). It uses time of flight principle by the help of a 3 GHz counter [77] which results into range measurement accuracy of 5cm. The angular resolution of the laser scanner is 0.5° and the measurement range is from 7cm to 50m. During first half of 40msec interval the range measurement in a semicircle is done while during the next 20msec the mirror is rotated back. From the maximum linear (V) and angular (W) velocity the distance and angle traversed by the robot can be calculated. For our robots the V=0.5m/sec and W=10°/sec results into ΔS=1cm and $\Delta\theta$=0.2° which is negligible compared to measurement error therefore, we can neglect the measurement delay during the robot motion.

A line segment is defined as when the difference between the two consecutive laser beams exceeds a certain threshold. In general the segmentation based techniques can be based on distance threshold method or can be in the form of line tracking method. In the later techniques the segmentation and line extraction are usually combined in to a single step. For the extraction of line segments from 2D laser range finder measurements various segmentation techniques have been evaluated in a simulated environment, which are briefly described as follows.

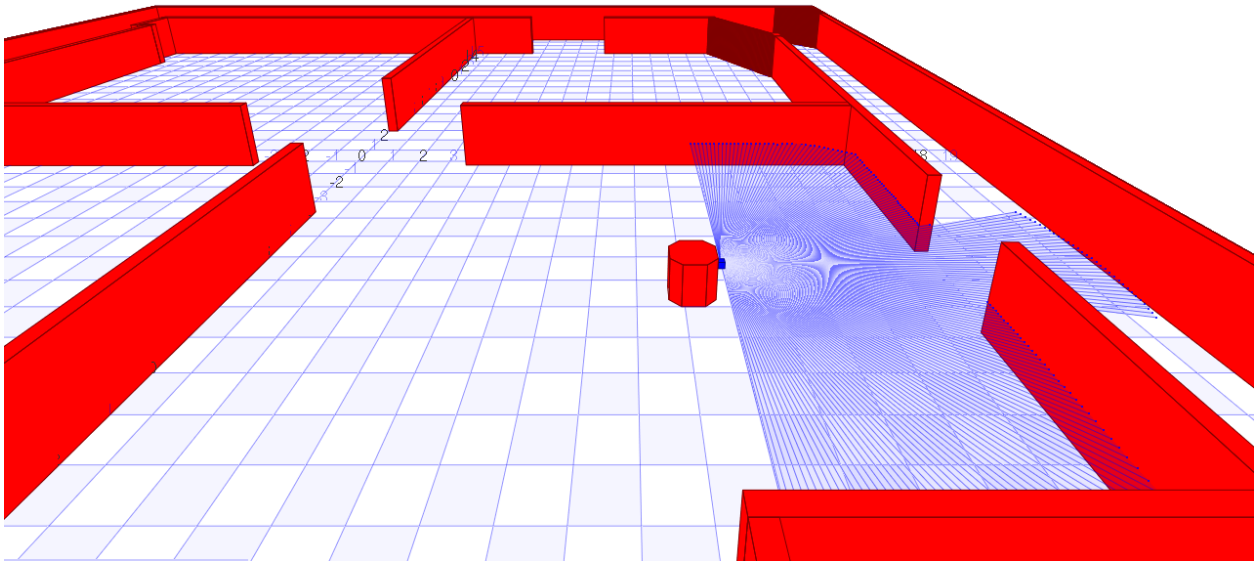

Figure 3.2 Simulated environment for evaluating different segmentation algorithms

Sequential Edge Following (SEF) works directly on the range measurement, therefore it does not require to transform laser scanner measurements from polar (raw laser scans) to Cartesian coordinates, although later on when we need to estimate the line parameters using linear regression we need the Cartesian coordinate of measurement points. SEF detect a line segment if the difference between two successive range measurements is greater than a threshold i.e. $|r_n - r_{n+1}| > d_{th}$. One disadvantage of the SEF is if the immediate point is affected with noise then then a new line segment is produced.

Line Tracking (LT) works sequentially on the laser scan measurements. LT produces a least square fit segment; segmentation and linear regression are in one step. At start a linear regression is applied on two points to estimate the line then the distance of the estimated line from the following third point is calculated, if the distance exceeds a certain threshold the estimated line segment is saved and new segmentation is performed from the third point otherwise the linear regression is performed once more including the third point until line-

point distance exceed for next point or all the points are processed. The same disadvantage of distance threshold as in the case of SEF also applies to LT when the next point which decides the break of line is disturbed by the noise. The next point bias the estimate more when the linear regression set is smaller. Both SEF and LT depend on the distance of the point from the laser scanner. SEF and LET can be improved by using previous and last point information into account.

Iterative End Point Fit (IEPF) [78] is a recursive algorithm which is executed when all data measurement points are available. As a pre-processing step it also requires the points to be converted into Cartesian coordinates. Then a line is estimated from first and last point afterward all the points' distances from the line is calculated. In case when no distance exceed a threshold this is the estimated line (or to enhance the parameters linear regression is performed on the point sets) otherwise the point with the maximum distance is selected as dividing point for two line segments which are again recursively checked iteratively for line-point distance. SEF and LT algorithms are fast compared to IEPF where IEPF is robust in both indoor and outdoor environments.

The decision to create cluster is based on a criteria $D(r_i, r_{i+1}) > D_{th}$. where $D(r_i, r_{i+1})$ is a Euclidean distance between two consecutive laser beam end points calculated by law of cosine i.e.

$$D(r_i, r_{i+1}) = \sqrt{r_i^2 + r_{i+1}^2 - 2r_i r_{i+1}\cos(\Delta\theta)}. \quad \text{Eq. 3.9}$$

The distance can be approximated by the following equation because of the very small angles among laser beams i.e. 0.5°

$$D(r_i, r_{i+1}) = |r_i - r_{i+1}| \quad \text{Eq. 3.10}$$

The important point in clustering is how to choose the threshold? Dietmayer [79] uses the following threshold condition

$$D_{th} = C_0 + C_1 \min(r_i, r_{i+1}) \quad \text{Eq. 3.11}$$

Where C_0 is a constant used for noise handling and

$$C_1 = \sqrt{2(1 - \cos(\Delta\theta))} = \frac{D(r_i, r_{i+1})}{r_i} \quad \text{Eq. 3.12}$$

The dependence of threshold on the range is because of radial measurement principle. Santos [80] included the parameter β aiming to reduce the dependence of the absolute distance of the point from the laser-scanner.

$$D_{th} = C_0 + \frac{C_1 \min(r_i, r_{i+1})}{\cot(\beta)\left(\cos\left(\frac{\Delta\theta}{2}\right) - \sin\left(\frac{\Delta\theta}{2}\right)\right)} \quad \text{Eq. 3.13}$$

Lee [81] proposed a simple method for line segments extraction threshold

$$D_{th} = \left|\frac{r_i - r_{i+1}}{r_i + r_{i+1}}\right| \quad \text{Eq. 3.14}$$

Kalman filter has also been used for segmentation process; interested reader may refer [82].

3.3.2. Feature Extraction

Features are distinguishable entities in mobile robot's sensor data which provides valuable information regarding the location of the mobile robot and mapping of the environment. Features or landmarks correspond to physical objects in the mobile robot environment. They bring different kind of information of environment objects into the map which helps the mobile robot to navigate using that map. Furthermore, they compress the sensor data size by modeling them into entities which constituted the map. This is a very important aspect of the large scale environment. Features usually depend on the type of sensor being used for the mobile robot e.g. for 2D laser range scanner the features could be lines, corner and circles, for 3D laser range scanner, TOF cameras or RGB-D cameras the features could be planes and for vision sensors features can be such as SIFT [83] or SURF [84].

Geometric features such as corners, lines, circles, planes and cylinders are most common features which are being used to model the environment from range sensor measurements. The geometric features are estimated by fitting the range measurements to the mathematical model of the feature. The literature on model fitting can be categorized into two broad categories i.e. Clustering (Hough Transformation) and Least Square Methods. A general form for the linear least square estimation process is shown in the Appendix B. During geometric feature extraction process the measurements are compared with a geometric model such as line or plane, the inliers are then used to estimate the parameters of the model. The parameter estimation problem can be mathematically seen as an optimization problem because of the over-determined system and measurement errors. One can use the least square method, RANSAC or Hough transformation to estimate the single or multiple models from the measurements. Two different types of geometric features for modeling the robot

environment are used i.e. line and planes. The extracted features are then used in the feature matching stage. A fitting function to a model must provide model parameters, error estimates on the parameters and statistical measure of goodness-of-fit.

3.3.2.1 Probabilistic Line Extraction

Among many primitive 2D geometric features line features are the prevalent in structured indoor environment. The Hessian normal form of line in polar coordinate is more desirable because it doesn't have the problem of representing lines parallel to x or y axis as in slope intercepts form. This implicit representation also allows fast calculation of point to the line distance. Least square estimation technique is used to estimate the parameters of a line from the laser scanner measurement cluster. Least square estimation technique provides a maximum likelihood estimation of the fitted parameters if the measurement errors are independent and Gaussian. Weighted least square fitting is also known as chi-square fitting. The sum of squares of weighted residual are called chi-square, i.e. the sum of square of normal distributed quantities. Weighted least square line fitting is used to estimate the parameters of a line if each laser beam has different error variance.

Laser range scanner takes n measurements of the environment in polar coordinates $z_i = (\rho_i, \theta_i)$ during one scan. We defined the line in Hessian normal form as follows

$$\rho \cos(\theta - \alpha) - r = 0 \qquad \text{Eq. 3.15}$$

Here r is the shortest Euclidian distance of the line's normal from the coordinate system's center and α is its angle with abscissa. Since there is an uncertainty in each variable ρ and θ therefore we have to minimize the term on right hand side of the above equation. Each variable can be represented as a random variable which has its own probability distribution function. We assumed that both random variables measurements are independent, furthermore, the PDF of both variables are Gaussian. The error of each measurement (ρ_i, θ_i) can be specified by the minimum normal distance of the measurement point and the line i.e. $\rho_i \cos(\theta_i - \alpha) - r = d_i$, from the estimated line (r, α). This approach results into a non-linear least square estimation which is computationally expensive to compute but not results into a bias estimate. The parameters of the line can be found by minimizing the sum square error of all the measurement points with respect to line parameters i.e.

$$SSE = \sum_{i=0}^{n} d_i^2 = \sum_{i=0}^{n} (\rho_i \cos(\theta_i - \alpha) - r)^2 \quad \text{Eq. 3.16}$$

$$\frac{\partial}{\partial r}\left(\sum_{i=0}^{n} (\rho_i \cos(\theta_i - \alpha) - r)^2\right) = 0 \quad \text{Eq. 3.17}$$

$$\frac{\partial}{\partial \alpha}\left(\sum_{i=0}^{n} (\rho_i \cos(\theta_i - \alpha) - r)^2\right) = 0 \quad \text{Eq. 3.18}$$

The above equations result into a non-linear least square estimation whose solution is calculated in [85]. The parameters of line's model in hessian normal form are calculated as follows:

$$\alpha = \frac{1}{2}\boldsymbol{atan2}\left(-2\sum_{i=0}^{n} (\bar{y} - y_i)(\bar{x} - x_i)\ ,\ \sum_{i=0}^{n} (\bar{y} - y_i)^2 - (\bar{x} - x_i)^2\right) \quad \text{Eq. 3.19}$$

$$r = \bar{x}\cos(\alpha) + \bar{y}\sin(\alpha) \quad \text{Eq. 3.20}$$

$$\bar{x} = \frac{1}{\mathrm{n}}\sum_{i=0}^{n} \rho_i \cos(\theta_i) \quad \text{Eq. 3.21}$$

$$\bar{y} = \frac{1}{\mathrm{n}}\sum_{i=0}^{n} \rho_i \sin(\theta_i) \quad \text{Eq. 3.22}$$

And the uncertainties of the line's model parameters (α, r) are because of the uncertainties in measurements (ρ, θ) which are calculated using error propagation law in [85]. These uncertainties are calculated as follows, assuming $\sigma_{\rho_i}^2$ and $\sigma_{\theta_i}^2$ are independent and angular uncertainties ($\sigma_{\theta_i}^2 = 0$) is negligible:

$$P_{\alpha r} = \begin{bmatrix} \sigma_\alpha^2 & \sigma_{\alpha r} \\ \sigma_{r\alpha} & \sigma_r^2 \end{bmatrix} \quad \text{Eq. 3.23}$$

$$\sigma_\alpha^2 = \sum_{i=0}^{n} \left[\frac{\partial \alpha}{\partial \rho_i}\right]^2 \sigma_{\rho_i}^2 \quad \text{Eq. 3.24}$$

$$\sigma_r^2 = \sum_{i=0}^{n} \left[\frac{\partial r}{\partial \rho_i}\right]^2 \sigma_{\rho_i}^2 \quad \text{Eq. 3.25}$$

$$\sigma_{\alpha r} = \sigma_{r\alpha} = \sum_{i=0}^{n} \left[\frac{\partial \alpha}{\partial \rho_i} \cdot \frac{\partial r}{\partial \rho_i}\right] \cdot \sigma_{\rho_i}^2 \quad \text{Eq. 3.26}$$

$$\frac{\partial \alpha}{\partial \rho_i} = \frac{N(\bar{x}\cos\theta_i - \bar{y}\sin\theta_i - \rho_i\cos 2\theta_i) - D(\bar{x}\sin\theta_i + \bar{y}\cos\theta_i - \rho_i\sin 2\theta_i)}{N^2 + D^2} \quad \text{Eq. 3.27}$$

$$\frac{\partial r}{\partial \rho_i} = \frac{\cos(\theta_i - \alpha)}{n} + \frac{\partial \alpha}{\partial \rho_i} \cdot (\bar{y}\cos\alpha - \bar{x}\sin\alpha) \quad \text{Eq. 3.28}$$

$$N = \frac{2}{n}\sum_{i=0}^{n}\sum_{j=0}^{n}(\rho_i\cos\theta_i)(\rho_j\sin\theta_j) - \sum_{i=0}^{n}\rho_i^2\sin 2\theta_i \quad \text{Eq. 3.29}$$

$$D = \frac{1}{n}\sum_{i=0}^{n}\sum_{j=0}^{n}\rho_i\cdot\rho_j\cos(\theta_i + \theta_j) - \sum_{i=0}^{n}\rho_i^2\cos 2\theta_i \quad \text{Eq. 3.30}$$

Position correction and map construction process can be speedup by storing other information regarding line segment such as direction vector (from one point to other), normal vector, length of segment, number of points in line segments and its normal distance to origin.

3.3.2.2 Probabilistic Plane Extraction

State of the art mobile robots use 3D range scanning devices such as laser scanner, time of flight cameras, stereo cameras and RGB-D cameras to sense the spatial environment and construct the map from acquired point clouds. 3D Geometric features such as planes are prevalent in the man-made environments such as offices and factory floors. Mobile robots can use such geometric features to construct a map for collision free autonomous navigation and localization in such environments. Various research works [86] [87] [88] [89] have been done until now to extract the 3D planes from the point cloud data acquired from different range sensor devices and build the 3D map of the environment. Asad [89] has proposed a mapping system for mobile robots which used height maps created from range images for path planning. Pathak [86] proposed a method for 3D mapping by a mobile robot, furthermore, his proposed method utilizes the uncertainty of the plane parameters to compute the uncertainty in the pose computed by scan registration. Weingarten et al. [88] proposed a method for plane fitting for laser range scanner data and fuses matching planes together to find a compact 3D model. Anderson et al. [90] uses an approach which fuses both color and range information to detect 3D planes. Apart from various mapping algorithms for mobile robots different sensors have also been used in combination with mapping algorithms to map 3D environments. Such sensors include laser scanners [91], stereo vision and monocular cameras [92] and time of flight camera [93]. A common approach for mapping is to align point clouds

by finding rotation and translation between consecutive 3D scans [94]. Henry [95] maps the environment using ICP and SIFT features. There exist numbers of other methods which extract the 3D planes from the raw point clouds. Borrmann [96] uses the Hough transform to extract the 3D plane from the raw point clouds. Triebel [97] uses expectation maximization, Gallo [98] used RANSAC to extract the planes and Pathek [99] used the split and merge techniques to detect the planes. In [100] two algorithms namely RANSAC and Hough transformation to extract the 3D planes from the raw point cloud are tested to compare the performance of real-time geometric map building from the Kinect equipped ground mobile robot. Recently most of the research work also used Kinect camera. The work in [101] [102] [103] has focused on extracted plane segmentation because of the sparsity, measurement range limitation and occlusion of the measurements. These research works have used the color image to complement the range limitation and sparsity of the depth measurement. The intensity information can help in segmentation of the 3D point cloud data by detecting edges in the intensity images corresponding to the area of interest in the 3D point cloud.

2D laser scanners are limited in use for mapping environments which contains simple geometric shapes; furthermore the obstacles which are above or below the scanned planes cannot be detected e.g. downward stairs. Where the stereo systems are dependent on lighting conditions and cannot detect planes in homogenous regions. Kinect sensor has brought acquiring colored 3D point clouds cheaper and quicker which in the past require expensive time of flight cameras. Furthermore, to acquire colored point clouds the system consisting of time of flight camera and image camera must be setup and calibrated but Kinect combines the 3D range finding capability and the color information. Since Kinect sensor acquires enormous amounts of data, 9.2 million 3D points in one sec, it is challenging to process the data in real time because of the limited amount of computation resources available on mobile robots, furthermore, raw 3D point clouds from Kinect sensor are not directly useable. Extracting multiple geometric features from the range data is computationally demanding and directly related to the number of parameters required to represent the geometric model to be found in the raw point clouds. In geometric mapping approach 3D planes can be used as geometric features because a plethora of 3D planes are available in structured environments.

Hough transform is a well-known algorithm in computer vision society to detect multiple models in the data compared to RANSAC which in its basic form assumes there is a single model present in the data. It can detect lines, planes, spheres and other parameterizable geometric objects in the input data. In spite of the robustness of the method against noisy

data one drawback of this algorithm is its high computational requirement therefore many variations of the Hough transform exists to detect the desired model parameters. Apart from standard Hough transform other variations which exists are, probabilistic Hough transform, random Hough transform, adaptive probabilistic Hough transform and progressive probabilistic Hough transform. The plane equation in Hessian normal form can be defined by a point p on the plane with normal vector n to the plane which is at a distance ρ from the origin, which is collinear to normal vector as shown in Figure 3.3. The normal vector ρ makes an angle θ with the z-axis and its projection in the x-y plane makes an angle φ with the x-axis. Therefore, the equation of the plane can be defined as

$$p_x \cdot \sin(\theta) \cdot \cos(\varphi) + p_y \cdot \sin(\theta) \cdot \sin(\varphi) + p_z \cdot \cos(\theta) = \rho \qquad \text{Eq. 3.31}$$

The dimension of the Hough space is equal to the number of parameters of our plane model i.e. (θ, φ, ρ). Each plane in $\mathbb{R}^3$ corresponds to a point in the Hough space and each point in $\mathbb{R}^3$ corresponds to a surface in Hough space. The surface represents all the possible planes where the point could belong to. Therefore, the transformation of the points $p_i \subset P$ from $\mathbb{R}^3$ to Hough space will generate surfaces in Hough space. The intersection of three surfaces in Hough space results in a point in Hough space which corresponds to a plane in $\mathbb{R}^3$ on which the three points which generates the surface lies on. All points whose surfaces in Hough space intersect at a point correspond to the same plane in $\mathbb{R}^3$. Figure 3.3 describes the model parameters of the geometric plane along with the coordinate system.

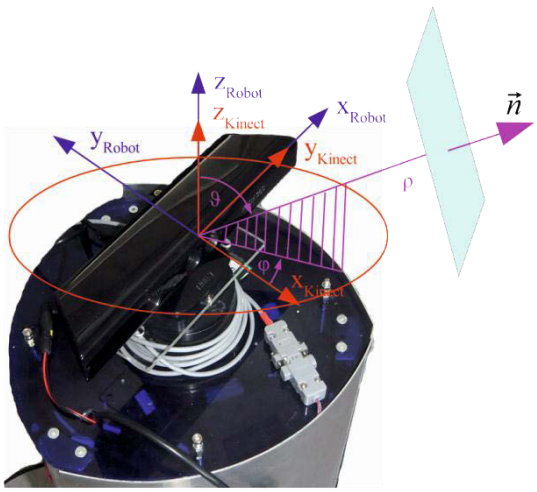

Figure 3.3 Plane definition in Hessian normal form

Random Hough transform is used to detect 3D planes in the raw 3D point clouds. Instead of generating surfaces for each point p_i in $\mathbb{R}^3$ into Hough space, which is very time consuming. The fact that a plane corresponds to a single point in Hough space is used, therefore, it is very fast to compute a plane from three random points from a small circular region and transform the estimated plane to Hough space, this results into a significant faster algorithm for real time implementation. The pseudo code of the randomized Hough transform is as follows:

Do until DetectedPlanes < 8 **and** TotalPoints > MinPoints
Randomly select (P_1, P_2, P_3) from a random circular region
Calculate plane from (P_1, P_2, P_3)
Transform the Calculate plane from $\mathbb{R}^3$ to Hough space
If local maxima is found in Hough space
Delete points corresponding to plane from input points
Calculate plane boundries
Reset Hough space
End if
End Do

Table 3.1 Randomized Hough transform algorithm

The discretization size of the Hough space depends on the accuracy required and the available memory. For the implementation purpose the Hough space was discretized into a step of 1cm for ρ which result into a range of 1cm to 500cm, 1° for φ from -180° to 180° and 1° for θ from 0° to 180°. Using the above discretization the memory requirement for Hough space is found to be 125MB. We have found out that the predominant part of the time required by the randomized Hough transform is required to reset the Hough space, therefore the choice of discretization for plane parameters has been chosen based on the possible orientation of the planes in the input raw 3D point clouds.

3.3.3. Feature prediction from map

Feature prediction from the map or data association is an important and crucial step for the correct working of the EKF based SLAM algorithm. Basically in this step the expected measurements by the robot are generated. This step requires the sensor observation model. TOM3D robot is equipped with the laser scanner to detect the line features from the environment. The lines along with their parameters uncertainties are extracted as described in section 3. The correction phase in fact calculates the amount of new information brought up by the laser scanner measurements. The amount of new information or innovation brought up by observing the already existing line feature is calculated as follows:

$$z_i = y_m^i - y_e^i = \begin{bmatrix} r_m^i \\ \alpha_m^i \end{bmatrix} - \begin{bmatrix} r_e^i \\ \alpha_e^i \end{bmatrix} \quad \text{Eq. 3.32}$$

Here y_e^i is the expected observation which is calculated by using the sensor observation model. The sensor observation model for the laser scanner system to extract the line feature is defined by the following equation

$$f(x_r, y_g^i) = \begin{bmatrix} r_e^i \\ \alpha_e^i \end{bmatrix} = \begin{bmatrix} r_g^i - x_r \cdot \cos(\alpha_g^i) - y_r \cdot \sin(\alpha_g^i) \\ \alpha_g^i - \theta_r \end{bmatrix} \quad \text{Eq. 3.33}$$

The sensor observation model takes as input the current robot pose $x_r = (x_t, y_t, \theta_t)^T$ and one of the already mapped line features $y_g^i = (r_g^i,\ \alpha_g^i)^T$ described in global coordinate frame and map it to the robot's local coordinate frame $y_e^i = (r_e^i,\ \alpha_e^i)^T$. The covariance of the expected feature observation is calculated as follows

$$S = [H_r \quad H_{l_i}] \cdot \begin{bmatrix} P_{rr} & P_{rl_i} \\ P_{l_i r} & P_{l_i l_i} \end{bmatrix} \cdot \begin{bmatrix} H_r^T \\ H_{l_i}^T \end{bmatrix} \quad \text{Eq. 3.34}$$

Where H_r is the Jacobian of the sensor observation model with respect to the robot pose and H_{l_i} is the Jacobian of the sensor observation model with respect to the i^{th} feature.

$$H_r = \begin{bmatrix} -\cos(\alpha_e) & -\sin(\alpha_e) & 0 \\ 0 & 0 & -1 \end{bmatrix} \quad \text{Eq. 3.35}$$

$$H_{l_i} = \begin{bmatrix} 1 & x_r \cdot \sin(\alpha_e) - y \cdot \cos(\alpha_e) \\ 0 & 1 \end{bmatrix} \quad \text{Eq. 3.36}$$

The crucial issue here is the data association of the measured feature with the i^{th} existing feature in the map. There are many different strategies for data association [68]. Here two strategies are being discussed namely Mahalanobis distance and K-D Tree.

3.3.3.1 Mahalanobis Distance

Mahalanobis distance is a distance measure which is based on the correlation of two variables and scale invariant. It basically measures the similarity of a measured data to a known data. The Euclidean distance measure cannot be used here because of the two reasons. First, both parameters of the line features are of different scales and, second, it doesn't takes into account the uncertainty of the parameters. The Mahalanobis distance criteria can be applied iteratively on all the features of the existing map to find out which expected feature from the existing map best matches to the measured feature. In other words we choose a feature with minimum Mahalanobis distance (Maximum Likelihood) below some threshold. Mathematically it is described as follows

$$z_i{}^T \cdot Z_i{}^{-1} \cdot z_i < n^2 \qquad \text{Eq. 3.37}$$

Here z_i is the innovation and Z_i is the covariance of the innovation and n is the squared Mahalanobis distance for a constant probability density curve with locus cantered at measured feature. The innovation covariance is found by adding the covariance of the expected measurement and the measured feature covariance i.e.

$$Z_i = \mathrm{S} + R \qquad \text{Eq. 3.38}$$

The covariance of the measured feature is found in section 3 is as follows

$$R = \begin{bmatrix} \sigma_r^2 & \sigma_{r\alpha} \\ \sigma_{\alpha r} & \sigma_\alpha^2 \end{bmatrix} \qquad \text{Eq. 3.39}$$

3.3.3.2 KD Tree

KD tree is a binary tree where K is the dimension of the data. It has storage requirements of $O(n)$ where n is the number of data point. It supports the nearest neighbor search scheme which is important for estimated feature extraction from the map. The nodes within the KD tree consist of two child pointers and a key. The number of item in the Key value represents the D or dimension of the data. Let's consider a concrete example in case of our SLAM problem. After extracting number of line features from the range scan data the next step is to extract the expected lines from the map at the given robot position. Here we assume that the map consists of a set of lines or in other words a set of pair of values which define the equation of line. Since we need two parameters r and α to define the line in Hessian normal form therefore, we need a 2D-tree data structure to represent our feature based map. Each

line entry in this data structure will be a node in the binary tree data structure of the KD-tree. The first node is called the root node and the subsequent data which follows is divided into two regions. We could imagine a hyper plane which divides the space into two parts, left side and right side of the plane. Because it's a binary tree, therefore, the child node could be on the left side or the right side. The decision to store the next line on left or right side is made as follows. If the r value of the given line is greater than or equal to the r value of the root node then the right side is further investigated otherwise the left side. Now if there no node exists at that position then the value is added as child node otherwise the α parameter is compared with the grandchild α value, the decision to traverse left or right as before until the node is registered at the appropriate level.

3.3.4. Map Update

If the data association process succeeds to find a match between a measured feature and any one of the existing feature then the map update step is performed. This step is in fact like the normal Kalman filter measurement update step. First we have to calculate the Kalman filter gain and then we update the states and their covariances. Mathematically

$$K_{l_i} = \begin{bmatrix} P_{rr} & P_{rl_1} \\ P_{l_1 r} & P_{l_1 l_i} \\ \vdots & \vdots \\ P_{l_n r} & P_{l_n l_i} \end{bmatrix} \cdot \begin{bmatrix} H_r^T \\ H_{l_i}^T \end{bmatrix} \cdot [Z_i]^{-1} \qquad \text{Eq. 3.40}$$

$$x = x + K_{l_i} \cdot z_i \qquad \text{Eq. 3.41}$$

$$P = P - K_{l_i} \cdot Z_i \cdot {K_{l_i}}^T \qquad \text{Eq. 3.42}$$

It is clear from the Eq. 3.40 that the measurement of i^{th} line feature will calculate the correction factor for all the line features in the map and the robot. The corrected state vector is calculated by adding a portion of innovation proportional to the correction factors as shown in Eq. 3.41. Similarly due to the availability of new information the uncertainty of the state vector is reduced by subtracting a portion of covariance proportional to the Kalman gain from already estimated state uncertainty as shown in Eq. 3.42.

3.3.5. New Features

In case if the measured feature failed to produce any match with existing feature a validation gate is performed i.e. if the feature is observed during last four or more observations then it is considered as a new feature and is need to be added to existing features. The validation gate is required because of the noise present in the sensor measurements. Similar to sensor

observation model we need an inverse sensor observation model to define the measured feature from sensor's local coordinate frame to global coordinate frame.

$$f(x_r, y_l^{n+1}) = \begin{bmatrix} r_g^{n+1} \\ \alpha_g^{n+1} \end{bmatrix} = \begin{bmatrix} r_l^{n+1} + x_r \cdot \cos(\alpha_l^{n+1} + \theta_r) + y_r \cdot \sin(\alpha_l^{n+1} + \theta_r) \\ \alpha_l^{n+1} + \theta_r \end{bmatrix} \quad \text{Eq. 3.43}$$

The state vector is augmented with the new feature $y_g^{n+1} = (r_g^{n+1}, \alpha_g^{n+1})$ and the state covariance matrix is also augmented and initialized with new feature covariance $P_{l_{n+1}l_{n+1}}$, the new feature to old feature covariance and the new feature to robot covariance. These covariance matrices are calculated as follows

$$P_{l_{n+1}l_{n+1}} = Y_r \cdot P_{rr} \cdot Y_r^T + Y_{l_{n+1}} \cdot R \cdot Y_{l_{n+1}}^T \quad \text{Eq. 3.44}$$

$$P_{l_i m} = Y_r \cdot [P_{rr} \quad P_{rl_1} \quad \dots \quad P_{rl_{n+1}}] \quad \text{Eq. 3.45}$$

$$P_{ml_i} = P_{l_i m}^T \quad \text{Eq. 3.46}$$

Where Y_r is the Jacobian of the inverse sensor model with respect to the robot pose and $Y_{l_{n+1}}$ is the Jacobian of the inverse sensor model with respect to the feature point. The covariance of the measured feature is the same as in Eq. 3.39.

$$Y_r = \begin{bmatrix} \cos(\alpha_l^{n+1} + \theta_r) & \sin(\alpha_l^{n+1} + \theta_r) & y_r \cdot \cos(\alpha_l^{n+1} + \theta_r) - x_r \cdot \sin(\alpha_l^{n+1} + \theta_r) \\ 0 & 0 & 1 \end{bmatrix} \quad \text{Eq. 3.47}$$

$$Y_{l_{n+1}} = \begin{bmatrix} 1 & y_r \cdot \cos(\alpha_l^{n+1} + \theta_r) - x_r \cdot \sin(\alpha_l^{n+1} + \theta_r) \\ 0 & 1 \end{bmatrix} \quad \text{Eq. 3.48}$$

Therefore, the augmented state covariance matrix looks like this

$$P = \begin{bmatrix} P_{rr} & P_{rm} & P_{rr}^T \cdot Y_r^T \\ P_{rm} & P_{mm} & P_{rm}^T \cdot Y_r^T \\ Y_r \cdot P_{rr} & Y_r \cdot P_{rm} & P_{l_{n+1}l_{n+1}} \end{bmatrix} \quad \text{Eq. 3.49}$$

3.4. Summary

This chapter describes in detail the core components of the SLAM algorithm for implementation purposes. Active range sensors such as laser-scanner have advantage over the passive sensors such as stereo camera systems because they are independent from illumination and object reflection. Furthermore, they are accurate with long range measurement where the stereo system have error variance which squares with the distance. There are many other issues in the EKF based SLAM which are not discussed here but which are important for the practical implementation of the EKF-SLAM algorithm, such as features' signatures (color, length etc.), intelligent update of only relevant features.

The advantages of the EKF based SLAM algorithm lies in the simplicity of applying EKF algorithm to the SLAM problem and it works well for small number of unique features. There are few drawbacks of the EKF-SLAM algorithm. The computation requirements grow quadratic ally to the number of features. It relies very heavily on the data association assumption, therefore, errors in the data association results into divergence and ultimately explosion of the filter. And the solution would not be optimal in case of non-Gaussian noise and strong non-linearity in motion and observation models.

The topics which are important for the SLAM implementation are clustering, feature extraction and data association. Various data clustering techniques which are useful and applicable to range sensors are described. The techniques used for extraction of geometric lines and planes are also described. Lines are extracted by using the non-linear least square estimate technique. Where the planes are extracted by using Hough transformation process. Then the features prediction step is explained which can use Mahalanobis distance based technique for feature prediction or the KD-Tree based approach. And finally the map update and augmentation process is described.

Chapter 4. Cooperative SLAM (CSLAM)

For mobile robots to act autonomously in their environment there are two fundamentally different approaches. One is the behavior based approach in which robots rely much on their sensory to take decision. The second approach is the model based approach in which the mobile robots model its surrounding environment. The model of the world around the mobile robot is in the form of a map. In chapter 2.5 we have seen the different representations of the maps which are useful to mobile robots. Mobile robots need the map to find their position in the environment and plan their actions in the environment. SLAM answers the localization and map building conundrum of the mobile robots in an unknown environment as both step depend on each other. Various working SLAM flavors exist now days such as GMapping, GridSLAM and DP-SLAM for research purpose. However no existing SLAM package is available for multiple robots up to the knowledge of the author. This chapter formalizes the cooperative SLAM strategy for multiple robots with different heterogeneous set of features.

4.1. SLAM for Heterogeneous features

The standard EKF based SLAM algorithm solution is for one type of features. In this section an EKF based SLAM algorithm is described for a single robot and heterogeneous features. By heterogeneous features means different kind of geometric features. One could extract and model different kind of geometric features such as corners, lines, circles and planes from the 2D range scan data. Line features can easily be extracted from the 2D range scan measurements of the laser range scanner such as SICK Laser scanner while the plane features can easily be extracted from the 3D range measurements from the depth cameras such as Kinect. Two parameters (r, α) are required to fully describe a line as shown in Eq. 4.1 and three parameters (r, θ, φ) are required to fully describe a plane as shown in Eq. 4.2.

$$p_x \cdot \cos(\alpha) + p_y \cdot \sin(\alpha) - r = 0 \qquad \text{Eq. 4.1}$$

$$p_x \cdot \cos(\theta) \cdot \sin(\varphi) + p_y \cdot \sin(\theta) \cdot \sin(\varphi) + p_z \cdot \cos(\varphi) - \mathrm{r} = 0 \qquad \text{Eq. 4.2}$$

The parameters of a geometric feature can be augmented to the state vector as a new feature on the discovery during the mobile robot moves in the environment. The set of features is defined as map. The re-observation of the existing features is used to correct the pose of the robot and helps to reduce the uncertainty of the robot pose and map. In the case of EKF based SLAM algorithm the state vector and covariance matrix can be described as follows

$$x = [x_r \quad y_r \quad \theta_r \quad r_{l_1} \quad \alpha_{l_1} \quad \cdots \quad r_{p_1} \quad \theta_{p_1} \quad \varphi_{p_1} \quad \cdots]^T \qquad \text{Eq. 4.3}$$

$$P = \begin{bmatrix} P_{rr} & P_{rm_l} & P_{rm_p} \\ P_{m_l r} & P_{m_l m_l} & P_{m_l m_p} \\ P_{m_p r} & P_{m_p m_l} & P_{m_p m_p} \end{bmatrix} \qquad \text{Eq. 4.4}$$

Equation 4.3 show the state vector composed of robot states and the map features. The first three elements are the pose of a mobile robot while the next tuple of two parameters represent the geometric line features and at the end tuple of three parameters represent the geometric plane feature present in the environment. Equation 4.4 shows the composition of state covariance matrix of robot and map features. The EKF based state estimation technique to perform the SLAM is as usual except in the update step where each measured feature update the robot pose and the subset of map composed of corresponding type of features

4.1.1. Prediction

In case of heterogeneous set of features such as lines and planes the state vector can be estimated as follows

$$x_{t+1} = \begin{bmatrix} f(x_r, u_t, w_t) \\ m_l \\ m_p \end{bmatrix} \qquad \text{Eq. 4.5}$$

Here $f(x_r, u_t, w_t)$ represents the states of the robot and m_l represents all of the existing line features and m_p represents the set of all existing plane features. It can be seen from the equation 4.5 that it is assumed the features remain static in the environment. The uncertainty in the robot states and the map features is propagated due to robot motion as follows

$$P_{t+1} = \begin{bmatrix} F_r \cdot P_{rr} \cdot F_r^T + F_n \cdot Q \cdot F_n^T & F_r \cdot P_{rm_l} & F_r \cdot P_{rm_p} \\ P_{rm_l} \cdot F_r & P_{m_l m_l} & P_{m_l m_p} \\ P_{rm_p} \cdot F_r & P_{m_p m_l} & P_{m_p m_p} \end{bmatrix} \qquad \text{Eq. 4.6}$$

The robot state uncertainty is propagated according to state transition model in addition to the uncertainty of the odometric inputs. The uncertainty due to robot motion also affect the cross-covariance's between the robot and the map features.

4.1.2. Update

The update step of the SLAM process in case of heterogeneous set of features is different for each type of feature. The update step for the line feature is the same as in Eq. 3.32 – Eq.3.42.

The line features only update the portion of the map containing the robot and line features. While the update step for the plane features is as follows

$$z_i = y_m^i - y_e^j = \begin{bmatrix} r_m^i \\ \varphi_m^i \\ \theta_m^i \end{bmatrix} - \begin{bmatrix} r_e^j \\ \varphi_e^j \\ \theta_e^j \end{bmatrix} \quad \text{Eq. 4.7}$$

In Eq. 4.7 z_i is the innovation calculated by subtracting j^{th} expected feature y_e^j from the i^{th} measured feature y_m^i. The data association between the i^{th} measured plane feature and the j^{th} existing feature is found by using the Mahalanobis distance threshold as already described by the Eq. 3.37. The measured feature is in the robot local coordinates frame where the existing plane features are stored in the global coordinate frame, therefore, the following sensor observation model transform one of the plane feature described in the global coordinate system and return's the plane feature parameter's in the robot's local coordinate frame

$$f(x_t, y_g^j) = \begin{bmatrix} r_e^j \\ \varphi_e^j \\ \theta_e^j \end{bmatrix} = \begin{bmatrix} r_g^j - x_r \cdot \sin(\theta_g^j)\cos(\varphi_g^j) - y_r \cdot \sin(\theta_g^j)\sin(\varphi_g^j) - z_r \cdot \cos(\theta_g^j) \\ \varphi_g^j - \theta_r \\ \theta_g^j \end{bmatrix} \quad \text{Eq. 4.8}$$

The above equation assumes that the robot is moving in a plane at a height of z_r with pose $x_t = (x_r, y_r, \theta_r)^T$. The expected feature's covariance is calculated as follows

$$S_j = \begin{bmatrix} H_r & H_{p_j} \end{bmatrix} \cdot \begin{bmatrix} P_{rr} & P_{rp_j} \\ P_{p_j r} & P_{p_j p_j} \end{bmatrix} \cdot \begin{bmatrix} H_r^T \\ H_{p_j}^T \end{bmatrix} \quad \text{Eq. 4.9}$$

Where H_r is the Jacobian of sensor observation model with respect to the robot pose and H_{p_j} is the Jacobian of the $f(x_t, y_g^j)$ with respect to the plane feature.

$$H_r = \begin{bmatrix} -\sin(\theta_g^j)\cos(\varphi_g^j) & -\sin(\theta_g^j)\sin(\varphi_g^j) & 0 \\ 0 & 0 & -1 \\ 0 & 0 & 0 \end{bmatrix} \quad \text{Eq. 4.10}$$

$$H_{p_j} = \begin{bmatrix} 1 & \sin(\theta_g^j)\left(x_r \sin(\varphi_g^j) - y_r \cos(\varphi_g^j)\right) & -\cos(\theta_g^j)\left(x_r \cos(\varphi_g^j) + y_r \sin(\varphi_g^j)\right) - z_r \cos(\theta_g^j) \\ 0 & 1 & 0 \\ 0 & 0 & 1 \end{bmatrix} \quad \text{Eq. 4.11}$$

The covariance of the innovation is measured by adding the covariance of the expected features and the covariance of the measured plane

$$Z_i = S_j + R_i \quad \text{Eq. 4.12}$$

The covariance of the measured plane is as follows

$$R_i = \begin{bmatrix} \sigma_r^2 & \sigma_{r\varphi} & \sigma_{r\theta} \\ \sigma_{\varphi r} & \sigma_{\varphi}^2 & \sigma_{\varphi\theta} \\ \sigma_{\theta r} & \sigma_{\theta\varphi} & \sigma_{\theta}^2 \end{bmatrix} \quad \text{Eq. 4.13}$$

Therefore, the update process for the map consisting of plane features is as follows

$$K_{p_i} = \begin{bmatrix} P_{rr} & P_{rp_1} \\ P_{p_1 r} & P_{p_1 p_i} \\ \vdots & \vdots \\ P_{p_n r} & P_{p_n p_i} \end{bmatrix} \cdot \begin{bmatrix} H_r^T \\ H_{p_i}^T \end{bmatrix} \cdot [Z_i]^{-1} \quad \text{Eq. 4.14}$$

$$x = x + K_{p_i} \cdot z_i \quad \text{Eq. 4.15}$$

$$P = P - K_{p_i} \cdot Z_i \cdot {K_{p_i}}^T \quad \text{Eq. 4.16}$$

The Eq. 4.16 which is used to update the covariance is computationally expensive but gives good numerical stability.

4.1.3. New Plane Features

The plane features which are failed to associate with the existing features are considered as new features and therefore, augmented to the existing feature list. A feature is measured in the robot local coordinated frame assuming sensor coordinate frame and robot coordinate frame are coincident and therefore, is required to transform into the global coordinate before appending to the existing feature's set. An inverse sensor model function is required which perform the local to global coordinate transformation. The inverse sensor model which transforms the featured defined in the hessian normal form and local spherical coordinate of the robot is as follows:

$$f(x_t, y_l^{n+1}) = \begin{bmatrix} r_g^{n+1} \\ \varphi_g^{n+1} \\ \theta_g^{n+1} \end{bmatrix} = \begin{bmatrix} r_g^{n+1} - x_r \cdot \sin(\theta_l^{n+1}) \cos(\varphi_l^{n+1} + \theta_r) - y_r \cdot \sin(\theta_l^{n+1}) \sin(\varphi_l^{n+1} + \theta_r) - z_r \cdot \cos(\theta_l^{n+1}) \\ \varphi_l^{n+1} + \theta_r \\ \theta_l^{n+1} \end{bmatrix} \quad \text{Eq. 4.17}$$

The state vector is augmented with $f\left(x_t, y_l^{n+1}\right)$ feature. It is assumed that the robot is moving in a planer surface. The covariance matrix of the state vector is also augmented as follows:

$$P = \begin{bmatrix} P_{rr} & P_{rm} & P_{rr}^T \cdot Y_r^T \\ P_{rm} & P_{mm} & P_{rm}^T \cdot Y_r^T \\ Y_r \cdot P_{rr} & Y_r \cdot P_{rm} & P_{p_{n+1} p_{n+1}} \end{bmatrix} \quad \text{Eq. 4.18}$$

$$P_{p_{n+1}p_{n+1}} = Y_r \cdot P_{rr} \cdot Y_r^T + Y_{p_{n+1}} \cdot R_{n+1} \cdot Y_{p_{n+1}}^T \quad \text{Eq. 4.19}$$

$$P_{p_i m} = Y_r \cdot [P_{rr} \quad P_{rp_1} \quad \dots \quad P_{rp_{n+1}}] \quad \text{Eq. 4.20}$$

$$P_{mp_i} = P_{p_i m}^T \quad \text{Eq. 4.21}$$

Where Y_r is the Jacobian of the inverse sensor model with respect to the robot pose and $Y_{p_{n+1}}$ is the Jacobian of the inverse sensor model with respect to the plane feature point.

$$Y_r = \begin{bmatrix} -\sin(\theta_g^j)\cos(\varphi_g^j + \theta_r) & -\sin(\theta_g^j)\sin(\varphi_g^j + \theta_r) & \sin(\theta_g^j)\left(x_r \sin(\varphi_g^j + \theta_r) - y_r \cos(\varphi_g^j + \theta_r)\right) \\ 0 & 0 & 1 \\ 0 & 0 & 0 \end{bmatrix} \quad \text{Eq. 4.22}$$

$$H_{p_j} = \begin{bmatrix} 1 & \sin(\theta_g^j)\left(x_r \sin(\varphi_g^j + \theta_r) - y_r \cos(\varphi_g^j + \theta_r)\right) & -\cos(\theta_g^j)\left(x_r \cos(\varphi_g^j + \theta_r) + y_r \sin(\varphi_g^j + \theta_r)\right) - z_r \cos(\theta_g^j) \\ 0 & 1 & 0 \\ 0 & 0 & 1 \end{bmatrix} \quad \text{Eq. 4.23}$$

4.2. SLAM for Multiple robot with known initial poses

When multiple robots are working together for the solution SLAM problem then first it is important to know how to setup the cooperative SLAM framework for multiple robots which can sense different kind of features. The following discussion limits the discussion to two differential drive based mobile robots moving in a planar environment which can be extended to multiple robots if required. The first robot is equipped with 2D laser range scanner so that it can detect the line features from the raw 2D point measurements. The second robot is equipped with a 3D range sensor device such as Kinect so that it can detect the plane features from the raw 3D point measurements. Here we assume that the initial pose of the each robot is known which is important for cooperative centralized map building.

The state vector and the uncertainty matrix estimated by the extended Kalman filter is as follows

$$x = \begin{bmatrix} x_{r_1} \\ x_{r_2} \\ m_l \\ m_p \end{bmatrix} \quad \text{Eq. 4.24}$$

$$P = \begin{bmatrix} P_{r_1 r_1} & P_{r_1 r_2} & P_{r_1 m_l} & P_{r_1 m_p} \\ P_{r_2 r_1} & P_{r_2 r_2} & P_{r_2 m_l} & P_{r_2 m_p} \\ P_{m_l r_1} & P_{m_l r_2} & P_{m_l m_l} & P_{m_l m_p} \\ P_{m_p r_1} & P_{m_p r_2} & P_{m_p m_l} & P_{m_p m_p} \end{bmatrix} \quad \text{Eq. 4.25}$$

Here $x_{r_1} = \left(x_{r_1}, y_{r_1}, \theta_{r_1}\right)^T$ is the state vector for the first robot and $x_{r_2} = \left(x_{r_2}, y_{r_2}, \theta_{r_2}\right)^T$ is the state vector for the second robot. $m_l = (l_1 \cdots l_2)^T$ is the subset of the total map m which consist of only line features extracted from the 2D range sensor and $m_p = (p_1 \cdots p_n)^T$ is the subset of m consists of plane features extracted from the 3D range sensor.

4.3. Summary

In this chapter a mathematical cooperative SLAM framework is formalized which is based on the extended Kalman filter. First an EKF based SLAM formulation is developed for the 2D geometric lines and 3D geometric planes. Each of the major implementation steps for the SLAM; prediction, update and the augmentation is described.

Later the formulation considers multiple robots in the formulization. The state vector is composed of individual robot state vector, 2D line features and the 3D plane features. The formulization assumes the initial relative robot pose are known.

Chapter 5.

Framework and Hardware Development

A mobile robot system usually consist of hardware components such as sensors, actuators and control unit for low level tasks related to mobile robots. These sensors, actuators and control algorithms are controlled by a firmware running in the control unit. Usually this control unit communicates with the high level algorithms running on a desktop computer for their tasks management or tele-control. Carrying out the task by a mobile robot requires the integration of several modules.

Therefore, a scalable cooperative multi-robot system is developed to address the current challenge of controlling, configuring and management of multiple ground and aerial robots with heterogeneous capabilities. The operation of the system for cooperative map building scenario is shown in Figure 5.1. Mobile agents can be created or configured dynamically at run-time in the existing team of mobile robots to perform tasks. Creation means assigning a unique ID, adding set of sensors and their poses via a graphical user interface for a physical mobile robot which is to be added into a team of mobile robots. Furthermore, to provide format for communication protocols of commands and reports between the mobile robot and computer control interface. Therefore, when sensor data is received from a mobile robot, it is parsed according to the robot's report protocol format and then stored in to a database. The mobile robots sensors data in the database is categorized according to the sensor type. The structured logging of sensor data according to sensor type into the database enables mapping and localization modules to quickly process the relevant information.

A mapping module which is a part of ground coordinator generates the online map and updates it automatically from the database. It makes the global map by using all range type sensors registered in the database from all mobile robots in the network. Based on the robot's ID, range sensor's data and pose from the database an online mesh is generated and rendered into the global map. 3D object models of robots along with their current pose are also rendered in to the map.

Another aspect of the system is the modular firmware architecture and a universal hardware board for ground mobile robots. The firmware architecture consists of multiple modules which can be enabled, disables or configured on the fly. Modules are defined as behaviors, sensors

drivers, obstacles avoidance algorithm, navigation algorithm or any other firmware code written to perform a specific function.

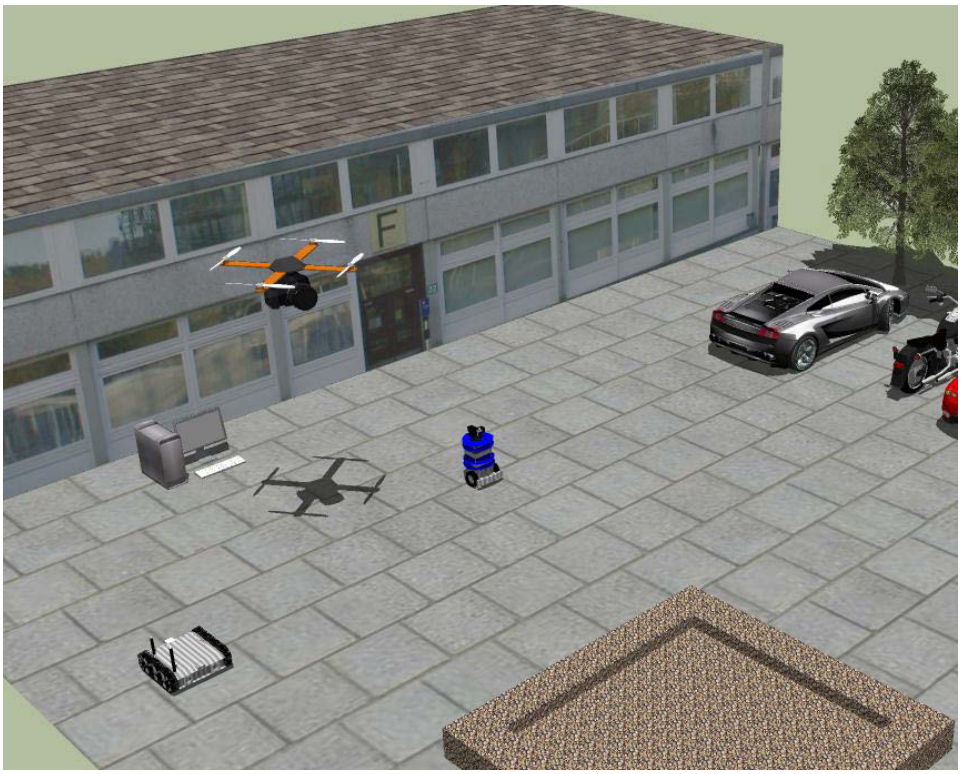

Figure 5.1 Heterogeneous mobile robots cooperation for map building in a partially structured environment

Each module can be considered to consist of four phase; initialization, input, processing and output phase. During initialization phase the settings related to the module are loaded which are stored into the EEPROM such as the sensors poll duration, reports duration and others. The control board is designed in a way to provide interfaces for all common robot sensors hence can be used on all ground based mobile robots. Some subsets of mobile robot sensors are common among other robots; this redundancy increases the robustness of the system and augments the resilience of system failure in case of individual mobile robot failure.

5.1. Overview of the system

The cooperative robot network can consist of multiple mobile robots with heterogeneous capabilities. Each robot is specific to the environment morphology and therefore has a set of sensors according to the environment it is designed for. The main purpose of the overall system is to create a general purpose framework where multiple robots with heterogeneous capability can be controlled, configured and managed. The application for using the cooperative multi-robot framework is to build a cooperative map of an environment and localize the robots within the map simultaneously. The multi-robot network is a server-

coordinator-agent based application. The server and the coordinators are the independent modules which can run concurrently on a computer or they can run on different computers to take advantage of computational efficiency. Information about the robots, there sensors configurations, data reports and control firmware settings are stored centrally into a database which is accessible to a server and coordinators. In general the hierarchy of multi-robot network is shown in Figure 5.2.

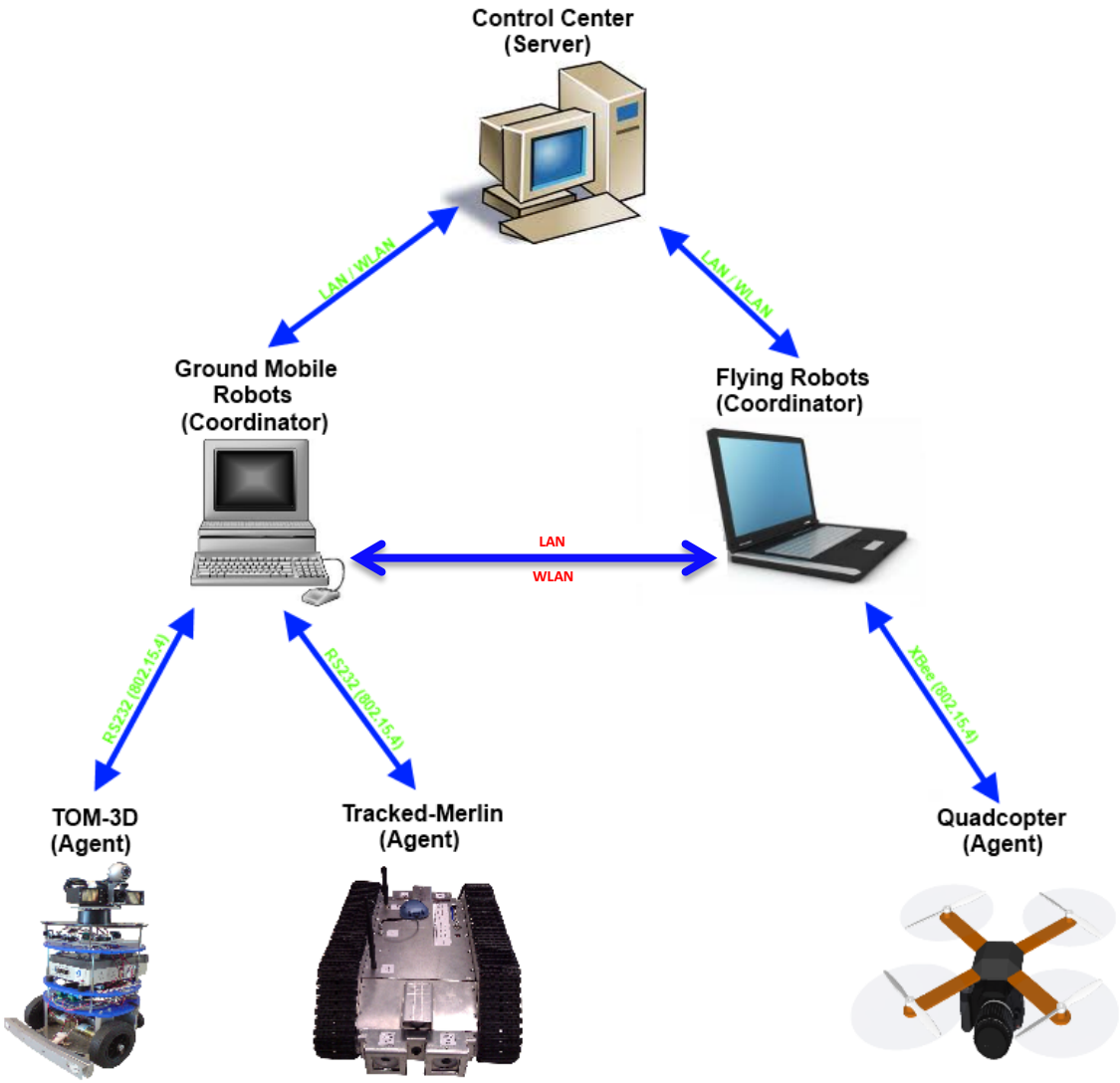

Figure 5.2 Cooperative heterogeneous multi-robot network architecture

The separation of the coordinators is based on the type of robots (ground or aerial) to ease the independent development and the nature of specific guidance and control requirements of the mobile robots. The following sections describes in detail the functionality and implementation for each of the overall system components; server, coordinates and agents.

5.1.1. Control Center

The control center (server) is responsible for the cooperative global map building, path planning and high level mission/task planning. The control center builds the global map by fusing the local maps which are constructed by the ground robot coordinator and the flying robot coordinator respectively. The map fusion is implemented when either the relative pose between the mobile robots is known or some common features in robots local map are found. The map fusion is therefore, a computationally intensive task which is to be performed by the server. The communication and cooperation between ground and aerial mobile robots coordinator are performed through the server. For instance, the server can command the ground mobile robots to explore an area which is not observable by aerial robot or command the flying robot to take the images of a planned path so that if there are some unforeseen dead-ends ahead that can be included before the mobile robots reach there. The control center and coordinator communicate to each other through UDP (User Datagram Protocol) hence they benefit from the interoperability, scalability, and standardization of the communication infrastructure. The UDP offers data throughput but don't have error checking. Therefore, a communication protocol structure is designed which is implemented for communication between server and coordinator. The communication protocol is general enough to be implemented between agents and coordinator. The general communication packet layout is as follows:

Packet Field	Field Size [Bytes]	Description
Header	2	Communication packet's beginning signature.
DestinationID	1	Unique number to identify the destination device(s) for the contained data.
PayloadSize	1	Number of bytes of data contained in this packet from next field onward excluding the checksum field.
SourceID	1	Unique number to identify the source device which has transmitted the contained data.
PacketType	1	Number to identify the type of data contained the packet.
Payload	0 ⋯ 255	The actual data bytes to be communicated among devices.
Checksum	1	Modulo 256 checksum

Table 5.1 General communication packet structure

The communication protocol is general enough to be implemented by all the robots, coordinators and the control center. The communication packets are divided into two broad categories

- Reports
- Commands

Reports are the communication packets which are sent by the agents or the coordinators in response to some command or event. The command packet contains the data for performing some action at agent or coordinate side. Usually the report packets are sent from agents to the coordinators and the command packets are sent from coordinator to the agents. The report and command packets can be identified by the Header values. For the implementation purpose the bytes (0x2A, 0x2A) are used as report packets header and the bytes (0x23, 0x23) are used as command packets header. The destination ID field contains a number between 1 and 255 as the destination device code. Zero is a special address which is reserved for broadcasting the communication packet to the entire network. At the moment the robust SLAM approach for single robot is GMapping, also known as Rao-Blackwellised particle filter, which required an accurate laser range finder and odometry data. Rao-Blackwellised filter is an efficient SLAM implementation which scales logarithmically with the number of landmarks. It uses an EKF of features estimate and a PF for robot state. The resampling process is crucial for PF. GMapping is the state of the art implementation of the SLAM algorithm. The research work can be extended to incorporate particle filter and extended Kalman filter like GMapping.

Particle filter approach when implemented on GPU for cooperative SLAM problem can help to overcome the computational requirement which arises because of handling very large state vectors, the computational time increase quadratically with the number of features in the map, and multiple hypotheses about robot pose. Particle filters is implemented on a GPU using CUDA because of the presence of the inherited parallelism. The particle filter approach also helps because it can handle non-linear robot motion and observation model where EKF fails if the non-linarites are too strong. It is robust against wrong data association because of resampling step and the computation cost is proportional to the number of particles. A TOF camera with higher field of view and resolution can also be used for further investigation.

In the case where GT data is not available, one could evaluate his method based on the qualitative impression of the resulting map. In the case when the blueprint of the experiment environment is available even the direct comparison among different algorithms is difficult as

different publications are evaluated with different dataset. The rawseeds project funded by European Union is an effort to provide GT data for SLAM algorithms. The communication packets are received asynchronously at the destination device. The bytes in the incoming data buffer are processed until the header bytes are found. The next byte which is the destination address, if matches' with the current device's ID then the following bytes are processed otherwise skipped until next header signature is found. On successful match of the destination ID, or broadcast ID, the next byte is processed which provides us the information about the size of packet's data in bytes which are extracted from the received bytes buffer and the modulo 256 checksum algorithm is performed over the data chunk. If the checksum calculation succeeds considering the transmitted checksum then the packet is processed further otherwise rejected.

5.1.2. Coordinator

Coordinators act as a middle layer between a command center (Server) and the mobile robots (Agents). The coordinator augments the hardware independence between the control center and agents. It translates the high level guidance commands from the control center to the low level commands, e.g. linear and angular velocities, then communicates to the agent over the available wireless hardware channel (XBee / RS232 / ZigBee). At the moment there are two separate coordinators which are designed for controlling a group of mobile robots. The first one is responsible for ground based mobile robots and the second for flying. Ground mobile robots coordinator, as shown in the Figure 5.3, can control configure and manage the ground mobile robots. The ground mobile robots coordinator can be used as a general purpose interface (middleware) to acquire data from any other custom made robot. Furthermore, it can create a cooperative local map which is built only by the ground robots; therefore, it can work independent of the control center. It can also send the ground mobile robot's pose, map or other coordinator related information to the server on request. The high level commands such as to move to a waypoint(s), explore the area with a specified robot or with the group of robots can also be commanded by the server.

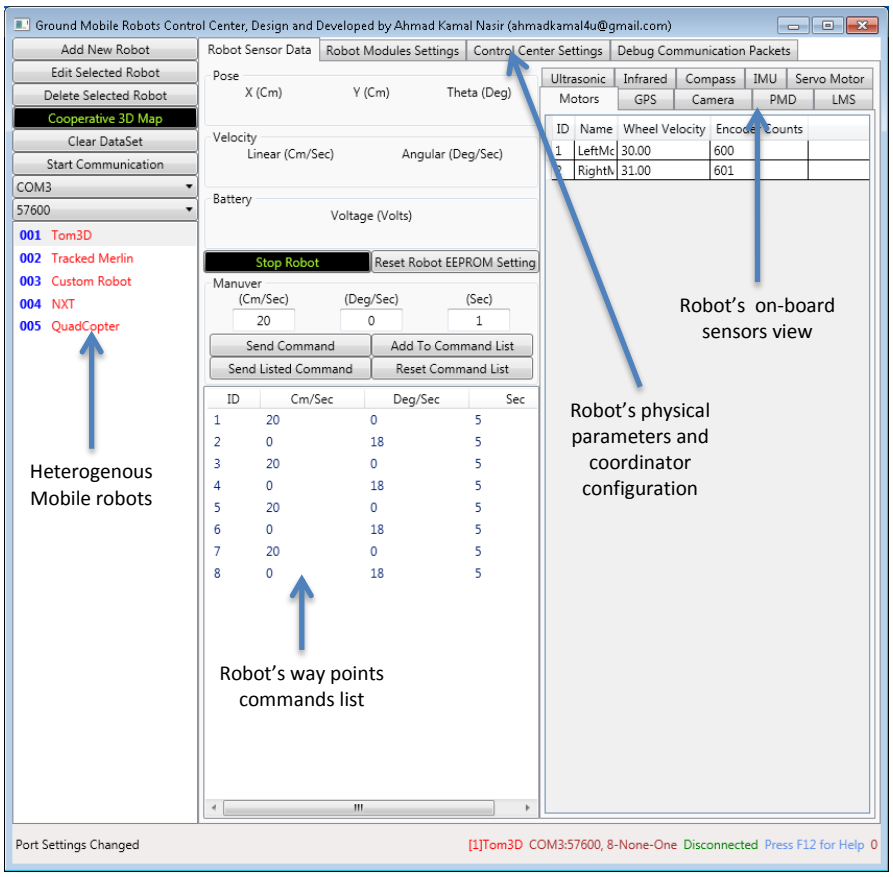

Figure 5.3 Ground mobile coordinator graphical user interface

The capability of each mobile ground robot is composed of different modules. Each physical module such as an ultrasonic sensor or a virtual module such as obstacle avoidance behavior can be configured by the coordinator. Apart from the module specific parameters each module is implemented in a standard format which is as follows

Field Name	Size [Bytes]	Description
EnableScan	1	Flag to enable/disable the module functionality
ScanInterval	1	Number of System Ticks between processing module related tasks
AutoReportSend	1	Enable/disable periodic transmission of module related reports
AutoReportInterval	1	Periodic report transmission interval

Table 5.2 General module related settings

The first tab of the ground robot coordinator," Robot Sensor Data", groups the robot sensor data for the currently selected robot in the list of the robot as shown at left in Figure 5.3. The second tab groups the robot's on-board module settings. Each physical or virtual module can be configured from the user interface. Figure 5.4 shows an interface for configuring the

robot's communication interface settings. The destination address for the robot's reports and the acknowledgements to the command sent can be configured separately to take advantage of the distributed processing. The automatic acknowledgement report in response to the command packet can also be enabled / disabled to reduce the robot network traffic.

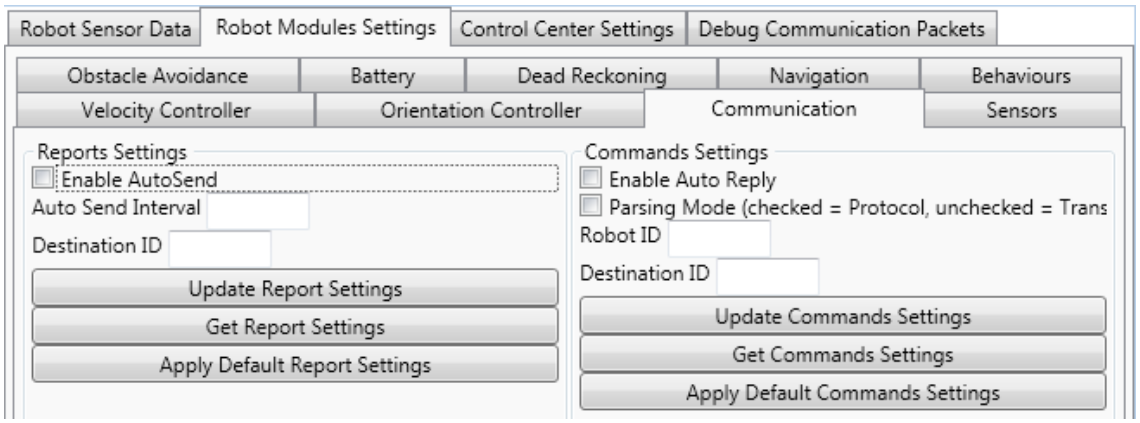

Figure 5.4 Ground mobile robot's communication module setting interface

Figure 5.5 displays the interface for configuring the electronic compass module. One can enable / disable the compass module for the currently selected robot and its poll time. The periodic interval for the compass module related report can also be configured in the interface. The module polling interval and the report interval are multiple of the system tick duration. E.g. assuming the system tick interval for the mobile robot is 20msec then a value of 50 for report interval means the report will be sent after each sec.

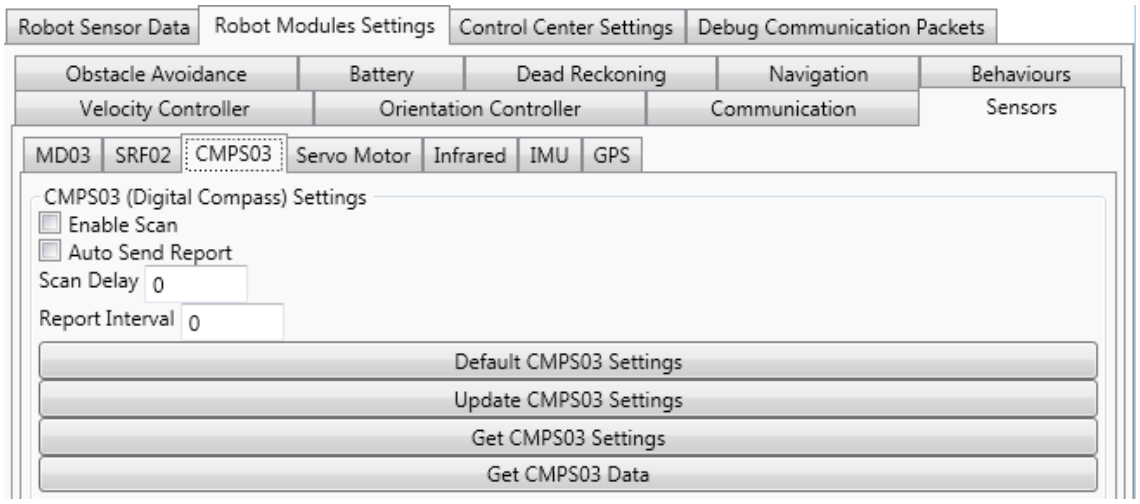

Figure 5.5 Ground mobile robot's electronic compass settings

Figure 5.6 shows the graphical interface for the motor controller module. Apart from the general module settings some MD03 motor control board related setting can be configured.

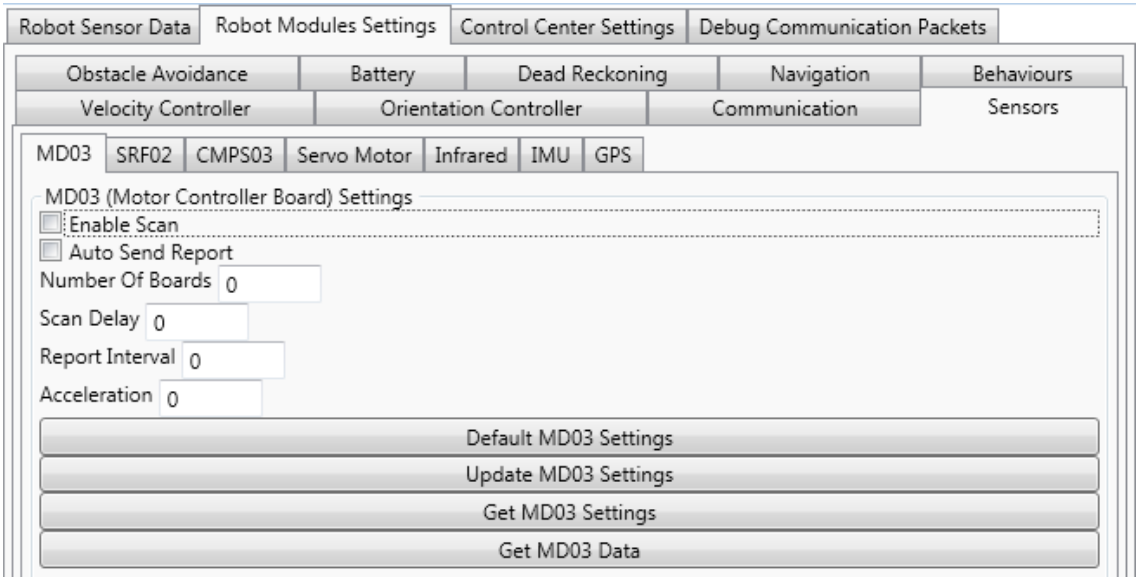

Figure 5.6 Ground mobile robot's motor controller settings

Figure 5.7 displays the settings related to the ultrasonic modules. One can specify the number of ultrasonic sensor's present on the robot. The firmware then poll an ultrasonic sensor sequentially after the polling interval expiries.

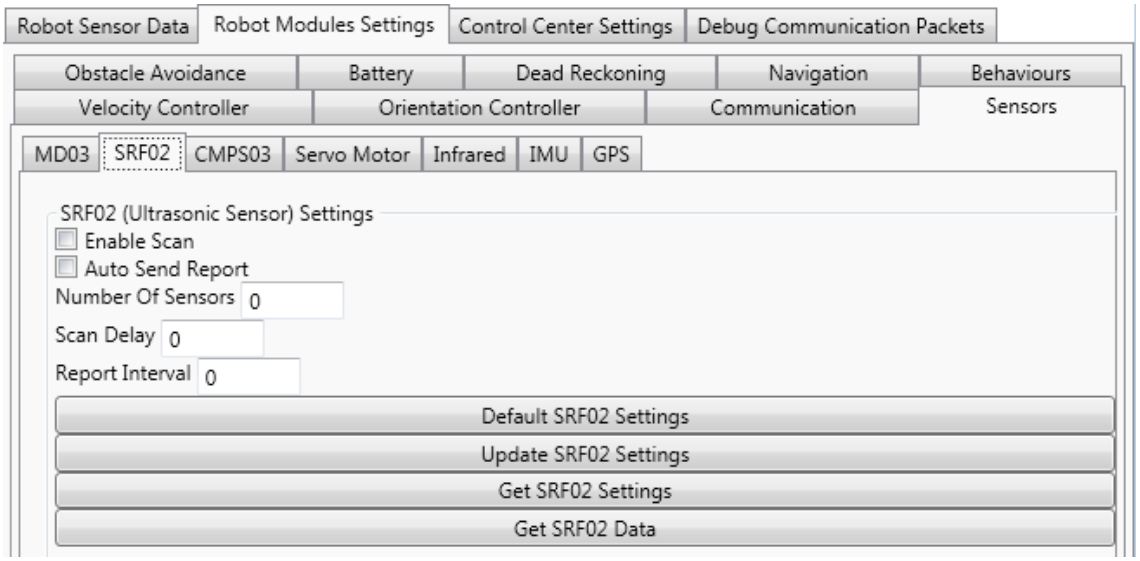

Figure 5.7 Ground mobile robot's ultrasonic sensor settings

There are some general set of commands which are implemented for each module which are

Command	**Description**
Default ModuleSettings	Apply the default module settings which are stored into the robot's EEPROM.
UpdateModuleSettings	Send the new module settings to the currently selected robot.

GetModuleSettings	Request the current settings of the specified module related to the selected robot.
GetModuleData	Command to manually request the module related data report.

Table 5.3 General module related commands

Figure 5.8 shows the interface to update the PID controller settings for the velocity control of left and right motor of the currently selected differential drive mobile robot.

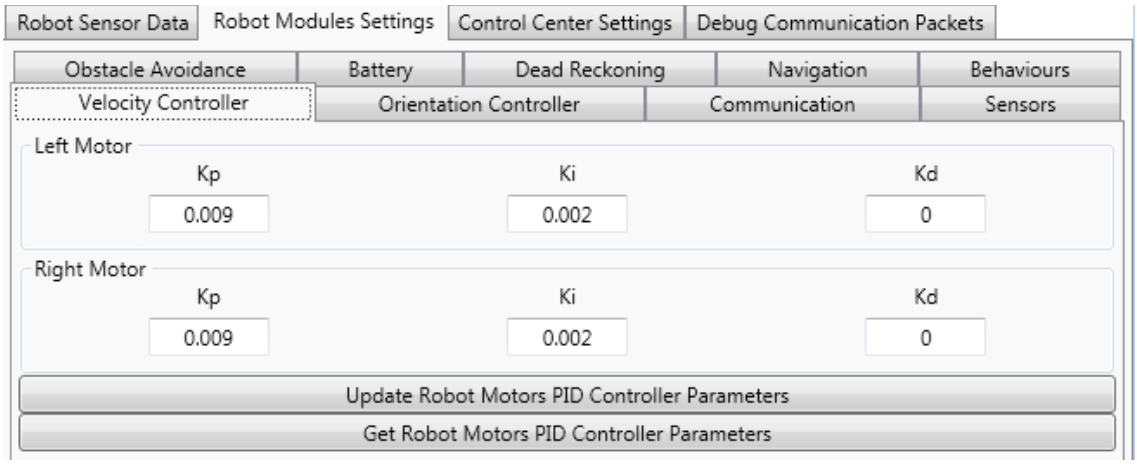

Figure 5.8 PID controller settings for the left and right motors of the selected differential drive robot

Figure 5.9 shows some coordinator related settings such as limit for the joystick control, robot's sensor data view update rate, velocity of sound to get the ultrasonic sensor range and overall coordinator system's tick interval.

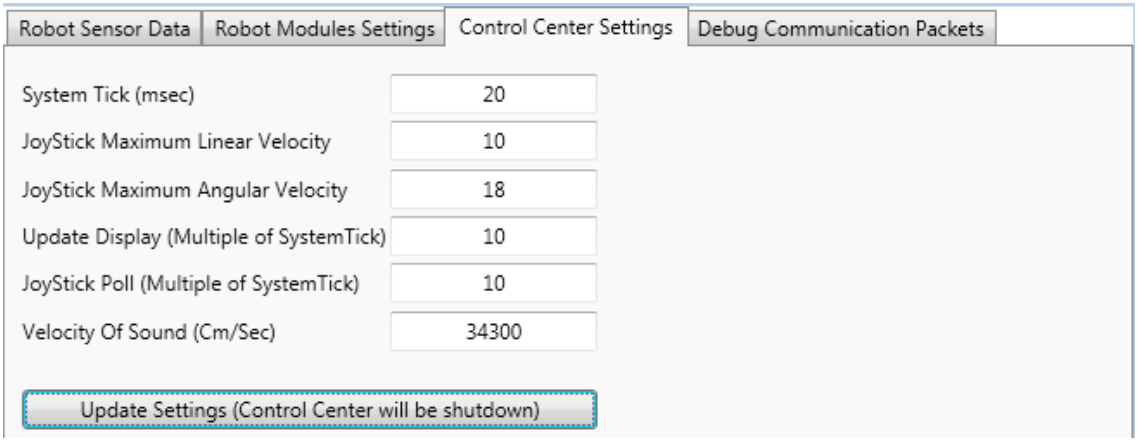

Figure 5.9 Settings related to ground mobile robot coordinator

To overcome the difficulties of troubleshooting a large robot network a graphical interface is provided, as shown in Figure 5.10, which hierarchly displays each robot's raw communication packets. This utility not only reveals the current module's settings and data report but also shows the format of a specific communication packet for a mobile robot.

Each communication report when arrives at the coordinator is parsed to check whether it is destined for it and also the data integrity of the communication packet is not compromised by calculating and verifying the packet checksum otherwise it is rejected. After the successful packet reception the packet type and Source ID are extracted so that the packet parsing settings according to the source robot and the report type are used to translate the packet contents.

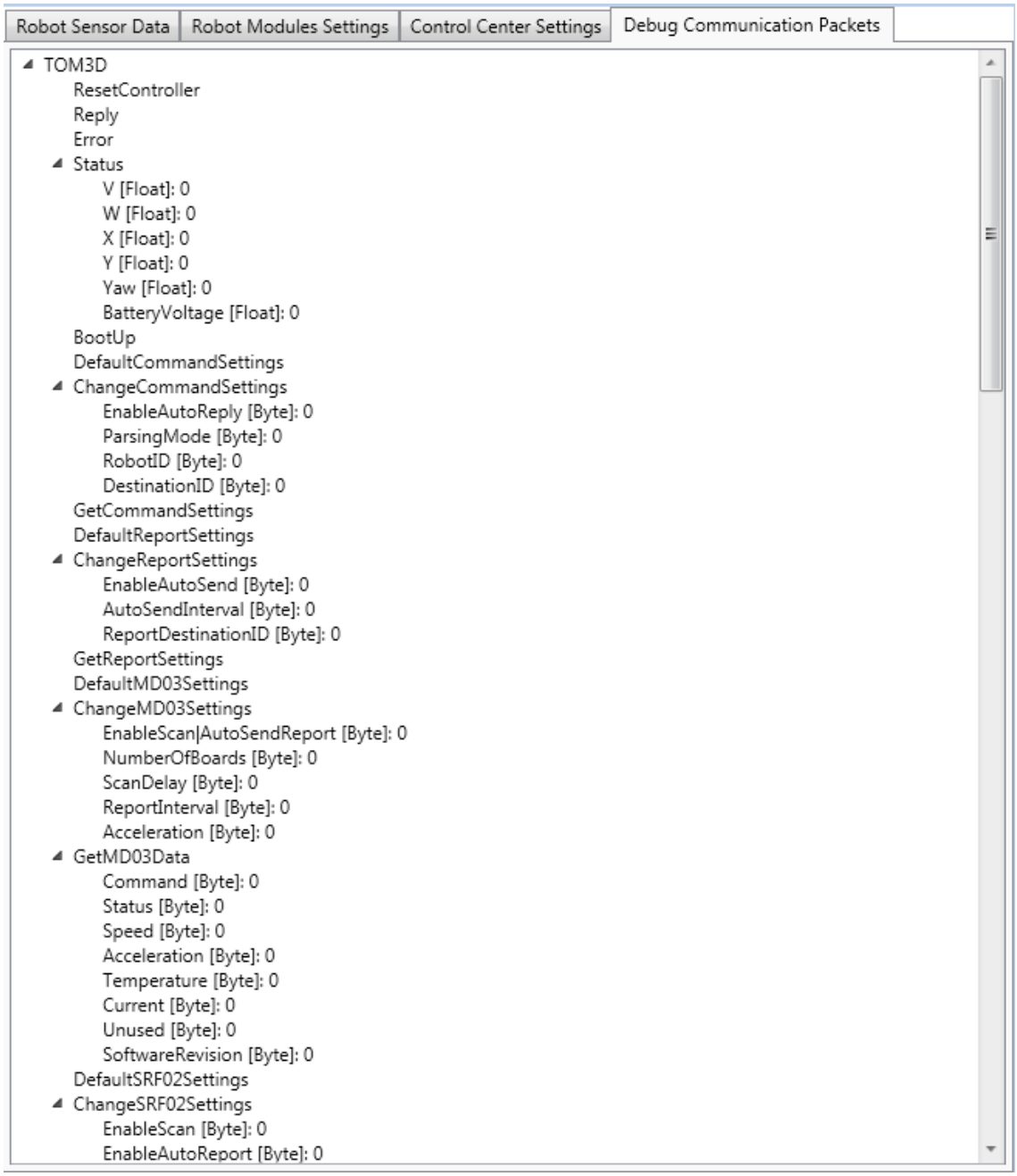

Figure 5.10 Communication packet debugging interface

The ground mobile robot coordinator not only configures and controls the existing mobile robots but also a new mobile robot can be added to the existing team of mobile robots. The

advantage is that the user only needs to add a robot to the database by the graphical wizard as shown in Figure 5.11. The user adds the sensor(s) available on the robot by specifying its pose(s) and some general settings which are common to a specific type of sensor type. The custom communication protocol layout for sending/receiving commands to/from the robot is also specified by the graphical interface. The sensor pose is useful for range sensors which require this information to build a map of the environment. Furthermore, a 3D model of the robot can also be specified which can be used to render on the combined map.

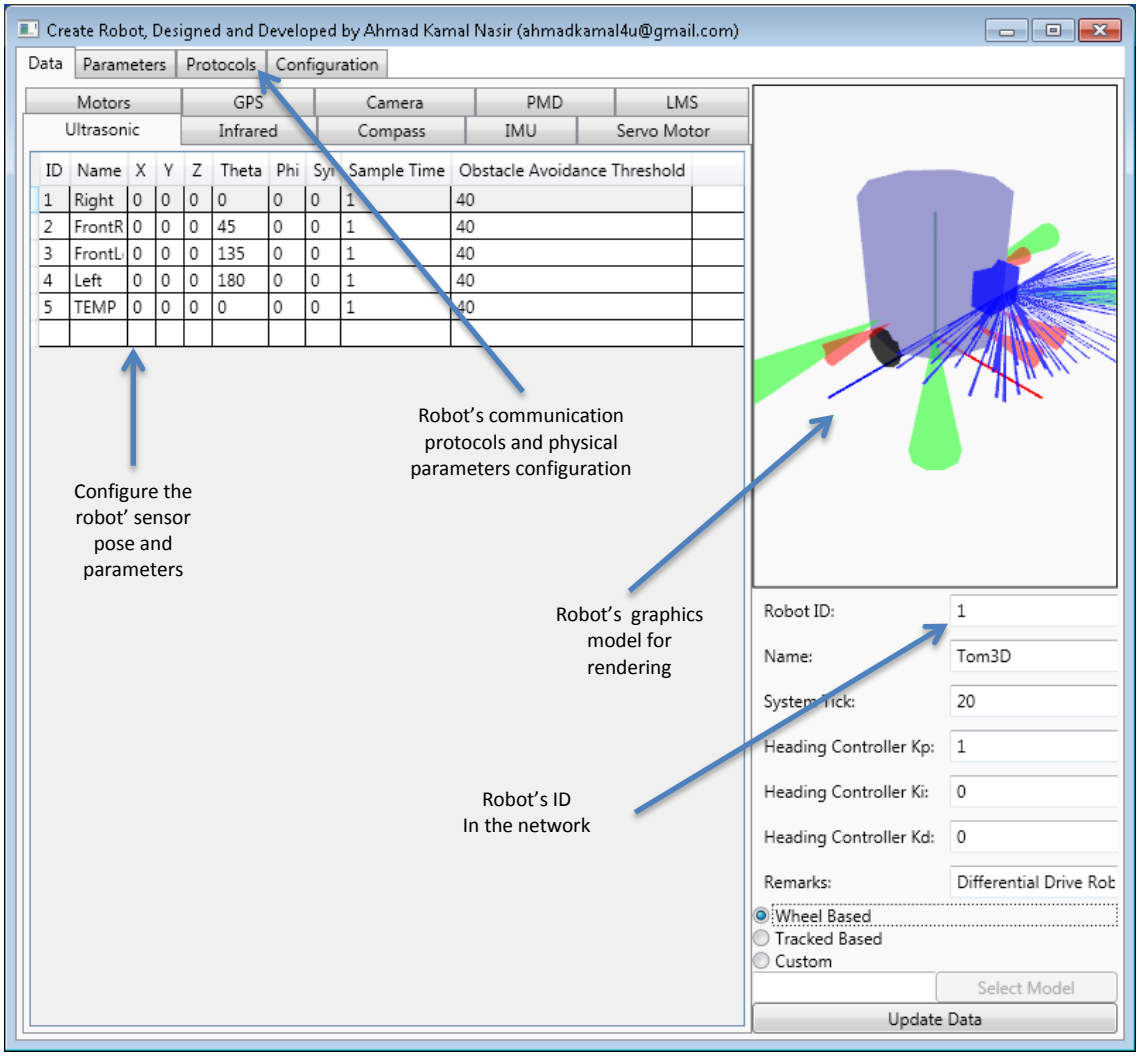

Figure 5.11 Add/Edit Ground mobile robot configuration

To ease in the creation of the cooperative map, the sensor's data reports received from different ground mobile robots are stored in a database table of that sensor type. For example the laser scans reports from all the robots equipped with laser range scanner are stored into the laser range scan table of the database. The tables of the database are shown in the Figure 5.12. This mechanism helps to fuse specific sensor information from different robots into the cooperative local map of the coordinator. To make an online map from the range

measurements acquired by ground mobile robots a separate add-in was developed which can generate the cooperative map. The application when runs query the robots poses and corresponding range sensor pose from the database and render them online.

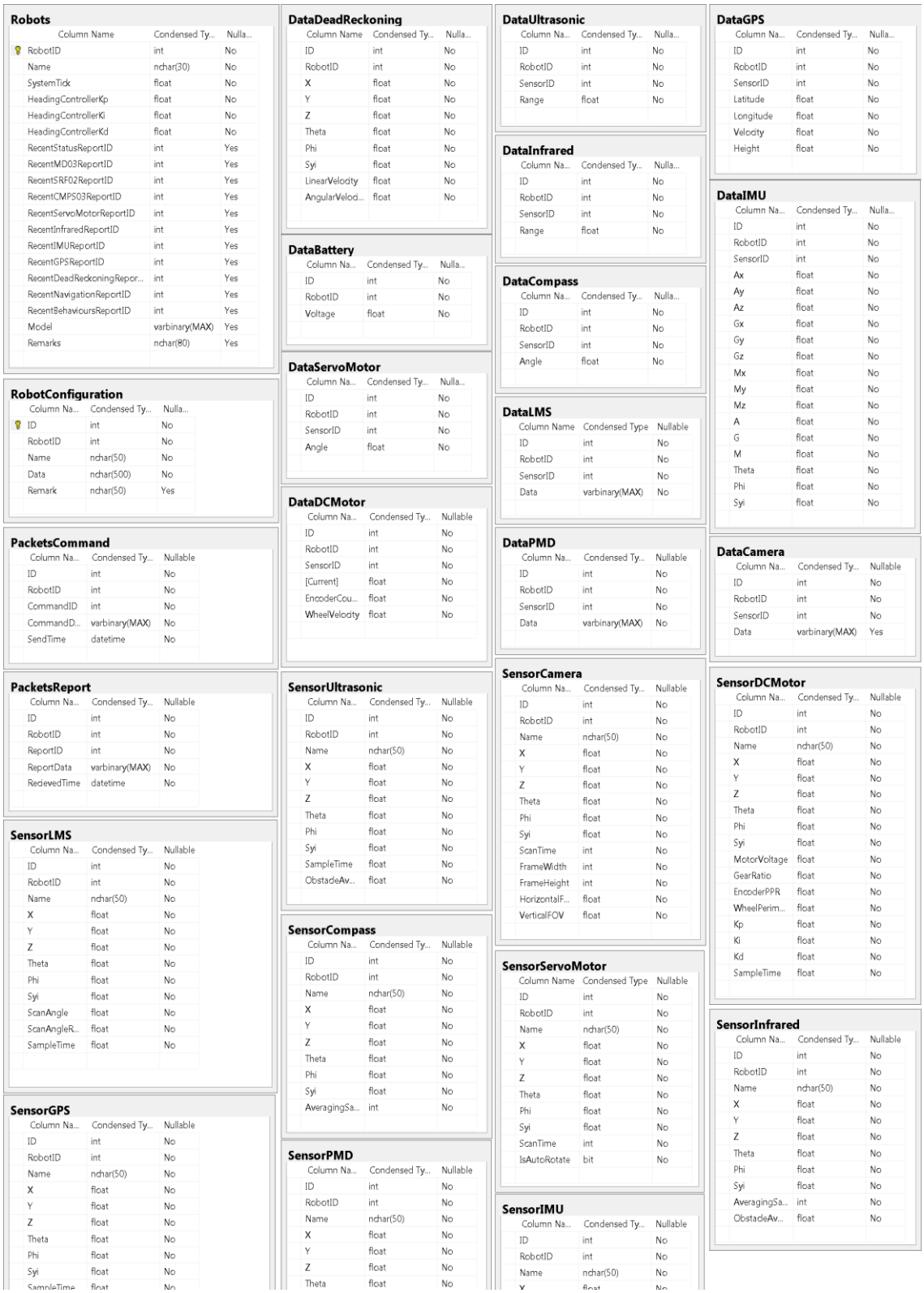

Figure 5.12 Structure of the database tables

The coordinator can also create and render a grid map of the environment which the team of mobile robots uses for navigation and there path planning.

Figure 5.13 shows a utility which creates a grid map of the environment and renders the robot over the map for the visual feedback to the user. Furthermore, this program at start-up read an existing grid map if available.

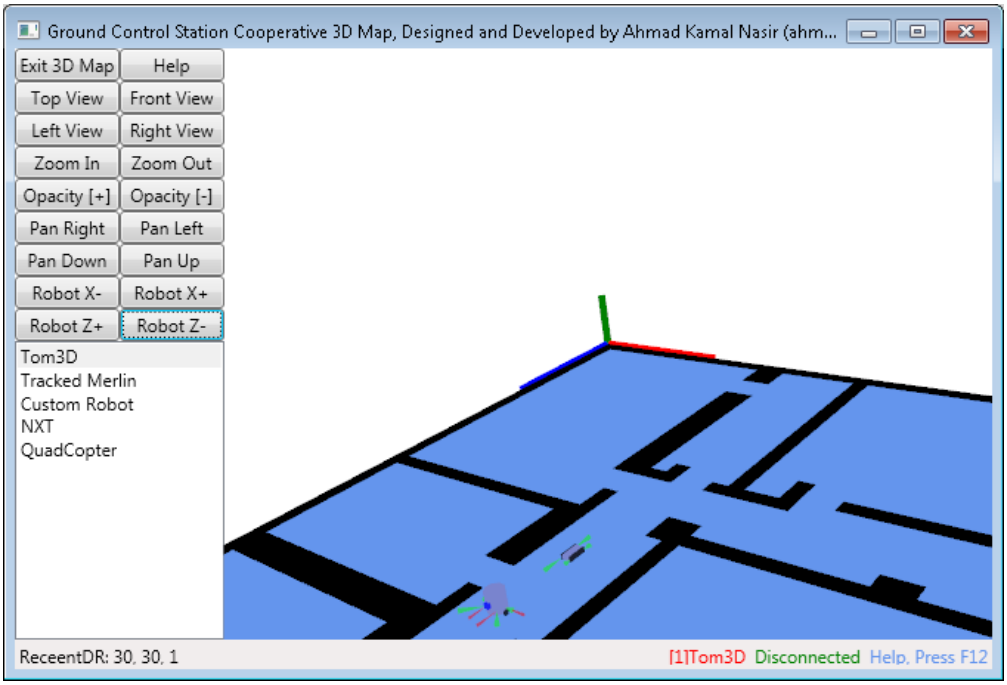

Figure 5.13 Online cooperative map generator utility

Figure 5.14 displays the top view of the grid map used by the two ground mobile robots for navigating cooperatively within the mapped indoor environment.

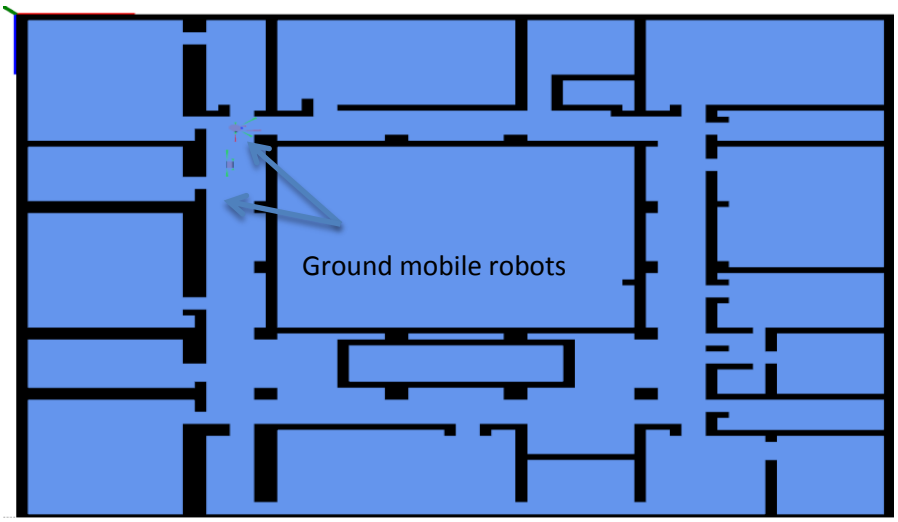

Figure 5.14 Ground mobile coordinator's local grid map

The coordinator software is running on a PC with a wireless transceiver with RS232 port. The transceiver is configured into a point-to-multipoint configuration. When the communication packets are received at the coordinator, they are parsed, verified (checksum) and queued. Robots communication packets are queued and later processed for mapping and data storage into a database. Each mobile robot can be controlled either in autonomous, semi-autonomous or manual mode. In the autonomous mode the mobile robots has been given a set of waypoints and the mobile robot follow the way points and avoid obstacles during execution of waypoints based on the information of ultrasonic and/or infrared sensor. In the semi-automatic mode the robots are given the set of way points but the robot trajectory execution can be overridden by the joystick. In the manual mode the robot follows the command from coordinator using joystick. The mounted RGB-D camera, Kinect, is connected to the embedded PC. A software utility is running on the embedded PC which parses the distance information and then sends the distance information via the WLAN to the ground based coordinator PC.

5.1.3. Agents

Agents are ground/aerial based mobile robots. They are responsible for the robots' control system of the guidance tasks. Furthermore, they have the navigation system for their local/internal tasks.

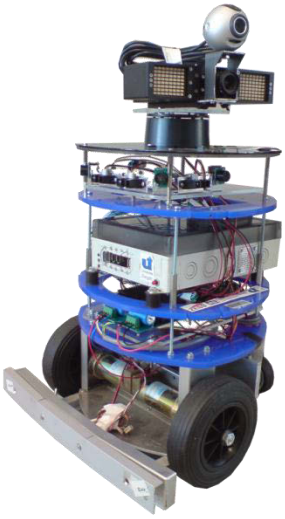

Figure 5.15 Tom3D ground mobile robot

Figure 5.16 Tracked Merlin ground mobile robot

The multi robot network consists of ground based mobile robots and aerial robots. At the moment the ground based robot system consists of two robots, TOM3D (Tele Operated Machine with a 3D PMD camera) as shown in Figure 5.15 and tracked MERLIN (Mobile Experimental Robot for Locomotion and Intelligent Navigation) as shown in Figure 5.16. Tracked MERLIN is a tracked based differential drive mobile robot designed for rough terrain

in an outdoor environment. TOM3D is a ground based mobile robot which is designed for indoor environment. Each robot is equipped with a different set of sensors e.g. TOM3D is equipped with gyroscope, accelerometer, digital compass, magnetometer, ultrasonic sensor, infrared sensor, bumper switches, a Kinect camera and a laser scanner.

For data processing of Kinect camera and laser scanner an embedded PC is mounted on TOM3D which runs a 1.8 GHz Pentium M processor and equipped with 1GB RAM. The wheels of TOM3D are integrated with high resolution quadrature encoders. The ground based tracked MERLIN mobile robot is equipped with digital compass, GPS, ultrasonic sensors and track drive motors integrated with quadrature encoders. Furthermore, it has front and rear wireless cameras and microphones. Both ground based robots are equipped with 2.4GHz, 802.15.4 based 500mW RF transceivers which can be configured in a point-to-multipoint mode. The camera images from the TOM3D robot are transmitted by the built-in WiFi of the embedded PC. Where the camera images from the Tracked MERLIN robot are transmitted by a 5.8GHz transmitter which can be multiplexed to transmit the front or rear camera by the control board.

5.2. Firmware and Hardware

The control board and the firmware are also designed to be modular so that they can be used and customized by any robot requirement. The firmware is developed with in such a way that a variety of sensor's drivers such as sonar, compass, IR, etc. are developed which can be enabled or disabled for a particular robot configuration.

5.2.1. Firmware

Each ground based mobile robot's control board is running a control system firmware. The firmware is designed in a modular way so that each robot's firmware can be reconfigured wirelessly to enable or disable a particular sensor and its configuration parameters for control and reports according to the availability of that sensor for that robot. Therefore the scalability was kept in mind while developing the firmware. Each module has some common general settings and communication packets which are described in Table 5.2 and Table 5.3. This format for the modules and communication packets was developed by keeping in mind that the future expansions to the existing features are easier to be implemented.

Since each robot has a different set of modules, therefore, for the ease of implementation of the firmware for different robots, all the module settings for a specific robot are grouped together in a configuration file. To develop a firmware for a robot the user can use DaVE [104]

for generating the initialization code for the Infineon C167 MCU by the help of a graphical environment. DaVE can generate a Keil compiler based project which can be opened by in the Keil IDE. Then all the developed drives, modules and a template configuration file are added to the project. The configuration file is modified according to the desired requirement of each module. For example the dead reckoning module uses the wheel diameter, gear ratio, pulses per revolution and wheel base parameters which can be configured. The robot's network id can be configured for communication module and the default value for report packet interval for each module can be configured. And then finally each of the modules can be inserted into the firmware at appropriate position in the main file. The control loop of the firmware architecture is divided into the three phases. During the first phase each modules acquire the sensor data and preprocess the data. If an error occurs during the sensor poll then the error report is prepared and added to the transmission queue. Input phase acquire the data such as from encoders, ultrasonic sensors, inertial measurement units, analog channels and etc. During the processing phase the computation are performed such as processing of coordinator commands, motors velocity controllers, dead reckoning and etc. and finally during the output phase the velocity control commands are applied, navigation commands are processed and the reports which have be queued are processed.

System peripheral initialization code generated by DaVE
Module's Initialization code • Load system settings from EEPROM • Initialize Commands Queue • Initialize Repors Queue • Send system boot-up report
System Control Loop Start
Input Phase
• Specify modules which acquire sensor data • Send error reports accordingly.
Processing phase
Ouput phase

System Conrol loop end

Table 5.4 Pseudo-code for modular robot firmware

The overall structure of the main file is as follows. The firmware has the responsibility to acquire the information from various onboard sensors and external attached boards and then preprocess the raw information. Furthermore, the reports are sent to the coordinator. Commands (Linear/Angular Velocities, configuration parameters, and waypoints) are received from the coordinator and processed by the firmware and then forwarded to control algorithms running onboard. Since the robots are intended to finish their assignments autonomously, it is very important for them to know their accurate positions in the environment in order to make next decision. The sensors used for the localization of ground robots are incremental encoders and low cost Inertial Measurement Unit (IMU). Due to the complementary properties of odometry and IMU, a Kalman Filter based algorithm (Simon, 2006) and its derivatives are used because of system motion constrains (Bruno, 2009).

5.2.2. Hardware

For all the ground based mobile robots, a multipurpose control board is developed based on a 16-bit Infineon MCU. The board has various digital and analog I/O channels for common robot sensors such as ultrasonic, infrared, digital compass, inertial measurement unit, global positioning system, wheel encoders and various digital and analog inputs and outputs. The schematic for the general purpose control board is shown in the Appendix C.

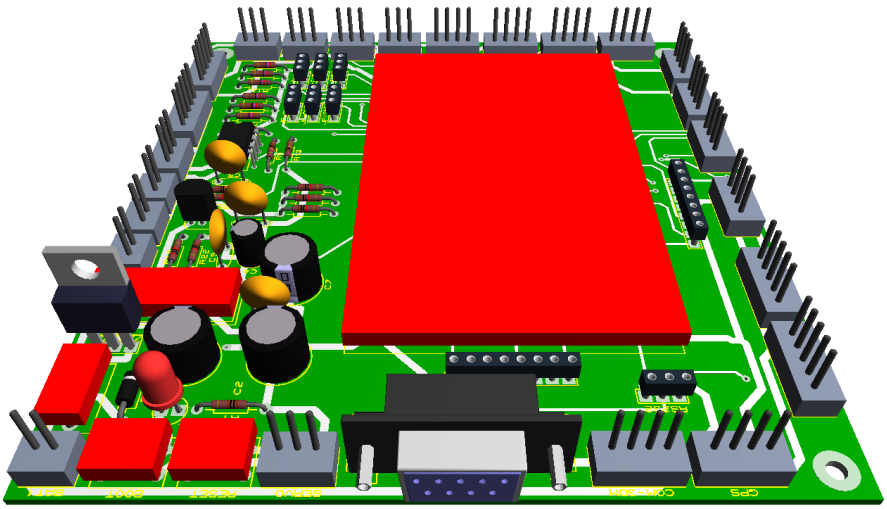

Figure 5.17 Hardware of general purpose ground robots control board

For the communication of the control board with the coordinator it is also equipped with a radio frequency modem as shown in . The radio frequency modem communicates with the control board via serial port and uses the IEEE 802.15.4 standard to communicate with the remote node. The communication modems are configured in a point to multi-point configuration. The master modem which is attached to the coordinator PC can receive the reports from all the slave modems mounted on the ground agents. Where the command transmitted by the master is received by all the slaves and the slave which is the destination of communication packet process it further where all the other reject and wait for another packet.

Figure 5.18 Agents Communication Modem based on IEEE 802.15.4

The communication packet uses module 256 checksum algorithms for transmission error checking. The wireless transceiver has the built-in error checking capability but this added error checksum mechanism ensures that the designed protocol remains independent from the hardware medium of transmission.

5.3. Simulation Environment

To overcome the difficulties of the hardware implementation, resources limitation and to reduce the algorithms development time a mobile robot simulation environment can be used. There are many commercial and open source mobile robot simulation softwares available in the market. Any mobile robot simulation software such as PSG, Webbots, USARSim or others can be used to simulate the robot's sensor data. The presented research work proposes USARSim. USARSim [46] is a simulation environment used in the presented research work which is based on the Unreal Tournament game engine. The simulation environment as shown in the Figure 5.19 provides us virtual ground and aerial robots in a map. The ground robot

platform utilized in the simulation experiment is based on a realistic looking model of Pioneer2 robot. The ground robot is equipped with a SICK laser scanner and wheel encoder for odometry. The quad-rotor used in this simulation environment is based on AirRobot UAV. The flying robot is equipped with an IMU and a downward looking camera. The top view of the simulation environment along with the ground robot trajectory is shown in the Figure 5.20. The ground robot is commanded to move in a square path inside the virtual environment and the flying robot is tracking the ground robot by downward looking camera. All the virtual sensors mounted on the ground and aerial robots are subject to random error.

The processing unit on the aerial robot captures camera images, as shown in top left corner of the Figure 5.19, and get the position coordinates relative to the ground robot using Haar-like based method. The quad-rotor position controller then takes the absolute coordinate of the ground robot $[x_{sl}, y_{sl}, z_{sl}]$ estimated by its SLAM algorithm, together with the relative position of aerial robot $[x_G, y_G, z_G]$ estimated form the camera and output the desired orientation angles $(\phi, \theta, \psi)$to keep tracking the ground robot. For the detail about the aerial and ground cooperation research work the interested reader can refer [105].

Figure 5.19 Aerial and Ground Robot Cooperative Localization In USARSim

USARSim based robot simulation can be run either by the unreal tournament 2003/2004 game or by the free UDK (Unreal Development Kit) software. If one owns an unreal tournament 2003/2004 game it also comes with a level editor called UnrealEd which can be used to create the environment map and robot models. The advantage is that the game can be run in Linux environment (with some patches) and many game related textures, models and maps are

already available. Where if one uses the UDK then it is missing the game related textures to model and maps, furthermore the simulation environment cannot be run in Linux environment because the development environment is targeted for windows. For a discussion about setting a simulation environment and acquiring robot's sensor data in user program the reader can refer to Appendix D. ROS is a famous simulation environment for mobile robots, to setup a simulation environment in ROS environment is described in Appendix E.

Figure 5.20 shows a plan view of a map for simulating mobile robots in a virtual environment.

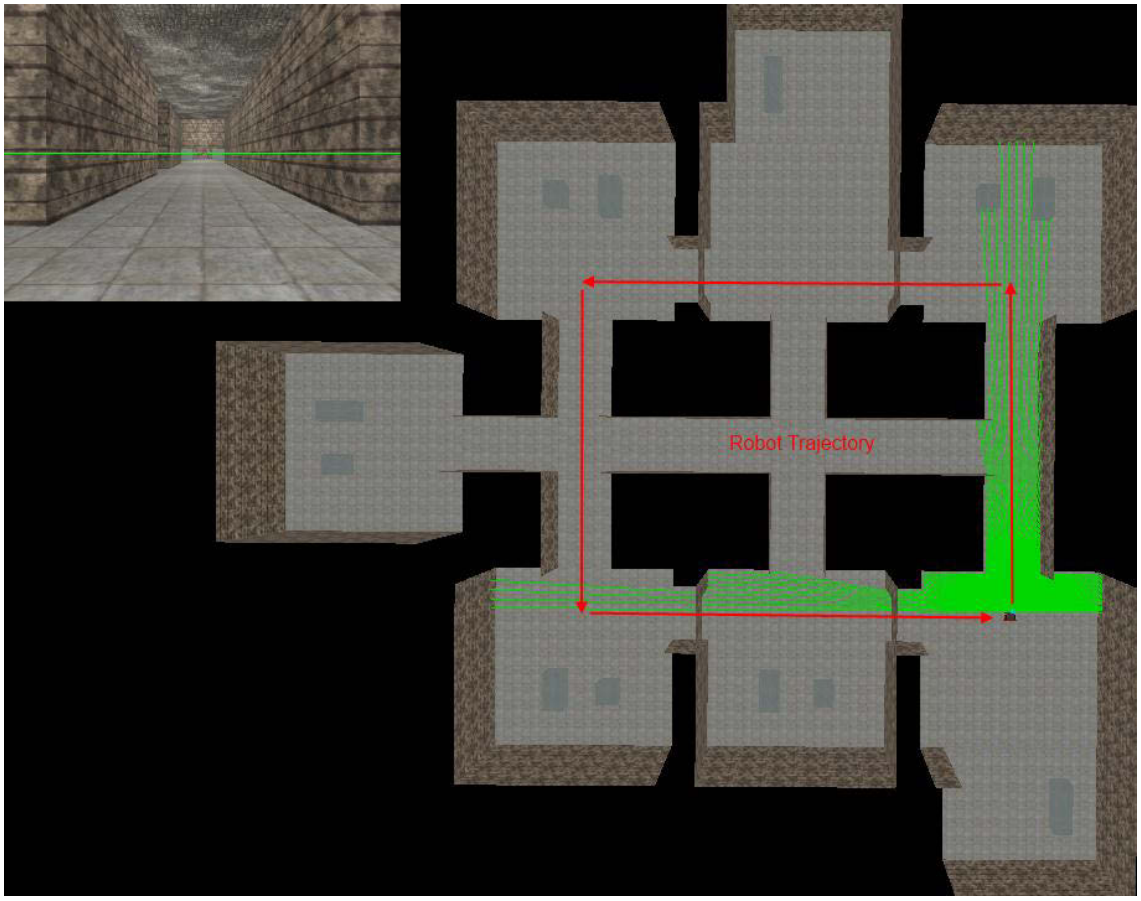

Figure 5.20 Plan view of simulation environment in USARSim

A differential drive robot is equipped with wheel odometry and a laser scanner, the green lines show the laser scan of the device. A user program (Client) can communicate with the robot simulation engine (Server) by establishing a TCP socket connection. After a successful connection between client and server the user program can send robot motion commands. The robot's laser scan and wheel encoder sensor data are periodically sent by the server which can be processed as required by the algorithm.

5.4. Summary

In this chapter the architecture of a multi-robot system is described, which consists of heterogeneous capabilities aerial and ground mobile robots for making online map cooperatively. The overall system consist of three parts; Control center, Coordinators and the Agents.

First the overall system architecture is described then other features such as communication protocol and ground Coordinator software interfaces are discussed for ground mobile robots. Afterwards, the hardware and firmware of ground and aerial mobile robots were introduced. And finally for rapid development of a multi-robot system a simulation environment based on USARSim is introduced. USARSim is a high-fidelity simulation environment for mobile robots based on the Unreal Tournament game engine. It is being interfaced to the proposed system so that it can acquire sensors data from multiple simulated robots with heterogeneous capabilities to generate the online map cooperatively

The overall system is designed in such a way that the future scalability of the robot network and the system features can be assured. The ground based mobile robot coordinator can be used as a general purpose robot control interface to acquire mobile robot's sensor data, so as to control the mobile robot using the joystick and remotely configure robot's firmware features using the graphic user interface on a windows based PC. Another novel feature of the ground mobile robots coordinator is the online generation and rendering of the meshes created from the mobile robots range data cloud points for online creation of the map.

Chapter 6.

Experiment and Results

In this chapter the results of cooperative feature based map built by a team of mobile robots and the results are discussed. The experiment is performed to test the cooperative SLAM formulization as described in Chapter 4. The experiment comprises of two differential drive robots. Both of the robots are equipped with a 2D laser range scanner for cooperative map building. To demonstrate the quick development the agents (ground mobile robots) are simulated in the USARSim environment. The agent's sensor data is acquired by the ground mobile robot coordinator and is stored in the database for future analysis.

6.1. Setup

To perform the cooperative SLAM algorithm a virtual environment as shown in the Figure 6.1 is used.

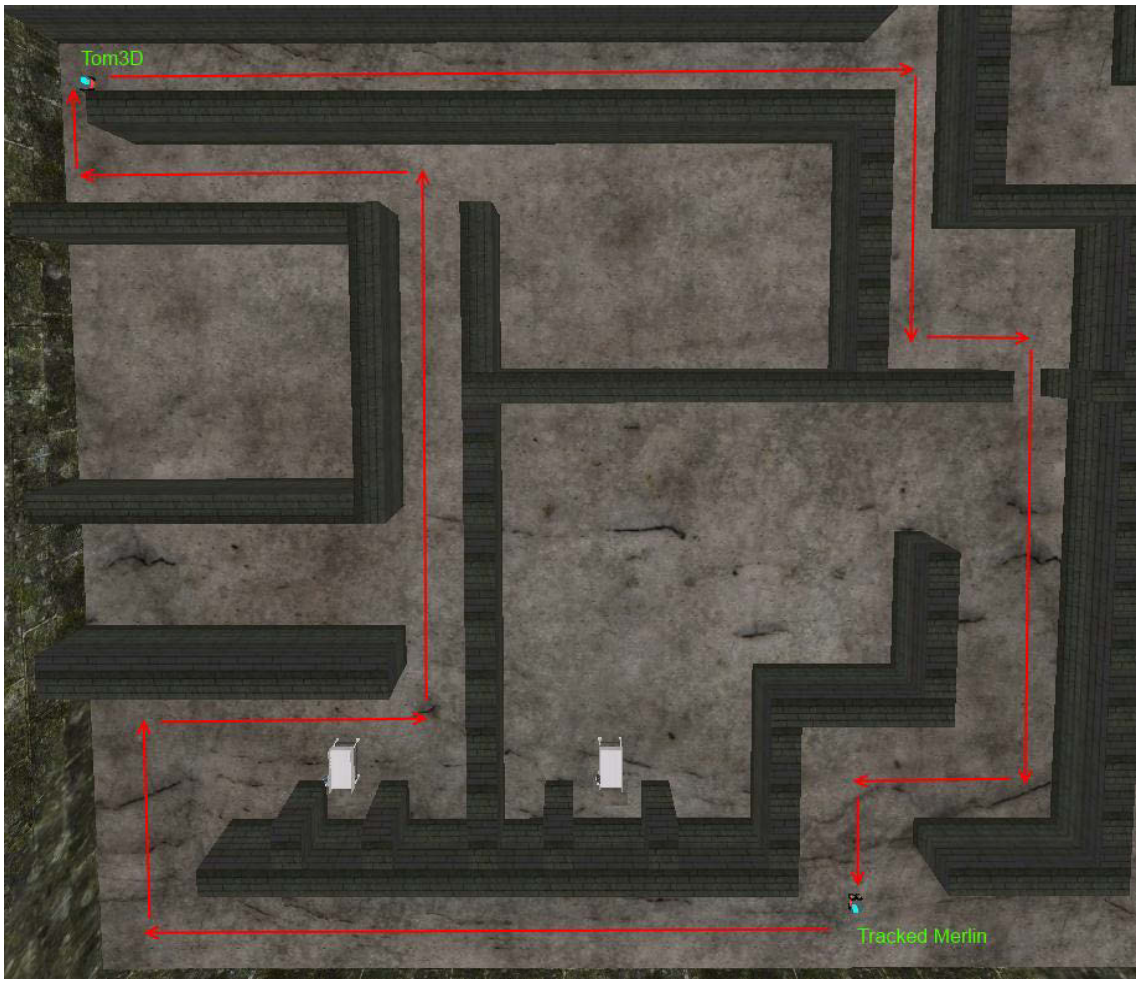

Figure 6.1 Cooperative SLAM experiment's simulation setup

The advantage of using the virtual map is that it provides us ground truth. Two differential drive mobile robots equipped with odometry modules and laser range scanner are used to perform the cooperative SLAM algorithm. The laser range readings are set to perturbed with Gaussian noise with 1cm standard deviation. The odometry module is based on the wheel encoder readings. The simulator implements a simple drift model for the odometry module. Both robots are configured to send the odometry messages at a rate of 10Hz while the laser range scans are transmitted at 5Hz.

The mobile robots are initialized at different initial poses. Each robot is programmed to follow a trajectory. The trajectory consists of many waypoints which the robot executes one after another. Each waypoint is in fact a robot pose (x, y, θ) which the robot has to acquire. The robots trajectories during the experiment are shown in the Figure 6.1. To reach a target pose $P_f = (x_f, y_f, \theta_f)$ from the current robot pose $P_i = (x_i, y_i, \theta_i)$ the robot execute a close loop position and orientation control in three steps. In the first step the robot is rotated from current robot orientation θ toward the waypoint orientation β. The orientation control consists of a P-Control which generates the angular velocity ω propotional to the difference of $\beta - \theta$. Once the error value reaches below a threshold value the orientation control phase is stopped. In the second step a position control is applied. The position control is implemented by using the state space controller as described in [106]. By considering the linear control law the closed loop system equation is as follows:

$$\begin{bmatrix} \dot{\rho} \\ \dot{\alpha} \\ \dot{\beta} \end{bmatrix} = \begin{bmatrix} -k_\rho \cdot \rho \cdot \cos(\alpha) \\ k_\rho \cdot \sin(\alpha) - k_\alpha \cdot \alpha - k_\beta \cdot \beta \\ -k_\rho \cdot \sin(\alpha) \end{bmatrix} \quad \text{Eq. 6.1}$$

The above model moves a mobile robot from an initial pose P_i to a final pose P_f but the trajectory generated is non-linear which might get obstructed with the obstacles, furthermore the control doesn't work to rotate the robot at the same position because the Jacobians are not defined at $\rho = \alpha = 0$. Therefore, the above controller is modified in such a way that K_β is set to zero and only K_ρ, K_α are used to drive the robot from $(x_i,\ y_i)$ to $(x_f,\ y_f)$. The position control is applied to calculate robot's linear and angular velocity as long as ρ doesn't become less than a threshold value during the positioning phase. During the third step orientation control is applied once again to rotate the robot from λ to the final orientation β. Thus a mobile robot move from an initial pose to a final pose in three phases; orientation, positioning and another orientation phase. Figure 6.2 visually describes the waypoint navigation process.

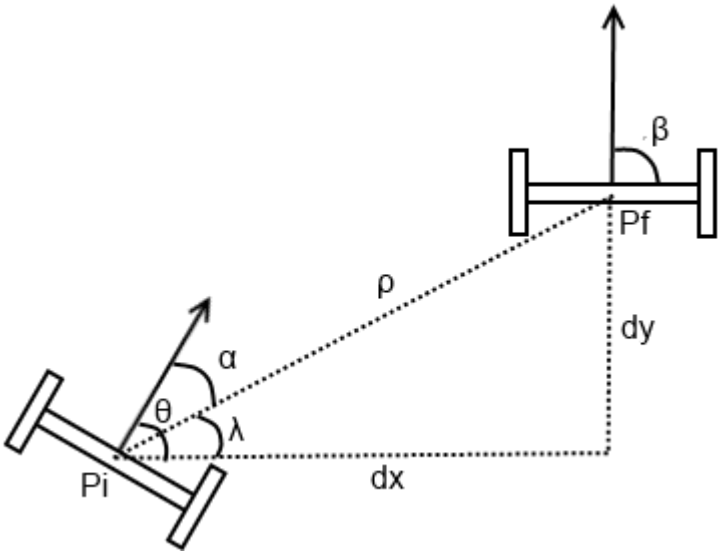

Figure 6.2 Waypoint navigation for differential drive mobile robot

The proportional gain for the orientation controller is chosen by experimentation. By increasing the gain we can control how fast the robot can rotate. For the position controller K_ρ is directly proportional to the robot linear velocity. For the stability of the control loop the gains are selected such that $K_\rho > K_\alpha$.

6.2. Map Management and Feature Fusion

As the cooperative SLAM algorithm experiment consists of two mobile robots, therefore, it is important to know how the state vector is organized, maintained and the map features are fused. The state vector is organized in such a way that the first three elements of the state vector correspond to the first robot states, the next three elements are for the second robot. In the beginning of the experiment there are no line features are present in the map, therefore the state vector only consist of robot poses. The state vector is augmented with line features as new line features are discovered. For example when the first line is detected by any one the robots, it is assigned the state vector position number seven and eight for that line feature and so on. As described in chapter 3 a geometric line feature equation is described in Hessian normal form. The ρ and α parameters of a detected line segment are in robot coordinate frame, therefore, they are transferred to global coordinate axis using robot pose before storing in to the state vector. Apart from storing the line features in the state vector a separate list of line segments is also maintained which not only includes the line segment ρ and α parameters but also the end points of the line segment. The end points of a line segment are calculated by the clustering algorithm. The line segment features list is used by the data association algorithm for matching detected line with the existing lines. Since there can be two line segments with same ρ and α values but are apart as shown in Figure 6.3,

therefore, following strategy is used to detect if the detected line segment corresponds to the existing line segment or the new it's a new line segment.

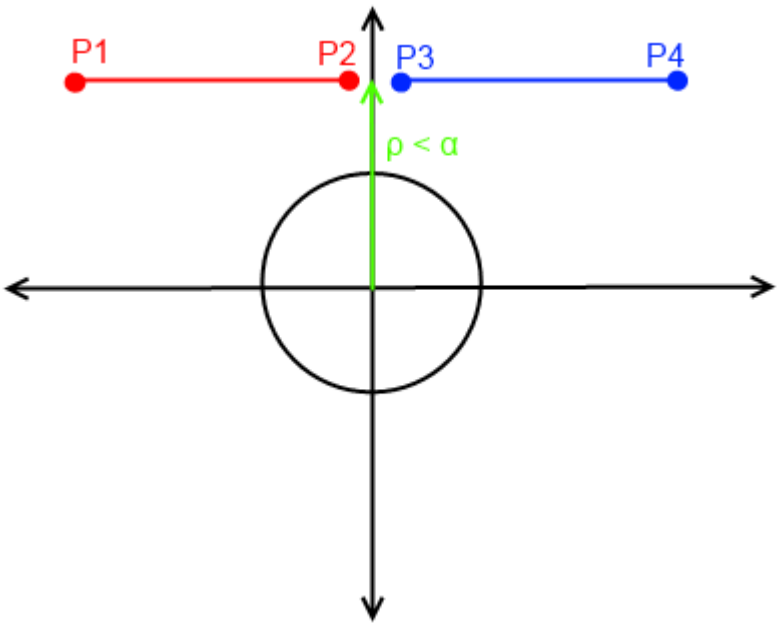

Figure 6.3 Two non-overlapping line segments with same parameters

To check whether the two line segments AB and CD overlaps as shown in Figure 6.4, the end points for one of the line segment (Say CD) is projected on to the other line segment (AB). By projection of the end point with in line segment means to check whether the end point C and D are within line segment AB. The two line segments will overlap only if when at least one of the two end points is within the line segment AB.

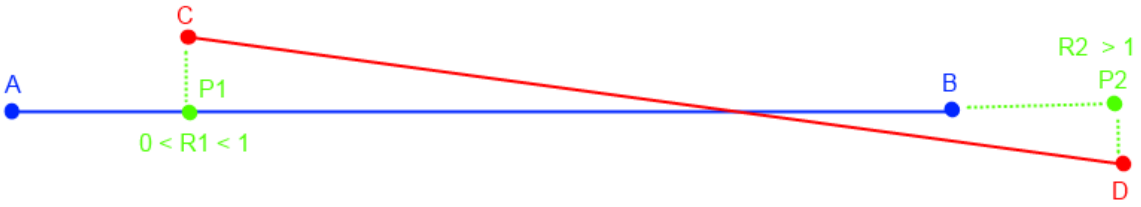

Figure 6.4 Projection of line segment's end points for overlapping check

To check whether the point C lies within the line segment formed by the point A and B. First the point C is projected on the line segment in case it does not exactly lie of the line segment. The point is projected in such a way that the projected $P1$ point is at a shortest distance from the point C. Then the projected point $P1$ is checked to see whether it lies between the point A and B. The ratio of the projected point distance from point A to the distance between points B from A is calculated. The ratio can be used to find if the projected point lies within the line segment AB. If the ratio is between 0-1 then the projected point lies within the line segment

otherwise not. If the ratio is negative then the projected point is away from point A else if ratio is greater than 1 the projected point is away from point B. Therefore, the line segment CD overlaps with the line segment AB only if one of ratio of the projected end point C or D is between zero and one. Mathematically the ratio is calculated as follows:

$$AC = (C.x - A.x, \quad C.y - A.y) \qquad \text{Eq. 6.2}$$

$$BA = (B.x - A.x, \quad B.y - A.y) \qquad \text{Eq. 6.3}$$

$$R1 = \frac{AC.x \cdot AB.x + AC.y \cdot AB.y}{AB.x^2 + AB.y^2} \qquad \text{Eq. 6.4}$$

6.3. Cooperative SLAM

The overall cooperative SLAM algorithm based on the EKF in the pseudocode is as follows

Initialize X, P, Q, R, FeatureList Establish TCP/IP Connection with the simulator
Parse the received message from Robot1
If the message contains odometry information then
Perform Robot1 pose prediction using robot motion model
Calculate and apply new motion commands (v, ω) for waypoint navigation
Else if the message contains laser range scan information then
Cluster the range scan using IEPF algorithm
Apply the non-linear least square estimation to estimate line's parameters and uncertainty
Apply the Mahalanobis distance based data association technique and validation gate
If the data association successes then
Perform the Map and Robots states correction
Else if the data association failed
Augment the state vector with the new feature
Perform the above steps for the Robot2

Table 6.1 Cooperative EKF-SLAM Pseudocode

During the initializing phase the Kalman filter and the other system variables are initialized. Then a connection with the USARSim engine is created and the robots are spawned in the virtual map. After the robots are initialized in the simulation environment they start sending the sensor messages. The main Kalman filter loop keep processing incoming messages from the robots and update the state vector accordingly. The messages from each robots are processed one after another.

6.4. Resultant Map

The resultant map generated by the cooperative EKF-SLAM algorithm is shown in the Figure 6.5. The robot were initialized at opposite ends of the map and given different trajectories.

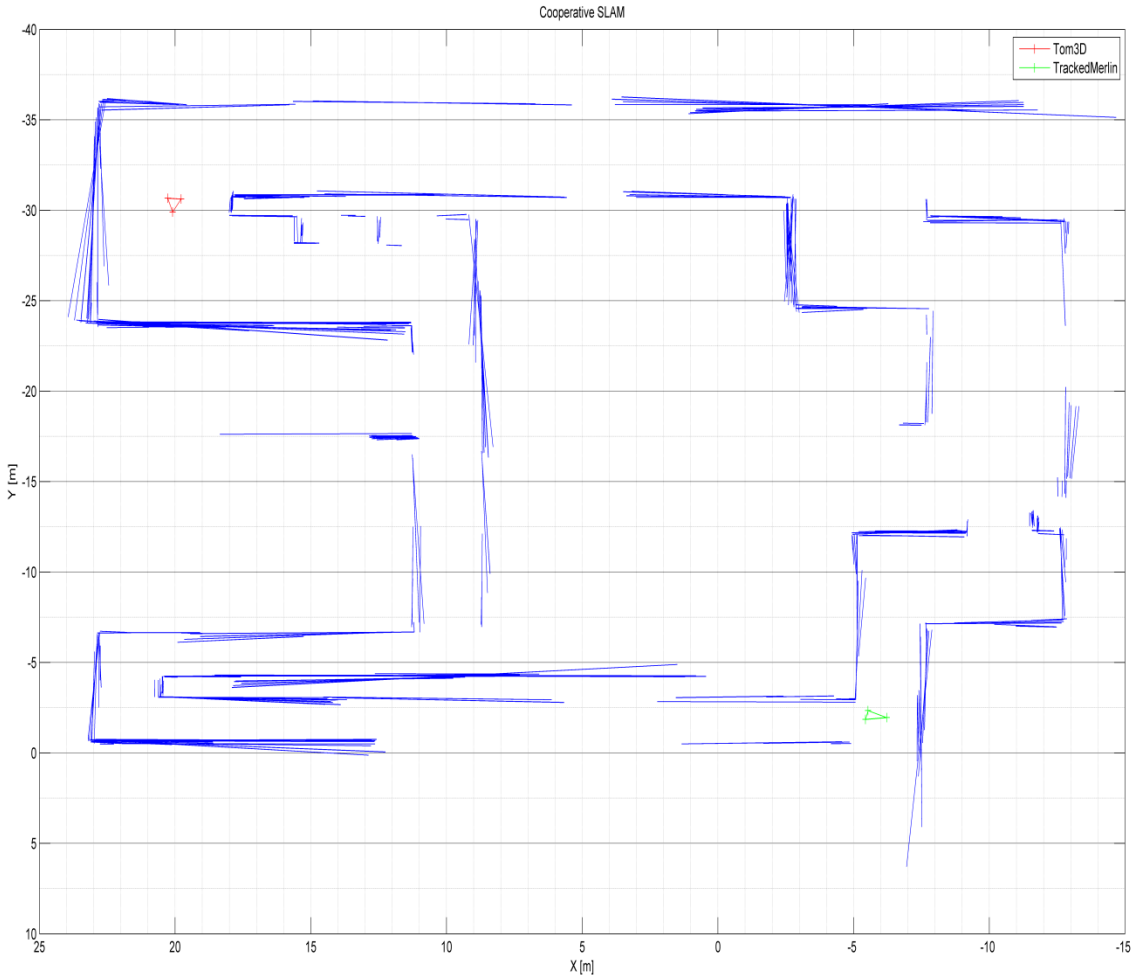

Figure 6.5 Cooperative EKF-SLAM generated line feature map

The line segments which are identified by the mobile robots are rendered as shown above. Many line segments are registered at the same location because of the noise in the laser range measurements, furthermore, during robot turning phase at the corners some new line segments are registered. By visual comparison the overall generated map quality is quite comparable to the ground truth map as shown in Figure 6.1. The cooperatively generated map by two robots was quickly generated as expected, furthermore the filter didn't diverge. Although the filter became slower as more and more features are being added to the map. This is because the data association routine requires more computation time to match the detected feature with the known existing features.

6.5. Summary

In this chapter the cooperative EKF-SLAM algorithm experiment and its results are discussed. To validate the cooperative EKF-SLAM algorithm a simulation environment is setup using USARSim setup. The simulation setup not only provides a ground truth data for result comparison but also it provides a fast method to experiment the Cooperative SLAM algorithms. To autonomously drive the robot in the modeled static environment a way point navigation controller is also implemented.

The navigation controller moves the robot from the current robot pose to a target pose in three steps. First by rotating toward the goal, then move toward the goal and finally rotation toward the target orientation.

The state vector is composed in such a way that searching for robot pose or features remains faster. The other characteristics of the line segments such as end points, length are stored in a separate list. The order of the line segments in the state vector is kept the same as in the state vector. Overlapping line segments are fused together while non-overlapping line segments with same parameters are detected also to avoid false data association. And finally the resultant map generated by the cooperative SLAM algorithm is discussed.

Chapter 7.

Discussion

In this thesis, a cooperative SLAM framework based on extended Kalman filter is formularized. Furthermore a cooperative software framework for heterogeneous mobile robots is developed. The background study related to the SLAM, the state of the art SLAM algorithms and the cooperative mobile robot simulation environments has been covered and the core topics for the SLAM implementations are discussed. SLAM is performed where a priori map of the environment is not available and it is not possible to use global positioning devices to find the accurate position of the mobile robot.

The proposed cooperative SLAM framework can use multiple mobile robots equipped with 2D and 3D range sensors for building the environment map assuming initial relative pose between mobile robots is known. The framework can also provide a general purpose interface to configure, control and manage a team of mobile robots and the sensor data.

In chapter 1 the motivation, research work scope and the related works regarding the SLAM problem and its solutions are discussed. In Chapter 2 Odometry based motion model for the differential drive mobile robots and the range sensor based observation model for mobile robots are discussed. Extended Kalman filter is used as the core estimation engine because of its simplicity for the Cooperative SLAM problem. The robot pose estimation is critical to the localization and mapping, therefore, two novel data fusion strategies are proposed. The geometric feature based map is selected for research work because it model the environment into the high level features which not only reduces the memory requirements but also helpful for semantic understanding of the environment.

Chapter 3 discusses the major modules which are necessary for successful implementation for the SLAM. Different algorithms regarding range sensor data segmentation, feature estimation, data association, map update and new feature augmentation in to the existing map are also discussed. Non-Linear least square estimation technique is used to extract the 2D geometric lines from the range data. The non-linear estimate is not biased toward the minimization of error with respect to x or y axis, instead it minimizes the error of the measured points with respect to the linear distance perpendicular to the estimated line. Two algorithms namely RANSAC and Hough transformation are used to extract the 3D geometric planes from the

point cloud. Hough transformation estimated planes more reliably while the RANSAC algorithm was comparatively little faster than Hough transformation to extract the planes.

In Chapter 4 a mathematical cooperative SLAM formulation is described based on the extended Kalman filter. The cooperative SLAM assumes that the initial relative pose among the mobile robot is known. Each time when the estimated feature associate with the existing feature, the two features coordinates are fused. For example in case of the 2D line feature, the end coordinates the extracted line and the existing lines are merged in such a way that the longest line is archived.

In Chapter 5 the software framework which is used to control, configure and manage the heterogeneous robots is discussed. Furthermore, for the rapid development of the algorithm a simulation environment which can be interfaced to the framework is also described. The framework is a step toward the standardization of the interfaces used for a team of mobile robots. Ground coordinator provides a general purpose interface to communicate with the mobile robots and manage their sensor data. The communication protocol provides a format which can be used to implement customized communication packets. The firmware is also designed in a modular way so that the customized modules can be developed and added later on. Each module implements some communication commands and reports protocol which are essential for configuring the module remotely. Similarly the Hardware board is designed to be as general purpose as possible so that hardware sensors can be attached as required. A simulation environment based on the USARSim is also introduced for the rapid development and prototyping of SLAM algorithms.

Chapter 6 discussed the results of the cooperative SLAM experiment. Two ground mobile robots are simulated in the USARSim. Both robots are attached with a 2D laser range scanner and odometry. Both robots data is acquired by the coordinator software and then a combined map is generated by the mathematical framework similar to as discussed in chapter 4.

7.1. Outlook

Apart from different algorithms used for the individual components of the SLAM the output of implemented SLAM solution depends on the choice of the sensor used for the environment observation. Few draw backs regarding different range sensors are as follows. Range sensors such as TOF cameras and RGB-D cameras are sensitive to sunlight and distance to target object. TOF cameras are also sensitive to color of the surface and they are too noisy and sparse to build the map in outdoor environment. Laser sensors measurements are corrupted

by the glass surface. Range measurement using stereo cameras can't be used in very homogenous environments and on mirror surfaces. The laser range finder is the most accurate sensor for mapping in both indoor and outdoor environment.

Feature based SLAM performance heavily depends also on data association technology. The simplest is the nearest neighbor approach. Neira proposed a joint compatibility approach to consider correlation among map features. For a feature map based SLAM approach a more sophisticated strategy is necessary such as octree.

7.2. Contributions

Following are the contribution of this thesis

- Overview of the SLAM algorithms.
- Overview of the start of art mobile robotics simulation software's.
- Two novel mobile robot's pose estimation approach
    - Multi-sensor data fusion based on Indirect Kalman Filter
    - Data fusion between Gyroscope and Stereo vision.
- Grid map and feature map creation utilities.
- Development of the mathematical cooperative SLAM formulization based on extended Kalman filter.
- Implementation of plane extraction and geometric map building technique toward SLAM implementation.
- Sensor data fusion methodologies based on Kalman filtering.
- Novel cooperative SLAM framework for controlling, configuring and managing a team of mobile robots
- Development of standard communication interfaces for cooperating among team of mobile robots.

7.3. Future Works

Despite of two decade research the SLAM problem is not fully solved. The SLAM is solved for indoor, structured, static and small environment. For outdoor and dynamic environment it still poses many challenges, furthermore the problem of loop closure and data associations are still required research works. The solutions to cooperative SLAM among many robots are still missing the map fusion part in case the initial relative robot pose are unknown. There is also a need of methods which run in real time with the available memory even for large maps with limited computational power.

Various other issues need to be investigated such as map complexity, dynamic environment and computational requirements. The map fusion when the relative pose is not known also need to be investigated. At the moment the robust SLAM approach for single robot is GMapping, also known as Rao-Blackwellised particle filter, which required an accurate laser range finder and odometry data. Rao-Blackwellised filter is an efficient SLAM implementation which scales logarithmically with the number of landmarks. It uses an EKF of features estimate and a PF for robot state. The resampling process is crucial for PF. GMapping is the state of the art implementation of the SLAM algorithm. The research work can be extended to incorporate particle filter and extended Kalman filter like GMapping.

Particle filter approach when implemented on GPU for cooperative SLAM problem can help to overcome the computational requirement which arises because of handling very large state vectors, the computational time increase quadratically with the number of features in the map, and multiple hypotheses about robot pose. Particle filters is implemented on a GPU using CUDA because of the presence of the inherited parallelism. The particle filter approach also helps because it can handle non-linear robot motion and observation model where EKF fails if the non-linarites are too strong. It is robust against wrong data association because of resampling step and the computation cost is proportional to the number of particles.

A TOF camera with higher field of view and resolution can also be used for further investigation.

In the case where GT data is not available, one could evaluate his method based on the qualitative impression of the resulting map. In the case when the blueprint of the experiment environment is available even the direct comparison among different algorithms is difficult as different publications are evaluated with different dataset. The rawseeds project [107] funded by European Union is an effort to provide GT data for SLAM algorithms.

Appendix A

The error model for wheel encoders, accelerometer, gyroscope and electronic compass are derived using error perturbation method to estimate the errors.

Encoder Velocity Error Model

The real and ideal velocity equations for robot are as follows:

$$V_{idl}(t+1) = \left(\frac{V_L(t) + V_R(t)}{2}\right) \tag{1}$$

$$\omega_{idl}(t+1) = \left(\frac{V_L(t) - V_R(t)}{L}\right) \tag{2}$$

$$Vx_{idl}(t+1) = V_{idl}(t) \cdot \cos(\omega_{idl}(t) \cdot \Delta T) \tag{3}$$

$$Vx_{idl}(t+1) = V_{idl}(t) \cdot \sin(\omega_{idl}(t) \cdot \Delta T) \tag{4}$$

$$V_{act}(t+1) = \left(\frac{V_L(t) + V_R(t) + S_L(t)V_L(t) + S_R(t)V_R(t)}{2}\right) \tag{5}$$

$$\omega_{act}(t+1) = \left(\frac{V_L(t) - V_R(t) + S_L(t)V_L(t) - S_R(t)V_R(t)}{L + S_D(t)L}\right) \tag{6}$$

$$Vx_{act}(t+1) = V_{act}(t) \cdot \cos((\omega_{act}(t) + \Delta\omega_{act}(t)) \cdot \Delta T) \tag{7}$$

$$Vy_{act}(t+1) = V_{act}(t) \cdot \sin((\omega_{act}(t) + \Delta\omega_{act}(t)) \cdot \Delta T) \tag{8}$$

The error models of encoder velocities after simplification are:

$$\Delta Vx_e(t+1) = Vx_{act}(t+1) - Vx_{idl}(t+1) \tag{9}$$

$$\Delta Vy_e(t+1) = Vy_{act}(t+1) - Vy_{idl}(t+1) \tag{10}$$

$$\begin{aligned}\Delta Vx_e(t+1) = &\left(\frac{S_L(t)V_L(t) + S_R(t)V_R(t)}{2}\right) \cdot \cos(\Delta\omega_e(t) \cdot \Delta T) \\ &- \left(\frac{V_L(t) + V_R(t)}{2}\right) \cdot \Delta\omega_e(t) \cdot \Delta T \cdot \sin(\Delta\omega_e(t) \cdot \Delta T)\end{aligned} \tag{11}$$

$$\begin{aligned}\Delta Vy_e(t+1) = &\left(\frac{V_L(t) + V_R(t)}{2}\right) \cdot \cos(\Delta\omega_e(t) \cdot \Delta T) \\ &+ \left(\frac{S_L(t)V_L(t) + S_R(t)V_R(t)}{2}\right) \cdot \Delta\omega_e(t) \cdot \Delta T \cdot \sin(\Delta\omega_e(t) \cdot \Delta T)\end{aligned} \tag{12}$$

$$\Delta\omega_e(t+1) = \left(\frac{V_L(t) - V_R(t)}{L}\right) \cdot S_D(t) - \left(\frac{S_L(t)V_L(t) - S_R(t)V_R(t)}{L}\right) \tag{13}$$

The velocity scale factor errors (S_L, S_R) and wheel distance error (S_D) are assumed to very slow time invariant, therefore

$$S_L(t+1) = S_L(t) \tag{14}$$

$$S_R(t+1) = S_R(t) \tag{15}$$

$$S_D(t+1) = S_D(t) \tag{16}$$

Accelerometer Velocity Error Model

The accelerometer error model for real and ideal linear velocities along with the scale (S_{ax}, S_{ay}) and bias factors (B_{ax}, B_{ay}) are as follows:

$$Vx_{idl}(t+1) = Vx_{idl}(t) + S_{ax}(t) \cdot Ax(t) \cdot \Delta T + B_{ax}(t) \quad (17)$$

$$Vy_{idl}(t+1) = Vy_{idl}(t) + S_{ay}(t) \cdot Ay(t) \cdot \Delta T + B_{ay}(t) \quad (18)$$

$$Vx_{act}(t+1) = Vx_{act}(t) + \left(S_{ax}(t) + \Delta S_{ax}(t)\right) \cdot Ax(t) \cdot \Delta T + \left(B_{ax}(t) + \Delta B_{ax}(t)\right) \quad (19)$$

$$Vy_{act}(t+1) = Vy_{act}(t) + \left(S_{ay}(t) + \Delta S_{ay}(t)\right) \cdot Ay(t) \cdot \Delta T + \left(B_{ay}(t) + \Delta B_{ay}(t)\right) \quad (20)$$

$$\Delta Vx_a(t+1) = Vx_{act}(t+1) - Vx_{idl}(t+1) \quad (21)$$

$$\Delta Vy_a(t+1) = Vy_{act}(t+1) - Vy_{idl}(t+1) \quad (22)$$

$$\Delta Vx_a(t+1) = \Delta Vx_a + \Delta S_{ax}(t) \cdot Ax(t) \cdot \Delta T + \Delta B_{ax}(t) \quad (23)$$

$$\Delta Vy_a(t+1) = \Delta Vy_a + \Delta S_{ay}(t) \cdot Ay(t) \cdot \Delta T + \Delta B_{ay}(t) \quad (24)$$

$$S_{ax}(t+1) = S_{ax}(t) \quad (25)$$

$$B_{ax}(t+1) = B_{ax}(t) \quad (26)$$

$$S_{ay}(t+1) = S_{ay}(t) \quad (27)$$

$$B_{ay}(t+1) = B_{ay}(t) \quad (28)$$

Gyroscope Error Model

The gyroscope error model for real and ideal angular velocities along with the scale (S_{gz}) and bias factor (B_{gz}) are as follows:

$$\omega_{idl}(t+1) = S_{gz}(t) \cdot \Omega(t) + B_{gz}(t) \quad (29)$$

$$\omega_{act}(t+1) = \left(S_{gz}(t) + \Delta S_{gz}(t)\right) \cdot \Omega(t) + \left(B_{gz}(t) + \Delta B_{gz}(t)\right) \quad (30)$$

$$\Delta\omega_g(t+1) = \omega_{act}(t+1) - \omega_{idl}(t+1) \quad (31)$$

$$\Delta\omega_g(t+1) = \Delta S_{gz}(t) \cdot \Omega(t) + \Delta B_{gz}(t) \quad (32)$$

$$S_{gz}(t+1) = S_{gz}(t) \quad (33)$$

$$B_{gz}(t+1) = B_{gz}(t) \quad (34)$$

Compass Angle Error Model

The compass error model for actual and ideal azimuth angle along with the bias factor (B_c) are as follows:

$$\theta_{idl}(t+1) = \theta_{idl}(t) + B_c(t) \quad (35)$$

$$\theta_{act}(t+1) = \theta_{act}(t) + \left(B_c(t) + \Delta B_c(t)\right) \quad (36)$$

$$\Delta\theta_c(t+1) = \theta_{act}(t+1) - \theta_{idl}(t+1) \quad (37)$$

$$\Delta\theta_c(t+1) = \Delta\theta_c(t) + \Delta B_c(t) \quad (38)$$

$$B_c(t+1) = B_c(t) \quad (39)$$

Appendix B

Least Square Estimation

Let's discuss an example of least square estimation which explains the Least Square Estimation (LSE) process. Consider a sensor outputs a signal , $Y(t)$, which is a function of time and described by the following mathematical equation

$$Y(t) = 2t + 3$$

Let's say some periodically measured output signal of the sensor at discrete time steps, Y_k^* are available. This discrepancy between ideal and measured signal is because of the measurement errors induced by the sensor system or because of the other un-modeled effects of the sensor system in the signal. For the simulation purpose purpose we can generate the sensor measurements using the mathematical model of the sensor. For simulation of the sensor's measurement error, the sensor output is contaminated with some random number generated by some noise model (Gaussian, Uniform, etc.). This random number must reflect the behavior of the discrepancies present in actual measurements. The simulated measurements can be produced by the following equation

$$Y_k^* = Y_k + \mathcal{N}(\mu, \sigma^2) = 2(k-1)T_s + 3 + randn(0, \sigma^2) \qquad wheres\ k = 0 \dots n$$

In the above equation the random number is modeled by a Normal/Gaussian distribution which is described by a mean, μ, and standard deviation, σ. In linear least square estimation one thinks that the estimation, $\hat{Y}_k$, of the obtained measurements can be modeled as polynomial, which is mathematically represented as follows

$$\hat{Y}_k = a_0 + a_1[(k-1)T_s] + a_2[(k-1)T_s]^2 + \cdots + a_n[(k-1)T_s]^n \qquad wheres\ k = 0 \dots n$$

Therefore the task is to calculate the coefficients of the above polynomial which can best represent, in least square sense, the measurements. Least square sense means that the **sum of the square of the errors**, between the measurements and selected polynomial, is the minimum. Mathematically it can be represented by the following equation

$$SSE = \sum_{k=1}^{n} \left(\hat{Y}_k - Y_k^*\right)^2$$

In the above example the sensor signal is represented by a first order polynomial, therefore, the polynomial chosen for estimating the sensor measurement is also of the first order, therefore

$$SSE = \sum_{k=1}^{n} (a_0 + a_1[(k-1)T_s] - Y_k^*)^2$$

The best estimate of the signal from the measurement is obtained only when the order of the polynomial matches the order of the signal. Overestimate (order of estimating polynomial is higher than actual signal polynomial) and under estimate (order of estimating polynomial is lower than actual signal polynomial) result in to sub optimal results in which the estimate diverges from the true/actual/ideal estimate. The minimum of the sum with respect to each parameter can be found by calculus, taking the derivative of the SSE with respect to each polynomial coefficient and equating it to zero.

$$\boldsymbol{\frac{\partial}{\partial a_0}(SSE) = 0 = \sum_{k=1}^{n} 2(a_0 + a_1[(k-1)T_s] - Y_k^*)}$$

$$0 = \sum_{k=1}^{n} (a_0 + a_1[(k-1)T_s] - Y_k^*)$$

$$0 = \sum_{k=1}^{n} (a_0) - \sum_{k=1}^{n} (Y_k^*) + \sum_{k=1}^{n} (a_1[(k-1)T_s])$$

$$\sum_{k=1}^{n} (Y_k^*) = \sum_{k=1}^{n} (a_0) + \sum_{k=1}^{n} (a_1[(k-1)T_s])$$

$$\sum_{k=1}^{n} (Y_k^*) = na_0 + a_1 \sum_{k=1}^{n} [(k-1)T_s] \qquad \boldsymbol{Eq(A)}$$

$$\boldsymbol{\frac{\partial}{\partial a_1}(SSE) = 0 = \sum_{k=1}^{n} 2(a_0 + a_1[(k-1)T_s] - Y_k^*)([(k-1)T_s])}$$

$$0 = \sum_{k=1}^{n} (a_0[(k-1)T_s] + a_1[(k-1)T_s]^2 - Y_k^*[(k-1)T_s])$$

$$0 = \sum_{k=1}^{n} (a_0[(k-1)T_s]) + \sum_{k=1}^{n} (a_1[(k-1)T_s]^2) - \sum_{k=1}^{n} (Y_k^*[(k-1)T_s])$$

$$\sum_{k=1}^{n}(Y_k^*[(k-1)T_s]) = a_0\sum_{k=1}^{n}([(k-1)T_s]) + a_1\sum_{k=1}^{n}([(k-1)T_s]^2) \qquad \boldsymbol{Eq(B)}$$

Eq (A) and Eq (B) have two unknowns (a_0 , a_1), therefore, solving two equations for two unknowns

$$\begin{bmatrix} a_0 \\ a_1 \end{bmatrix} = \begin{bmatrix} n & \sum_{k=1}^{n}[(k-1)T_s] \\ \sum_{k=1}^{n}[(k-1)T_s] & \sum_{k=1}^{n}[(k-1)T_s]^2 \end{bmatrix}^{-1} \begin{bmatrix} \sum_{k=1}^{n} Y_k^* \\ \sum_{k=1}^{n}[(k-1)T_s]Y_k^* \end{bmatrix}$$

In this example we have estimated the parameters of equation which is a function of time. In general the estimation equation can be parameter of any independent variable or in other words the measurements can be a function of any variable. Mathematically it can be described as follows

$$\hat{Y}_k = a_0 + a_1x + a_2x^2 + a_3x^3 + \cdots + a_nx^n$$

$$\begin{bmatrix} a_0 \\ a_1 \\ a_2 \\ \vdots \\ a_n \end{bmatrix} = \begin{bmatrix} n & \sum_{k=1}^{n}X_k & \sum_{k=1}^{n}X_k^2 & \cdots & \sum_{k=1}^{n}X_k^n \\ \sum_{k=1}^{n}X_k & \sum_{k=1}^{n}X_k^2 & \sum_{k=1}^{n}X_k^3 & \cdots & \sum_{k=1}^{n}X_k^{n+1} \\ \sum_{k=1}^{n}X_k^2 & \sum_{k=1}^{n}X_k^3 & \sum_{k=1}^{n}X_k^4 & \cdots & \sum_{k=1}^{n}X_k^{n+2} \\ \vdots & \vdots & \vdots & \ddots & \vdots \\ \sum_{k=1}^{n}X_k^n & \sum_{k=1}^{n}X_k^{n+1} & \sum_{k=1}^{n}X_k^{n+2} & \cdots & \sum_{k=1}^{n}X_k^{n+n} \end{bmatrix}^{-1} \begin{bmatrix} \sum_{k=1}^{n}Y_k^* \\ \sum_{k=1}^{n}X_kY_k^* \\ \sum_{k=1}^{n}X_k^2Y_k^* \\ \vdots \\ \sum_{k=1}^{n}X_k^nY_k^* \end{bmatrix}$$

$$\begin{bmatrix} a_0 \\ a_1 \\ a_2 \end{bmatrix} = \begin{bmatrix} n & \sum_{k=1}^{n}X_k & \sum_{k=1}^{n}X_k^2 \\ \sum_{k=1}^{n}X_k & \sum_{k=1}^{n}X_k^2 & \sum_{k=1}^{n}X_k^3 \\ \sum_{k=1}^{n}X_k^2 & \sum_{k=1}^{n}X_k^3 & \sum_{k=1}^{n}X_k^4 \end{bmatrix}^{-1} \begin{bmatrix} \sum_{k=1}^{n}Y_k^* \\ \sum_{k=1}^{n}X_kY_k^* \\ \sum_{k=1}^{n}X_k^2Y_k^* \end{bmatrix}$$

Appendix C

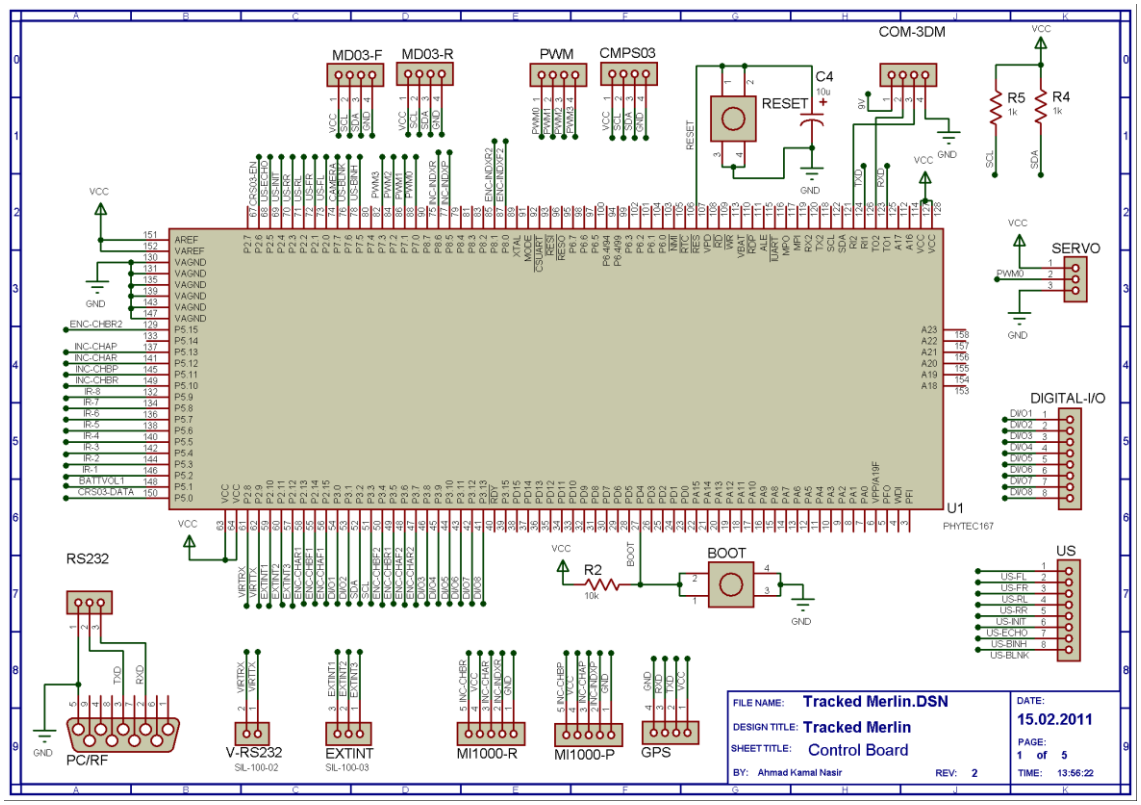
COM-3DM
MD03-F
MD03-R
PWM
CMPS03
RESET
C4
R5
R4
SERVO
DIGITAL-I/O
US
RS232
BOOT
R2
U1
PHYTEC167
PC/RF
V-RS232
SIL-100-02
EXTINT
SIL-100-03
MI1000-R
MI1000-P
GPS
FILE NAME: Tracked Merlin.DSN
DESIGN TITLE: Tracked Merlin
SHEET TITLE: Control Board
BY: Ahmad Kamal Nasir
REV: 2
DATE: 15.02.2011
PAGE: 1 of 5
TIME: 13:56:22

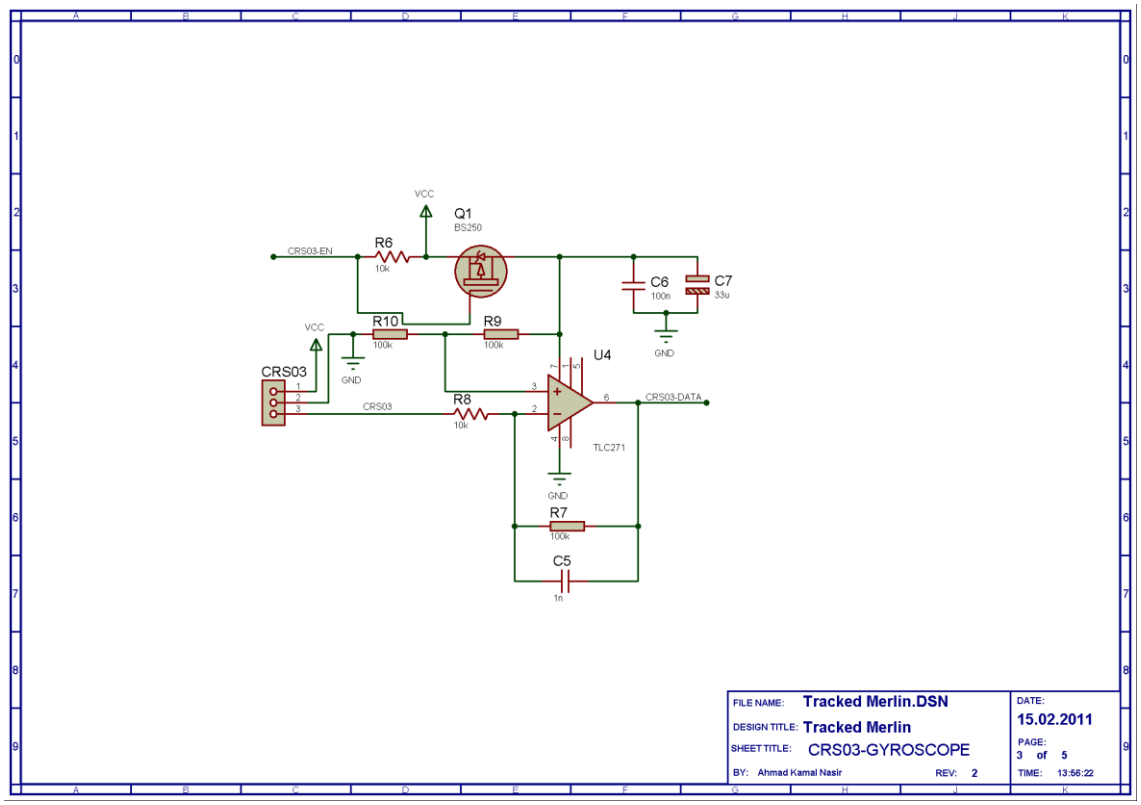
Q1
BS250
R6
10k
R10
100k
R9
100k
R8
10k
R7
100k
C6
100n
C7
33u
C5
1n
U4
TLC271
CRS03
CRS03-EN
CRS03-DATA
FILE NAME: Tracked Merlin.DSN
DESIGN TITLE: Tracked Merlin
SHEET TITLE: CRS03-GYROSCOPE
BY: Ahmad Kamal Nasir
REV: 2
DATE: 15.02.2011
PAGE: 3 of 5
TIME: 13:56:22

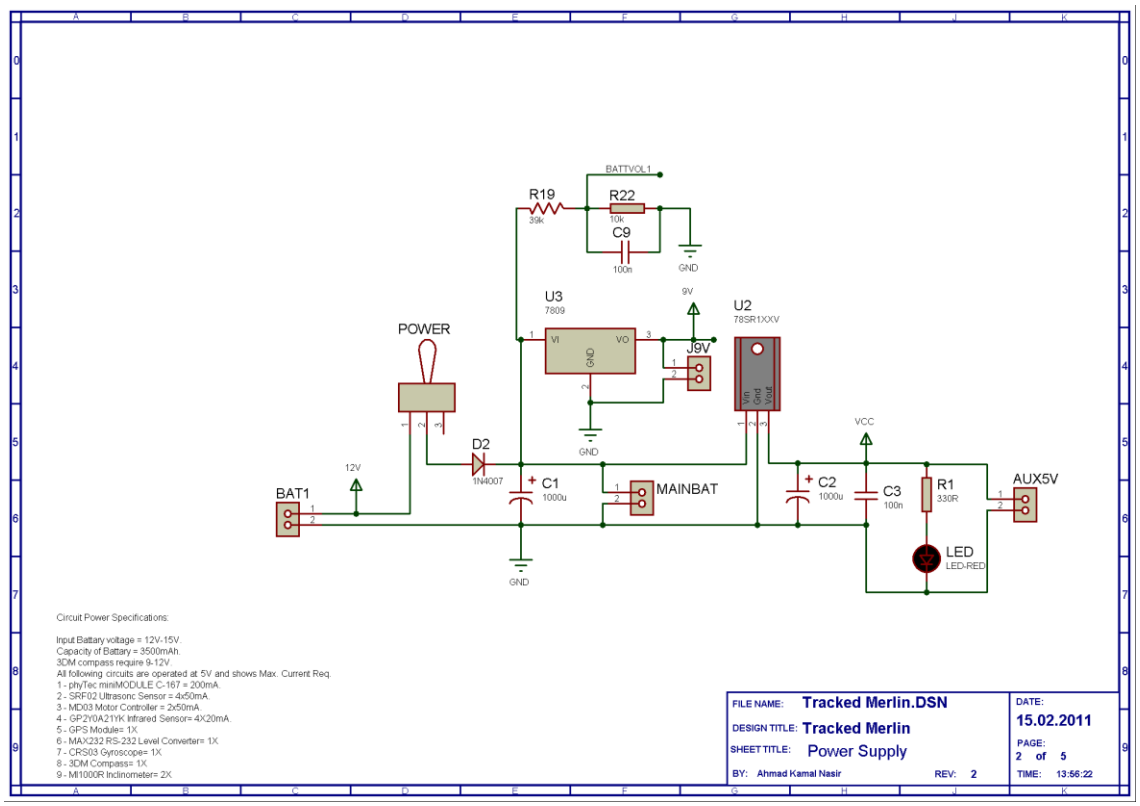
BATTVOL1
R19
39k
R22
10k
C9
100n
GND
U3
7809
9V
U2
78SR1XXV
POWER
J9V
D2
1N4007
12V
BAT1
C1
1000u
MAINBAT
C2
1000u
C3
100n
VCC
R1
330R
AUX5V
LED
LED-RED
Circuit Power Specifications:
Input Battary voltage = 12V-15V.
Capacity of Battary = 3500mAh.
3DM compass require 9-12V.
All following circuits are operated at 5V and shows Max. Current Req.
1 - phyTec miniMODULE C-167 = 200mA.
2 - SRF02 Ultrasonc Sensor = 4x50mA.
3 - MD03 Motor Controller = 2x50mA.
4 - GP2Y0A21YK Infrared Sensor= 4X20mA.
5 - GPS Module= 1X.
6 - MAX232 RS-232 Level Converter= 1X.
7 - CRS03 Gyroscope= 1X.
8 - 3DM Compass= 1X.
9 - MI1000R Inclinometer= 2X.
FILE NAME: Tracked Merlin.DSN
DESIGN TITLE: Tracked Merlin
SHEET TITLE: Power Supply
BY: Ahmad Kamal Nasir
REV: 2
DATE: 15.02.2011
PAGE: 2 of 5
TIME: 13:56:22

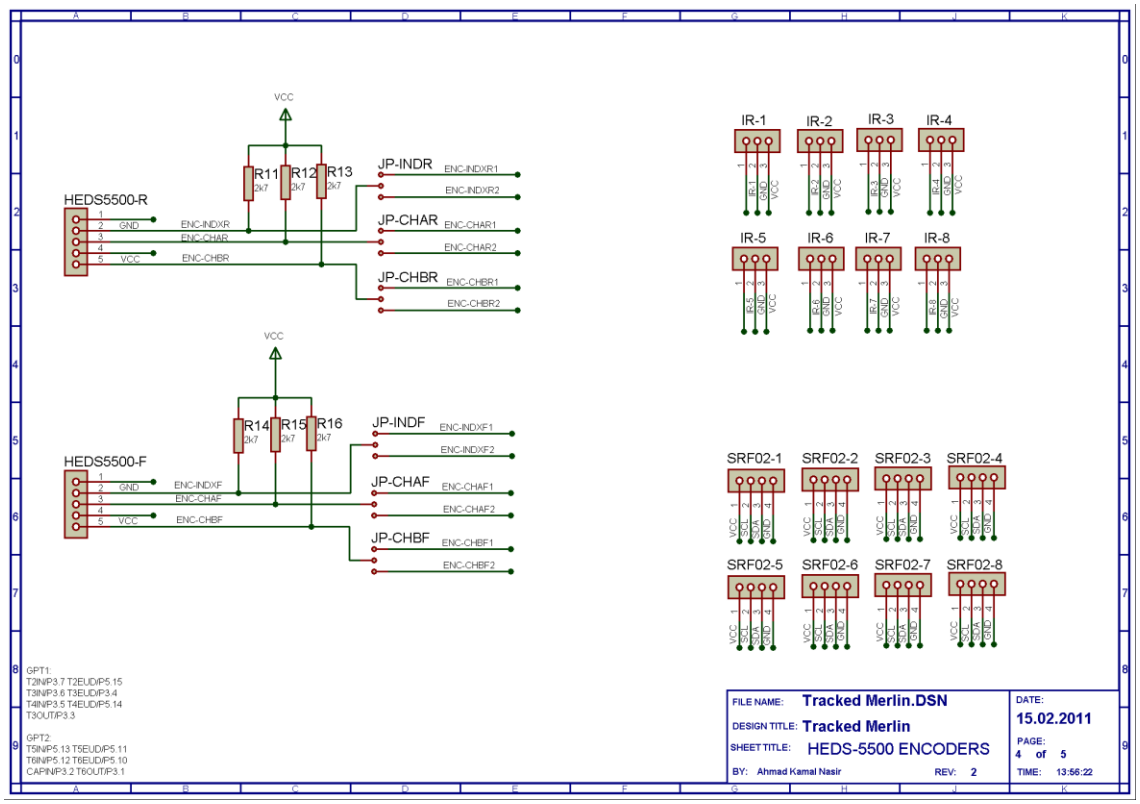
VCC
R11
R12
R13
2k7
HEDS5500-R
GND
ENC-INDXR
ENC-CHAR
ENC-CHBR
JP-INDR
ENC-INDXR1
ENC-INDXR2
JP-CHAR
ENC-CHAR1
ENC-CHAR2
JP-CHBR
ENC-CHBR1
ENC-CHBR2
R14
R15
R16
HEDS5500-F
ENC-INDXF
ENC-CHAF
ENC-CHBF
JP-INDF
ENC-INDXF1
ENC-INDXF2
JP-CHAF
ENC-CHAF1
ENC-CHAF2
JP-CHBF
ENC-CHBF1
ENC-CHBF2
IR-1
IR-2
IR-3
IR-4
IR-5
IR-6
IR-7
IR-8
SRF02-1
SRF02-2
SRF02-3
SRF02-4
SRF02-5
SRF02-6
SRF02-7
SRF02-8
GPT1:
T2IN/P3.7 T2EUD/P5.15
T3IN/P3.6 T3EUD/P3.4
T4IN/P3.5 T4EUD/P5.14
T3OUT/P3.3
GPT2:
T5IN/P5.13 T5EUD/P5.11
T6IN/P5.12 T6EUD/P5.10
CAPIN/P3.2 T6OUT/P3.1
FILE NAME: Tracked Merlin.DSN
DESIGN TITLE: Tracked Merlin
SHEET TITLE: HEDS-5500 ENCODERS
BY: Ahmad Kamal Nasir
REV: 2
DATE: 15.02.2011
PAGE: 4 of 5
TIME: 13:56:22

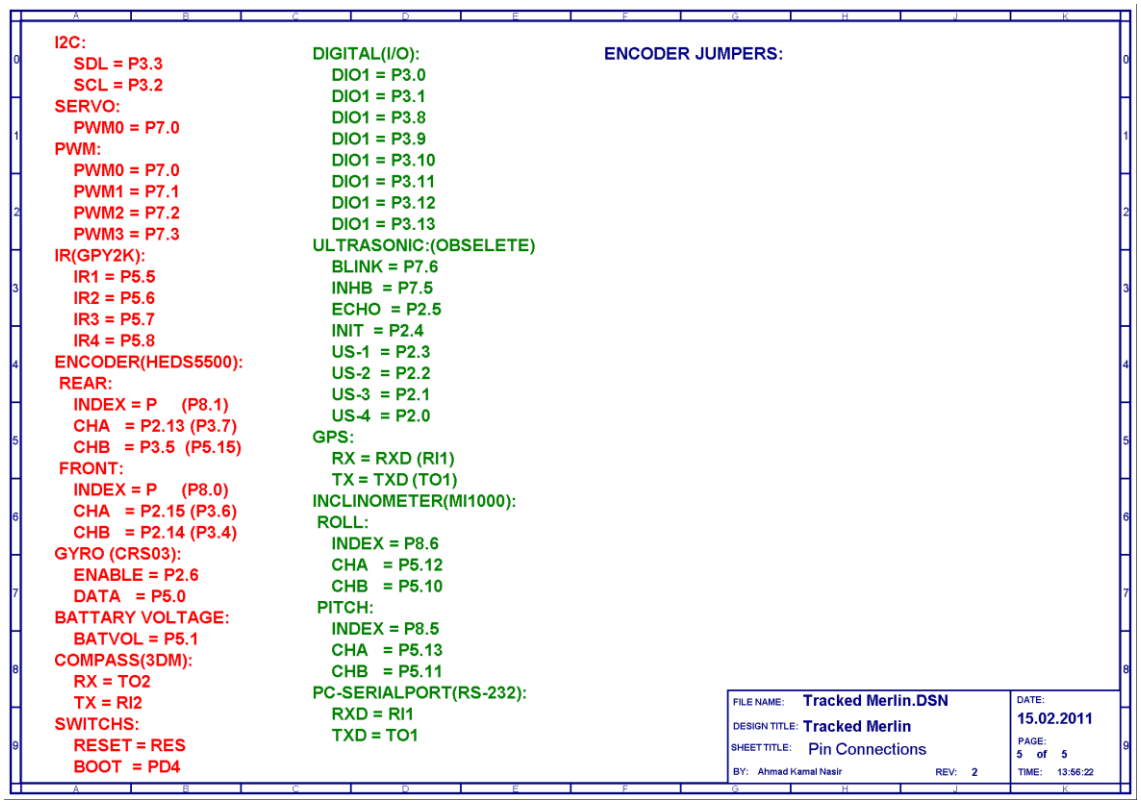

I2C:
SDL = P3.3
SCL = P3.2
SERVO:
PWM0 = P7.0
PWM:
PWM0 = P7.0
PWM1 = P7.1
PWM2 = P7.2
PWM3 = P7.3
IR(GPY2K):
IR1 = P5.5
IR2 = P5.6
IR3 = P5.7
IR4 = P5.8
ENCODER(HEDS5500):
REAR:
INDEX = P (P8.1)
CHA = P2.13 (P3.7)
CHB = P3.5 (P5.15)
FRONT:
INDEX = P (P8.0)
CHA = P2.15 (P3.6)
CHB = P2.14 (P3.4)
GYRO (CRS03):
ENABLE = P2.6
DATA = P5.0
BATTARY VOLTAGE:
BATVOL = P5.1
COMPASS(3DM):
RX = TO2
TX = RI2
SWITCHS:
RESET = RES
BOOT = PD4

DIGITAL(I/O):
DIO1 = P3.0
DIO1 = P3.1
DIO1 = P3.8
DIO1 = P3.9
DIO1 = P3.10
DIO1 = P3.11
DIO1 = P3.12
DIO1 = P3.13
ULTRASONIC:(OBSELETE)
BLINK = P7.6
INHB = P7.5
ECHO = P2.5
INIT = P2.4
US-1 = P2.3
US-2 = P2.2
US-3 = P2.1
US-4 = P2.0
GPS:
RX = RXD (RI1)
TX = TXD (TO1)
INCLINOMETER(MI1000):
ROLL:
INDEX = P8.6
CHA = P5.12
CHB = P5.10
PITCH:
INDEX = P8.5
CHA = P5.13
CHB = P5.11
PC-SERIALPORT(RS-232):
RXD = RI1
TXD = TO1

ENCODER JUMPERS:

FILE NAME: Tracked Merlin.DSN
DESIGN TITLE: Tracked Merlin
SHEET TITLE: Pin Connections
BY: Ahmad Kamal Nasir REV: 2
DATE: 15.02.2011
PAGE: 5 of 5
TIME: 13:56:22

Appendix D

Create an C# based TCP/IP Client to communicate with a simulated robot in USARSim

This guide will help to create an application in C# which can communicate with simulated robots in USARSim environment. USARSim provides a simulation environment for robots. Many commercial ground, aerial robot models environment maps and virtual sensors and actuators are included.

Setting up a Simulation Environment

This guide assumes that we are using a Windows-7 operating system with 8GB Ram and a graphics card. After we have downloaded and installed the Dec-2011 UDK release, we have to download the USARSim v1.3 and extract all the files in the same directory where we have installed the UDK. This process will copy the necessary maps, models and configuration files at the desired location. After extracting, e.g. the destination path C:\UDK\UDK-2011-12\, the USARSim related files one can execute the make file in the base UDK directory to compile the simulation entities.

Running Simulation Environment

After the simulation environment is setup we can run any one of the provided map in the C:\UDK\UDK-2011-12\USARRunMaps environment, a batch file which will load a map and run the game server. If everything was correct then the game server is started at the local machine (**127.0.0.1:3000**) and load the specified map. Initially the map is without any robots. The robots are spawned as bots in the game map. We can execute the game related commands by typing them at the command terminal (**Appears by pressing TAB**).

Communication with game engine

After the game engine is started and running we can send commands to spawn the robots and communicate robot sensors and actuators data. The communication between the game server and a client (user program) must be by using TCP/IP communication protocol format. The user must first establish a TCP/IP connection to already game server (IPAddress:Port) and then the navigation and actuators commands can be sent and sensors data can be received. For the detailed description of the command formats please refer to the documentation of the USARSim. For the communication, sensors parameters, and robots sensors settings look at the C:\UDK\UDK-2011-12\UDKGame\Config\DefaultUSAR.ini.

Client Application

The client or user application to communicate with the simulated robot is developed using the C# application using visual studio 2010 development environment. Follow the steps below to create an application which uses TCP/IP communication. First create a windows application. To perform TCP/IP communication we are provided with socket class in C#.

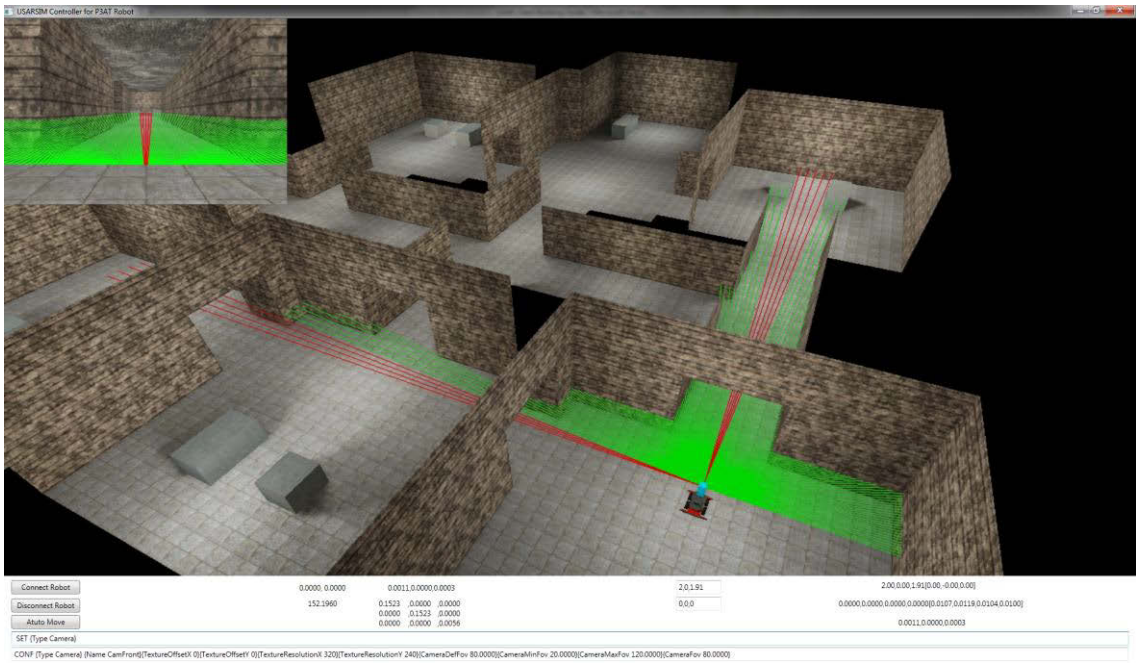

Figure 0.1 An example client application receiving simulation data

The methodology of the TCP/IP communication used to develop the application is as follows. We create a TcpClient class and assign it the game server IPEndPoint (IPAddress:Port). Then we create a thread which is passed a function to process the incoming data.

```
System.Net.Sockets.TcpClient tcpConn = new System.Net.Sockets.TcpClient ("127.0.0.1",3000);
System.Threading.Thread tcpRxThread = new System.Threading.Thread(ProcessRxData);
tcpRxThread.start(tcpConn);
```

Here first a TCP connection is created with the game serve IP address and port number. Then a thread is created which will execute the specified function as its parameter. And finally the thread is started with the created TCP connection passed as its function argument.

To capture the image data, connect to the image server at 127.0.0.1:5003 using another TCP connection. The image can be acquired by sending the request. At the moment two request commands are supported

- OK
- U[X][Y][WIDTH][HEIGHT]

The image stream data obtained is in the following format

Byte[0]	Image Formats(0=Raw[BGR],1-5=JPEG[BEST,GOOD,NORMAL,FAIR,BAD])
Byte[1,2,3,4]	Image Size
Byte[5,6]	Image Width, if Image Format is Raw
Byte[7,8]	Image Height, if Image Format is Raw
Byte[5…n]	Image Data in case Image Format is JPEG
Byte[9…n]	Image Data in case Image Format is Raw

ProcessRxData

The description of the ProcessRxData function is as follwos:

```
Void ProcessRxData ( object tcpConnection){
System.Net.Sockets.TcpClient conn = (System.Net.Sockets.TcpClient)tcpConnection;
System.Net.Sockets.NetworkStream stream = conn.GetStream();
While ( conn!= null && conn.Connected==true){
If (conn.Available > 0){
try{
byte[] buff = new byte[conn.Available];
stream.Read(buff,0,conn.Available);
DisplayData(Encoding.ASCII.GetString(buff).Insert(0,conn.Available.ToString("[0]")));
}
catch(Exception ex){
DisplayData(ex.Message);
}
} // end if
} // end While
DisplayData(string.Format("Connection closed with {0}\r\n", conn.Client.RemoteEndPoint));
} // end ProcessRxData
```

DisplayData

DisplayData is a utility function to display the data into a form control such as textbox. This function is required because the thread is running in other process wheres the textbox is on another thread. The function DisplayData is as follows:

```
Void DisplayData( String data){
data = String.Format("{}\r\n",data);
if(txtbox.Dispatcher.Thread!=Thread.CurrentThread){
txtbox.Dispatcher.Invoke(new Action(delegate(){txtbox.AppendText(data);}),null);
}
else{
txtbox.AppendText(data);
}
}
```

Important Commands and Messages Format

Following are the some of the commands which are useful for communicating with the existing Poineer3 robot. The robot sensors and actuators configuration are defined in the DefaultUSAR configuration file under [USARBot.P3AT] section. Each sensor and actuator configurations are also described in the same file under their respective section label. The communication protocol for commands and messages is based on Gamebots protocol. All messages and commands follow the following format:

DATA_TYPE {SEGMENT1} {SEGMENT2}

DATA_TYPE: INIT, STA, SEN, DRIVE etc.

SEGMENT: Name/Value pair seprated by space e.g. "Loction 1.0 2.0 3.0"

A message or command is composed of one DATA_TYPE and one or multiple SEGMENTS separated by space and ends with "\r\n".

Messages

Following are some of the important communication packet format received from the USARSim.

STA

A state message tells about the robot or mission package's state. It depends on the type of robot. The format of status messages for a ground robot is as follows:

STA {Type string } {Time float } {FrontSteer float } {RearSteer float }{LightToggle bool } {LightIntensity int } {Battery int }

{Type string } "string' describes the vehicle type. In this case: "GroundVehicle".
{Time float } "float' is the UT time in seconds. It starts from the time the UT server starts execution. {FrontSteer float } Current front steer angle of the robot, in radians.
{RearSteer float } Current rear steer angle of the robot, in radians.
{LightToggle bool } Indicate whether the headlight is turned on. 'bool' is true/false.
{LightIntensity int } Light intensity of the headlight. Right now, it always is 100.
{Battery int }" int ' is the battery lifetime in second. It's the total time remaining for the robot to run.

SEN

Sensor message contains sensor data. After it is an optional Time segment, {Time *float* }, that reports the current time in seconds in the virtual world. Whether the Time segment will appear or not is decided by the sensor's "bWithTimeStamp' variable

Range Sensor

SEN {Type string } {Name string Range float } {Name string Range float }

{Type string }" string ' is the sensor type. It can be either "Sonar" or "IR" which means it's a Sonar sensor or IR sensor.

Laser Sensor

SEN {Type string } {Name string } {Resolution float } {FOV float } {Range r1,r2,r3 "}

{Type string }" string ' is the sensor type. It can be "RangeScanner" or "IRScanner".
{Name string }" string ' is the sensor name.
{Resolution float } float ' is the sensor's resolution in radians.
{FOV float }" float ' is the sensor's field of view in radians.
{Range r1,r2,r3 "} " r1,r2,r3 is a series of range values in meters.

Odometry sensor

SEN {Type Odometry} {Name string } {Pose x,y,theta }

{Name string }" string ' is the sensor name.
{Pose x,y,theta }" x,y ' is the estimated robot position relative to the start point in meters.
theta is the head angle in radians relative to the start orientation.

GPS Sensor

SEN {Type GPS} {Name string } {Latitude int , float , char } {Longitude int , float , char } {Fix int } {Satellites int }

{Name string }" string ' is the sensor name, as given in the USARBot.ini robot's definition.
{Latitude int , float , char } int, float, char provide the latitude degree, minute (as a decimal), and cardinal description (i.e. "N' or "S'), respectively. There are only two possible values for the char parameter: 'N' for North and 'S' for South.
{Longitude int , float , char }" int ', float ', char " provide the longitude degree, minute (as a decimal), and cardinal description (i.e. "E' or "W'), respectively. There are only two possible values for the char parameter: 'E' for East and 'W' for West.
{Fix int }" int ' indicates whether or not a position was acquired. The fix is the same as the GGA format. Namely, a value of 0 means that the GPS sensor failed to acquire a position and a value of 1 means that a position was acquired.
{Satellites int }" int ' gives the number of satellites tracked by the GPS sensor. This number is an implicit source of accuracy. The more satellites are tracked, the higher the position accuracy.

INS Sensor

The Inertial Navigation Sensor is a sensor that provides estimates of the vehicles current location and orientation, based on measurements of angular velocity and linear acceleration relative to the vehicles current pose.

SEN {Type INS} {Name string } {Location x,y,z } {Orientation r,p,y } "

{Name string }" string ' is the sensor name.
{Location x,y,z } "x,y,z', are float variables for estimated vehicle locations.
{Orientation r,p,y } "r,p,y', are float variables for estimated vehicle orientation in radians. All radians are in the range [0,2PI].

Encoder sensor

SEN {Type Encoder} {Name string Tick int } {Name string Tick int }

{Name string Tick int }" string ' is the sensor name. " int ' is the tick count.

Touch sensor

SEN {Type Touch} {Name string Touch bool } {Name string Touch bool }

{Name string Touch bool } string ' is the sensor name. bool indicates whether the sensor is touching something. Value 'True' means the sensor is touching something.

RFID sensor

This sensor contains an integer id and a boolean bSingleshot variable that determines whether the tag is a single shot tag or a multi shot tag. They are deployed by placing them in UnrealEd. If the tag's id is set to -1 (the default), then the tag id will be set to a unique value automatically. Other values for the id will not be changed. If the tags are within the MaxRange of the RFID sensor mounted on the robot then the server sends the following message to the client:

SEN {Type RFIDTag} {Name string } {ID int }{Location float, float, 'float }

{Name string }" string ' is the sensor name.

Commands

In USARSim all the values in the commands are case insensitive. However, the data_type and names are case sensitive and the format must be exactly followed. The supported commands are:

INIT

Add a robot to UT world, it has the following format:

INIT {ClassName robot_class } {Name robot_name } {Location x,y,z } {Rotation r , p , y }

{ClassName robot_class } robot_class is the class name of the robot. It can be USARBot.ATRVJr, USARBot.Zerg, USARBot.P2AT, USARBot.P2DX, USARBot.Hummer, and any other robots built by the user.

{Name robot_name } robot_name is the robot's name. It can be any string you want. If you omit this block, USARSim will give the robot a name.

{Location x,y,z } x,y,z is the start position of the robot in meters from the world origin. For different arenas, we need different positions. The recommended positions can be queried by the command GETSTARTPOSES, as described in Getting_Starting_Poses_From_Maps. Worlds are available in the "maps" file release area on sourceforge.

{Rotation r , p , y } r,p,y is the starting roll, pitch, and yaw of the robot in radians with North being 0 yaw.

DRIVE

Control the Robot. There are seven kinds of control command. The first kind controls the left and right side wheels of a skid steered robot. The second kind controls the front and rear wheels of an Ackerman steered robot. The third kind controls an underwater robot. The fourth kind controls an aerial vehicle. The fifth kind controls the wheels of an OmniDrive robot. The sixth kind controls a specified joint of the robot. The seventh kind controls the angle of multiple joints of a robot, which is convenient for flipper, leg, and arm control.

DRIVE {Left float } {Right float } {Normalized bool } {Light bool } {Flip bool }

{Left float } float is spin speed for the left side wheels. If we are using normalized values, the value range is -100 to 100 and corresponds to the robot's minimum and maximum spin speed. If we use absolute values, the value will be the real spin speed in radians per second.
{Right float } Same as above except the values affect the right side wheels.
{Normalized bool } Indicates whether we are using normalized values or not. The default value is "False' which means absolute values are used to control wheel spin speed.
{Light bool } bool ' is whether turn on or turn off the headlight. The possible values are True/False.
{Flip bool } If a robot rolls over or otherwise tips off of its wheels, this will "right" the robot. If bool ' is True, this command will flip the robot to its "wheels down' position.

Appendix E

Simulation of Map Building in ROS with Mobile Robots Equipped with Odometry and Laser Range Scanner

A simulation world is created in Stage (2D simulation system). The simulation environment consists of a map and two differential drive mobile robots. The robots are equipped with a laser range scan system and an odometry system. The map is in fact a top view (plan) of the building which is stored as a PNG file format. The simulation world file (simulation.world) of the Stage simulation system depends on the robot model files; TOM3D.inc, Trackedmerlin.inc and a map file (Map.inc).

It is assumed that the following packages are already installed on the ROS system:

- Stage
- Rviz
- Gmapping

Furthermore, eclipse indigo c/c++ IDE for linux developers is also installed on the development system. The ROS system is installed under Ubuntu 10.04.4 is electric desktop distribution which is fully installed. The stage world files along with its dependent model files are displayed at the end of this document.

The stage simulation system is publishing odometry and laser scanner data on /odom and /base_scan topics. While to control the movement of the robot another topic it is subscribed to a topic names cmd_vel. To communicate with the simulated system a ROS package has been created into as follows:

roscreate-pkg simulation roscpp stage std_msgs nav_msgs sensor_msgs geometry_msgs
cd simulation
make eclipse-project

Then import the above created project into eclipse and add the controller.cpp file which is displayed at the end of this document. After that modify the CMakeLists.txt file, at the end of the file write the following line **rosbuild_add_executable(controller src/controller.cpp)**. Build the eclipse project.

After successful compilation of the package. Create a launch file as shown at the end of the document. This launch file will run the roscore and load the stage simulation system along with the world file and also run the controller node which will communicate with the relevant

topics to interact with the simulation. To create the map of the simulated envriornment run the following command at the command prompt:

rosrun gmapping slam_gmapping scan:=base_scan

To save a snapshot of the mapped environment one can use the following command

rosrun map_server map_saver

To visualize the map building process we need the rviz package to be installed. To run the rviz system type the following command at the terminal

rosrun rviz rviz

When the rviz system is successfully launched then add a map display into it and set its node to /map which is being published by the gmapping system. One can record also the simulation experiment by the following ros command

rosbag record –o dataset /odom /base_pose_ground_truth /base_scan /cmd_vel

To use the exsisting dataset (bag file) use the following commands

rosparam set /use_set_time true
rosbag play dataset.bag

Bibliography

[1] "IRobot," 14 Nov 2012. [Online]. Available: http://www.irobot.com/global/de/home.aspx. [Accessed 14 Nov 2012].

[2] "Google gets first self-driven car license in nevada," [Online]. Available: http://www.reuters.com/article/2012/05/08/uk-usa-nevada-google-idUSLNE84701320120508. [Accessed 14 Nov 2012].

[3] "KUKA mobile robot," 14 Nov 2012. [Online]. Available: http://youbot-store.com/. [Accessed 14 NOV 2012].

[4] "DARPA Grand Challenge," 14 Nov 2012. [Online]. Available: http://en.wikipedia.org/wiki/DARPA_Grand_Challenge. [Accessed 14 NOV 2012].

[5] W. Burgard, A. B. Cremers, D. Fox, D. Haehnel, G. Lakemeyer, D. Schulz, W. Steiner and S. Thrun, "The Interactive Museum Tour-Guide Robot," in *Proc. of the 15th National Conference on Artificial Intelligence*, Madison, Wisconsin, 1998.

[6] I. Ehrenberg, C. Floerkmeir and S. Sarma, "Inventory Management with and RFID-equipped Mobile Robot," in *3rd Annual IEEE Conference on Automation Science and Engineering*, Scottsdale, AZ, USA, Sep 22-25, 2007.

[7] W. D. Smart, "Is a Common Middleware for Robotics Possible?," in *Proceedings of the IROS 2007 workshop on Measures and Procedures for the Evaluation of Robot Architectures and Middleware*, San Diego, USA, Oct. 29-Nov.2, 2007.

[8] H. Durrant-Whyte and T. Bailey, "Simultaneous Localization and Mapping (SLAM): Part I The Essential Algorithms," in *IEEE Robotics & Automation Magazine, vol. 13, no. 2, pp. 99-110*, 2006.

[9] P. Besl and H. McKay, "A method for registration of 3-D shapes," in *IEEE Transactions on Pattern Analysis and Machine Intelligence*, Feb 1992.

[10] A. Censi, L. Iocchi and G. Grisetti, "Scan Matching in the Hough Domain," in *IEEE*

International Conference on Robotics and Automation, 2005, 18-22 April 2005.

[11] A. Diosi and L. Kleeman, "Fast Laser Scan Matching using Polar Coordinates," in *International Journal of Robotics Research*, Oct. 2007.

[12] H.-C. Lee, S.-H. Lee, S.-H. Lee, T.-S. Lee, D.-J. Kim, K.-S. Park, K.-W. Lee and B.-H. Lee, "Comparison and analysis of scan matching techniques for Cooperative-SLAM," in *8th International Conference on Ubiquitous Robots and Ambient Intelligence*, 23-26 Nov. 2011.

[13] R. C. Smith and P. Cheeseman, "On the Representation and Estimation of Spatial Uncertainty," *The International Journal of Robotics Research, vol. 5, no. 4,* pp. 56-68, 1986.

[14] H. F. Durrant-Whyte, "Uncertain geomatries in robotics," in *IEEE International Conference on Robotics and Automation, vol. 4*, Oxford, U.K., 1987.

[15] L. Crowley, "World modeling and position estimation for a mobile robot using ultrasonic ranging," in *IEEE Conference on Robotics and Automation*, Scottsdal, AZ, USA, 1989.

[16] J. Leonard and H. Durrant-Whyte, "Simultaneous map building and localization for an autonomous mobile robot," in *IEEE/RSJ International Workshop on Intelligent Robots and Systems.*, Osaka, Japan, 3-5 Nov 1991.

[17] J. Vandorpe, H. Van Brussel and H. Xu, "Exact dynamic map building for a mobile robot using geometrical primitives produced by a 2d range," in *IEEE International Conference on Robotics and Automation*, Sacramento CA USA, 22-28 Apr 1996.

[18] J. Gonzalez, A. Ollero and A. Reina, "Map building for a mobile robot equipped with a 2D laser rangefinder," in *IEEE International Conference on Robotics and Automation*, San Diego, CA, USA, 8-13 May 1994.

[19] N. Ayache and O. Faugeras, "Registrating And Fusing Noisy Visual Maps," in *International Journal of Robotics Research*, Dec 1988.

[20] J. J. Leonard and H. F. Durrant-Whyte, Directed Sonar Sensing for Mobile Robot Navigation, Springer-Verlag GmbH, 1992.

[21] K. Murphy, "Bayesian map learning in dynamic environments," in *Neural Info Proc. Systems*, 2000.

[22] M. Montemerlo and S. Thrun, "Simultaneous localization and mapping with unknown data association using FastSLAM," in *IEEE International Conference on Robotics and Automation*, Taipei, 14-19 Sept. 2003.

[23] G. Grisetti, C. Stachniss and W. Burgard, "Improved Techniques for Grid Mapping With Rao-Blackwellized Particle Filters," in *IEEE Transactions on Robotics*, Feb. 2007.

[24] A. Eliazar and R. Parr, "DP-SLAM: Fast, Robust Simultainous Localization and Mapping Without Predetermined Landmarks," in *International Joint Conference on Artificial Intelligence*, 2003.

[25] D. Haehnel, W. Burgard, D. Fox and S. Thrun, "An efficient fastslam algorithm for generating maps of large-scale cyclic environments fram raw laser range measurements," in *IEEE/RSJ Int. Conf. on Intelligent Robots and Systems*, 2003.

[26] C. Stachniss, U. Frese and G. Grisetti, "OpenSLAM," 12 2011. [Online]. Available: http://www.openslam.org/. [Accessed 14 Nov 2012].

[27] "Robot Operating System," 23 Oct 2012. [Online]. Available: http://www.ros.org/wiki/. [Accessed 14 Nov 2012].

[28] J. Fenwick, P. Newman and J. Leonard, "Cooperative concurrent mapping and localization," in *IEEE International Conference on Robotics and Automation*, 2002.

[29] T. Tong, H. Yalou, Y. Jing and S. Fengchi, "Multi-robot cooperative map building in unknown environment considering estimation uncertainty," in *Control and Decision Conference*, 2-4 July 2008.

[30] D. Rodriguez-Losada, F. Matia and A. Jimenez, "Local maps fusion for real time multirobot indoor simultaneous localization and mapping," in *IEEE International Conference on Robotics and Automation*, Apr 26 - May 1 2004.

[31] A. Howard, "Multi-robot Simultaneous Localization and Mapping using Particle Filters," in *International Journal of Robotics Research*, Dec 2006.

[32] N. Adluru, L. Latecki, M. Sobel and R. Lakaemper, "Merging maps of multiple robots," in *19th International Conference on Pattern Recognition*, 8-11 Dec. 2008.

[33] F. Chanier, P. Checchin, C. Blanc and L. Trassoudaine, "Map fusion based on a multi-map SLAM framework," in *IEEE International Conference on Multisensor Fusion and Integration for Intelligent Systems*, 20-22 Aug. 2008.

[34] P. Jayasekara, L. Palafox, T. Sasaki, H. Hashimoto and B. Lee, "Simultaneous localization assistance for multiple mobile robots using particle filter based target tracking," in *5th International Conference on Information and Automation for Sustainability*, 17-19 Dec. 2010.

[35] S. Williams, G. Dissanayake and H. Durrant-Whyte, "Towards multi-vehicle simultaneous localisation and mapping," in *IEEE International Conference on Robotics and Automation*, 2002.

[36] H. S. Lee and K. M. Lee, "Multi-robot SLAM Using Ceiling Vision," in *IEEE/RSJ International Conference on Intelligent Robots and Systems*, 10-15 Oct. 2009.

[37] X. Zhou and S. Roumeliotis, "Multi-robot SLAM with Unknown Initial Correspondence: The Robot Rendezvous Case," in *IEEE/RSJ International Conference on Intelligent Robots and Systems*, 9-15 Oct. 2006.

[38] M. Wu, F. Huang, L. Wang and J. Sun, "Cooperative Multi-Robot Monocular-SLAM Using Salient Landmarks," in *International Asia Conference on Informatics in Control, Automation and Robotics*, -2 Feb. 2009.

[39] B. Gerkey, A. Howard, N. Koenig and R. Vaughan, "The Player Project," Nov 2012. [Online]. Available: http://playerstage.sourceforge.net/. [Accessed 14 Nov 2012].

[40] N. Koenig and A. Howard, "Design and use paradigms for Gazebo, an open-source multi-robot simulator," in *IEEE/RSJ International Conference on Intelligent Robots and Systems*, 28 Sept.-2 Oct. 2004.

[41] B. Petersen and J. Fonseca, 2006. [Online]. Available: Writing player/stage drivers. [Accessed 14 Nov 2012].

[42] R. T. Vaughan, B. P. Gerkey and A. Howard, "On device abstractions for portable, reusable robot code," in *IEEE/RSJ Intl. Conf. on Intelligent Robots and Systems*, Las Vegas, Nevada, 2003.

[43] M. Quigley, E. Berger and A. Y. Ng, "STAIR: Hardware and Software Architecture," in *AAAI Mobile Robot Workshop*, Vancouver, BC, Canada, July 23, 2007.

[44] M. Quigley, B. Gerkey, K. Conley, J. Faust, J. L. E. B. R. W. Tully Foote and A. Y. Ng, "ROS: an open-source Robot Operating System," in *Proceedings of the Open-Source Software workshop at the International Conference on Robotics and Automation*, 2009.

[45] M. Montemerlo, N. Roy and S. Thrun, "Perspectives on standardization in mobile robot programming: The carnegie mellon navigation (CARMEN) toolkit," in *IEEE/RSJ Int. Conf. on Intelligent Robots and Systems*, Las Vegas, USA, 2003.

[46] S. Carpin, M. Lewis, J. Wang, S. Balakirsky and C. Scrapper, "USARSim: a robot simulator for research and education," in *IEEE International Conference on Robotics and Automation*, Roma, Italy, 10-14 April 2007.

[47] "Sourceforge," 26 February 2013. [Online]. Available: http://sourceforge.net/apps/mediawiki/usarsim/index.php?title=Communication_%26_Control_(Messages_and_commands).

[48] J. Jackson, "Microsoft robotics studio: A technical introduction," in *IEEE Robotics & Automation Magazine*, Dec. 2007.

[49] "Anykode Marilou," 23 11 2012. [Online]. Available: http://www.anykode.com/index.php. [Accessed 23 11 2012].

[50] J. Kerr and K. Nickels, "Robot operating systems: Bridging the gap between human and robot," in *44th Southeastern Symposium on System Theory*, 11-13 March 2012.

[51] W. Li, T. Zhang and K. Klihnlenz, "A Vision-Guided Autonomous Quadrotor in An Air-Ground Multi-Robot System," in *IEEE International Conference on Robotics and Automation*, 9-13 May 2011.

[52] G. S. Sukhatme, J. F. Montgomery and R. T. Vaughan, "Experiments with Cooperative

Aerial-Ground Robots," in *Citeseer*, 2001.

[53] "Autonomous Intelligent Systems," Nov 2012. [Online]. Available: http://www.informatik.uni-freiburg.de/~burgard/.

[54] Nov 2012. [Online]. Available: http://robots.stanford.edu/research.html.

[55] Nov 2012. [Online]. Available: http://robots.unizar.es/html/home.php.

[56] Nov 2012. [Online]. Available: http://www.acfr.usyd.edu.au/index.shtml.

[57] 14 Nov 2012. [Online]. Available: http://robotics.umd.edu/research/projects/Blankenship_Cooperative_Slam.php. [Accessed 14 Nov 2012].

[58] Nov 2012. [Online]. Available: http://mars.cs.umn.edu/index.html.

[59] Nov 2012. [Online]. Available: http://asrl.utias.utoronto.ca/~kykleung/DSLAM/.

[60] J. Borenstein and L. Feng, "UMBmark: A Benchmark Test for Measuring Odometry Errors in Mobile Robots," in *SPIE Conference on Mobile Robots*, Philadelphia, USA, Oct. 22-26,1995.

[61] N. Roy and S. Thrun, "Online self-calibration for mobile robots," in *IEEE International Conference on Robotics and Automation*, 1999.

[62] "Kinect for Windows," Microsoft, [Online]. Available: http://www.microsoft.com/en-us/kinectforwindows/. [Accessed 29 Nov 2012].

[63] "ASUS," [Online]. Available: http://www.asus.com/Multimedia/Xtion_PRO/. [Accessed 26 Feburary 2013].

[64] D. Simon, Optimal State Estimation: Kalman, H Infinity, and Nonlinear Approaches, 1 ed., USA: Wiley-Interscience, 2006, p. 552.

[65] R. Douc and O. Cappe, "Comparison of resampling schemes for particle filtering," in *Proceedings of the 4th International Symposium on Image and Signal Processing and Analysis*, 2005.

[66] S. Thrun, W. Burgard and D. Fox, Probabilistic Robotics, The MIT Press, 2005.

[67] A. Eliazar and R. Parr, "DP-SLAM: Fast, Robust Simultaneous Localization and Mapping without Predetermined Landmarks," in *in Proc. of 18th Int. Joint Conf. on Artificial Intelligence*, 2003.

[68] A. J. Cooper, "A comparison of data association techniques for Simultaneous Localization and Mapping," Massachusetts Institute of Technology, Massachusetts Institute of Technology. Dept. of Aeronautics and Astronautics, 2005.

[69] A. K. Nasir and H. Roth, "Pose Estimation by Multisensor Data Fusion of Wheel Encoders, Gyroscope, Accelerometer and Electronic Compass," in *Embedded Systems, Computational Intelligence and Telematics in Control*, University of Würzburg, Germany, 2012.

[70] A. K. Nasir, C. Hille and H. Roth, "Data Fusion of Stereo Vision and Gyroscope for Estimation of Indoor Mobile Robot Orientation," in *Embedded Systems, Computational Intelligence and Telematics in Control*, University of Würzburg, Germany, 2012.

[71] T. Larsen, N. Andersen, O. Ravn and N. Poulsen, "Incorporation of time delayed measurements in a discrete-time Kalman filter," in *Proceedings of the 37th IEEE Conference on Decision and Control*, 1998.

[72] M. Ronen and A. Lipman, "The V-scope: An Oscilloscope for motion," in *The Physics Teacher*, 1991.

[73] J. Canny, "A Computational Approach to Edge Detection," in *IEEE Transactions on Pattern Analysis and Machine Intelligence*, 1986.

[74] I. Sobel and G. Feldman, A 3x3 Isotropic Gradient Operator For Image Processing, R. Duda and P.Hart, Pattern Classification and Scene Analysis ed., New York: Wiley, 1973, pp. 271-272.

[75] P. Hart, N. Nilsson and B. Raphael, "A Formal Basis for the Heuristic Determination of Minimum Cost Paths," in *IEEE Transactions on Systems Science and Cybernetics*, 1968.

[76] E. W. Dijkstra, A note on two problems in connexion with graphs, vol. 1, 1959, pp. 269-

271.

[77] E. Sick, "Sick PLS Laser Scanner Operating Instructions," Sick GmbH, Optik- Elektronik, Waldkirch, Germany, 1995.

[78] R. Duda and P. hart, Pattern classification and scene analysis, New York, USA: John Wiley & Sons, 1973.

[79] K. Dietmayer, J. Sparbert and D. Streller, "Model based Object Classification and Object Tracking in Traffic scenes from Range Images," in *Proceedings of IV IEEE Intelligent Vehicles Symposium*, Tokyo, 2001.

[80] S. Santos, J. Faria, F. Soares, R. Araujo and U. Nunes, "Tracking of Multi-Obstacles with Laser Range Data for Autonomous Vehicles," in *Proc. 3rd National Festival of Robotics Scientific Meeting (ROBOTICA),*, Lisbon, Portugal, 2003.

[81] K. J. Lee, "Reactive navigation for an outdoor autonomous vehicle," Master Thesis. University of Sydney, Department of Mechanical and Mechatronic Engineering, 2001.

[82] G. A. Borges and M.-J. Aldon, "Line Extraction in 2D Range Images for Mobile Robotics," in *Journal of Intelligent and Robotic Systems*, July 2004.

[83] D. Lowe, "Object recognition from local scale-invariant features," in *The Proceedings of the Seventh IEEE International Conference on Computer Vision*, 1999.

[84] H. Bay, A. Ess, T. Tuytelaars and L. V. Gool, "SURF: Speeded Up Robust Features," in *9th European Conference on Computer Vision*, Graz, Austria, May 7 - 13, 2006.

[85] K. O. Arras, "Feature-Based Robot Navigation in Known and Unknown Environments," Swiss Federal Institute of Technology Lausanne, Lausanne, EPFL, 2003.

[86] K. Pathak, N. Vaskevicius, J. Poppinga, M. Pfingsthorn, S. Schwertfeger and A. Birk, "Fast 3D mapping by matching planes extracted from range sensor point-clouds," in *IEEE/RSJ International Conference on Intelligent Robots and Systems*, 10-15 Oct. 2009.

[87] E. Bayro-Corrochano and M. Bernal-Marin, "Generalized hough transform and conformal geometric algebra to detect lines and planes for building 3D maps and robot navigation," in *IEEE/RSJ International Conference on Intelligent Robots and Systems*, 18-

22 Oct. 2010.

[88] J. Weingarten, G. Gruener and R. Siegwart, "Probabilistic plane fitting in 3D and an application to robotic mapping," in *IEEE International Conference on Robotics and Automation*, 26 April-1 May 2004.

[89] M. Asada, "Map building for a mobile robot from sensory data," in *IEEE Transactions on Systems Man and Cybernetics*, Nov-Dec 1990.

[90] H. Andreasson, R. Triebel and W. Burgard, "Improving plane extraction from 3D data by fusing laser data and vision," in *IEEE/RSJ International Conference on Intelligent Robots and Systems*, 2-6 Aug. 2005.

[91] M. Y. Yang and W. Forstner, "Plane detection in point cloud data," University of Bonn, 25 Jan 2010.

[92] J. Biswas and M. Veloso, "Depth camera based indoor mobile robot localization and navigation," in *IEEE International Conference on Robotics and Automation*, 14-18 May 2012.

[93] N. Vaskevicius, A. Birk and K. Pathak, "Fast plane detection and polygonalization in noisy 3d range images," in *IEEE/RSJ International Conference on Intelligent Robots and Systems*, 22-26 Sept. 2008.

[94] A. Nuchter, H. Surmann, K. Lingemann, J. Hertzberg and S. Thrun, "6D SLAM with an application in autonomous mine mapping," in *IEEE International Conference on Robotics and Automation*, April 26-May 1, 2004.

[95] P. Henry, M. Krainin, E. Herbst, X. Ren and D. Fox., "RGB-D mapping: Using depth cameras for dense 3d modeling of indoor environments," in *12th International Symposium on Experimental Robotics*, Delhi, India , Dec 18-21.

[96] D. Borrmann, J. Elseberg, K. Lingemann and A. Nuchter, "The 3d hough transform for plane detection in point clouds - A review and a new accumulator design," in *Journal 3D Research, Springer*, March 2011.

[97] R. Triebel, W. Burgard and F. Dellaert, "Using hierarchical EM to extract planes from 3d

range scans," in *IEEE International Conference on Robotics and Automation*, 2005.

[98] O. Gallo, R. Manduchi and A. Rafii, "CC-RANSAC: fitting planes in the presence of multiple surfaces in range data," *Pattern Recognition Letters,* pp. 403-410, 2011.

[99] K. Pathak, A. Birk, N. Vaskevicius and J. Poppinga, "Fast registration based on noisy planes with unknown correspondences for 3d mapping," *IEEE Transactions on Robotics,* vol. 26, no. 3, pp. 424-441, June 2010.

[100] A. K. Nasir, C. Hille and H. Roth, "Plane Extraction and Map Building Using a Kinect Equipped Mobile Robot," in *Workshop on Robot Motion Planning:2012 IEEE/RSJ International Conference on Intelligent Robots and Systems*, Vilamoura, Algarve, Portugal, October 7-12, 201.

[101] D. Holz, S. Holzer, R. B. Rusu and S. Behnke, "Real-Time Plane Segmentation using RGB-D Cameras," in *15th RoboCup International Symposium*, Istanbul, Turkey, July 2011.

[102] R. B. Rusu, N. Blodow, Z. C. Marton and M. Beetz, "Close-range Scene Segmentation and Reconstruction of 3D Point Cloud Maps for Mobile Manipulation in Human Environments," in *IEEE/RSJ International Conference on Intelligent Robots and Systems*, St. Louis, MO, USA, 2009.

[103] C. Erdogan, M. Paluri and F. Dellaert, "Planar Segmentation of RGBD Images Using Fast Linear Fitting and Markov Chain Monte Carlo," in *Ninth Conference on Computer and Robot Vision*, 28-30 May 2012.

[104] "Dave," Infineon Technologies, [Online]. Available: http://www.infineon.com/cms/en/product/microcontrollers/development-tools,-software-and-kits/dave-tm-version-2-low-level-code-generation/channel.html?channel=db3a3043134dde6001134ee4d3b30265. [Accessed 15 March 2013].

[105] A. K. Nasir, A. Hsino and K. H. Hubert Roth, "Aerial Robot Localization Using Ground Robot Tracking Toward Cooperative SLAM," in *19th IFAC Symposium on Automatic Control in Aerospace*, Würzburg, Germany, 2013.

[106] R. Siegwart, I. R. Nourbakhsh and D. Scaramuzza, Introduction to Autonomous Mobile

Robots, The MIT Press, 2011.

[107] "The Rawseeds project," [Online]. Available: http://www.rawseeds.org/home/. [Accessed 27 March 2013].

[108] "Web bots: Robot Simulator," Cyberbotics, 24 11 2012. [Online]. Available: http://www.cyberbotics.com/. [Accessed 24 11 2012].

[109] A. J. Cooper, "A Comparison of Data Association Techniques for Simultaneous Localization and Mapping," Massachusetts Institute Of Technology, 2005.